AD-A108 233   ASHLAND CHEMICAL CO COLUMBUS OH
IMPROVED GRAPHITE FIBER ADHESION.(U)
SEP 81 G GYNN, R N KING, S F CHAPPELL   F33615-79-C-5060
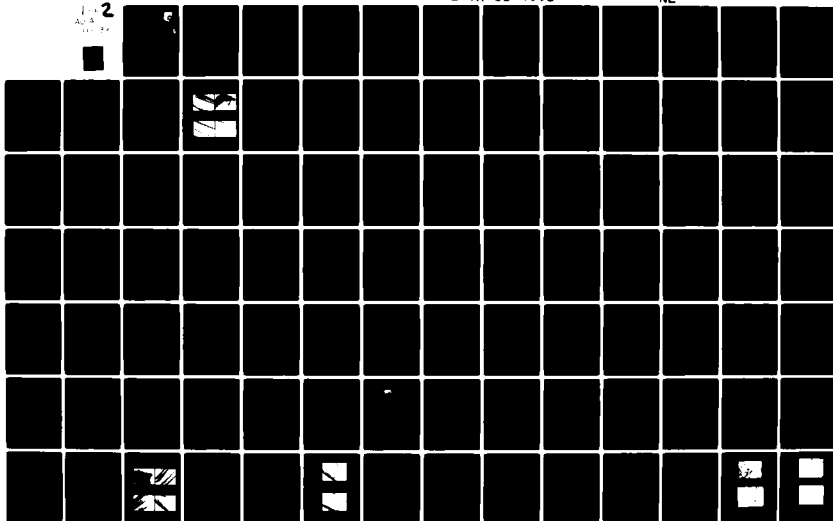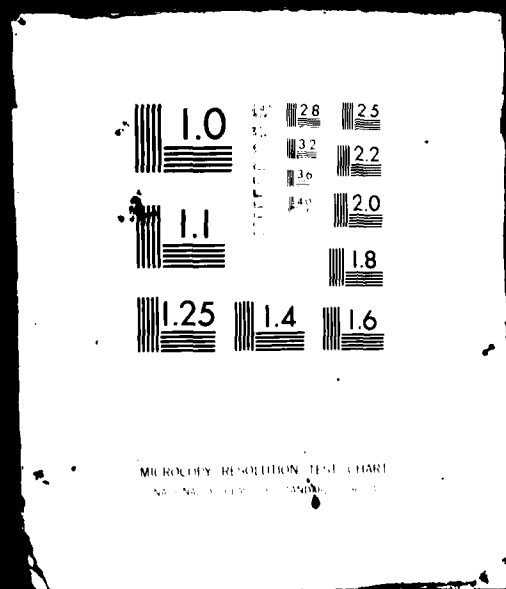AFWAL-TR-81-4096

F/G 11/4

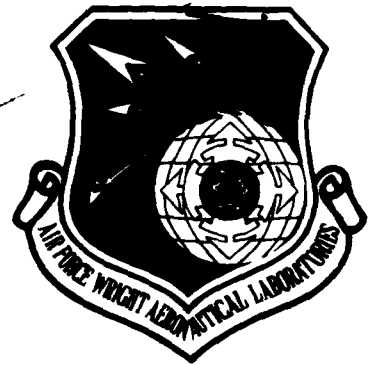UNCLASSIFIED

NL

AD-A 108233

AFWAL-TR-81-4096

LEVEL II

AD A108233

IMPROVED GRAPHITE FIBER ADHESION

ASHLAND CHEMICAL COMPANY — 393702
RESEARCH AND DEVELOPMENT DIVISION
COLUMBUS OH 43216

September 1981

Final Report for Period 10 September 1979 - 11 June 1981

Approved for public release; distribution unlimited

MATERIALS LABORATORY
AIR FORCE WRIGHT AERONAUTICAL LABORATORIES
AIR FORCE SYSTEMS COMMAND
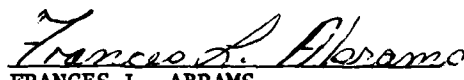WRIGHT-PATTERSON AIR FORCE BASE, OHIO 45433

81 12 08 040

NOTICE

When Government drawings, specifications, or other data are used for any purpose other than in connection with a definitely related Government procurement operation, the United States Government thereby incurs no responsibility nor any obligation whatsoever; and the fact that the Government may have formulated, furnished, or in any way supplied the said drawings, specifications, or other data, is not to be regarded by implication or otherwise as in any manner licensing the holder or any other person or corporation, or conveying any rights or permission to manufacture, use, or sell any patented invention that may in any way be related thereto.

This report has been reviewed by the Office of Public Affairs (ASD/PA) and is releasable to the National Technical Information Service (NTIS). At NTIS, it will be available to the general public, including foreign nations.

This technical report has been reviewed and is approved for publication.

FRANCES L. ABRAMS
Project Engineer

THEODORE J. REINHART, JR, Chief
Composites, Adhesives & Fibrous
Materials Branch

FOR THE COMMANDER

FRANKLIN D. CHERRY, Chief
Nonmetallic Materials Division

SECURITY CLASSIFICATION OF THIS PAGE (When Data Entered)

REPORT DOCUMENTATION PAGE	READ INSTRUCTIONS BEFORE COMPLETING FORM

1. REPORT NUMBER	2. GOVT ACCESSION NO.	3. RECIPIENT'S CATALOG NUMBER
AFWAL-TR-81-4096	AD-A108 233	

4. TITLE (and Subtitle)	5. TYPE OF REPORT & PERIOD COVERED
IMPROVED GRAPHITE FIBER ADHESION	Final Technical Report 10 Sep 79 - 11 Jun 81
	6. PERFORMING ORG. REPORT NUMBER

7. AUTHOR(s)	8. CONTRACT OR GRANT NUMBER(s)
Mr G. Gynn Dr M. L. Deviney Dr R. N. King Dr S. F. Chappell	

9. PERFORMING ORGANIZATION NAME AND ADDRESS	10. PROGRAM ELEMENT, PROJECT, TASK AREA & WORK UNIT NUMBERS
Materials Laboratory (AFWAL/MLBC) AF Wright Aeronautical Laboratories (AFSC) Wright-Patterson Air Force Base, Ohio 45433	Program Element 62102F, Project 2419, Task 241903 Work Unit 24190315

11. CONTROLLING OFFICE NAME AND ADDRESS	12. REPORT DATE
Materials Laboratory (AFWAL/MLB) AF Wirght Aeronautical Laboratories (AFSC) Wright-Patterson Air Force Base, Ohio 45433	September 1981
	13. NUMBER OF PAGES
	120 122

14. MONITORING AGENCY NAME & ADDRESS(if different from Controlling Office)	15. SECURITY CLASS. (of this report)
	Unclassified
	15a. DECLASSIFICATION/DOWNGRADING SCHEDULE

16. DISTRIBUTION STATEMENT (of this Report)

Approved for public release; distribution unlimited.

17. DISTRIBUTION STATEMENT (of the abstract entered in Block 20, if different from Report)

18. SUPPLEMENTARY NOTES

19. KEY WORDS (Continue on reverse side if necessary and identify by block number)

graphite fibers   ESCA
surface characterization   graphite fiber treatments
radiotracer analysis   electrodeposition
surface energetics   graphite-resin interface

20. ABSTRACT (Continue on reverse side if necessary and identify by block number) Several different commercial graphite fibers were characterized as to surface chemistry by XPS analysis, radiotracer analysis, thermal desorption/mass spectrometry, and surface energetics via contact angle measurements. These fibers were then treated by selective oxidation and devolatilization. Various interphase resins were then electro-deposited on the fibers. Composites were made from three matrix resins using the electrodeposited fibers and tested before and after exposure to moisture aging. No improvement in shear strength due to the electrodeposited interphase resins was noted.

DD FORM 1 JAN 73 1473   EDITION OF 1 NOV 65 IS OBSOLETE

SECURITY CLASSIFICATION OF THIS PAGE (When Data Entered)

FOREWORD

This report was prepared by Ashland Chemical Company, Ventures Research and Development Division, Polymer and Surface Chemistry Sections, Dublin, Ohio under Air Force Contact F33615-79-C-5060, "Improved Graphite Fiber Adhesion." The work was sponsored by the Composites, Adhesives and Fibrous Materials Branch (AFWAL/MLBC), Nonmetallic Materials Division, Air Force Wright Aeronautical Laboratories (AFSC), Wright-Patterson Air Force Base, Ohio 45433. Ms. F. L. Abrams was the Project Monitor. The work was done during the period September 1979 - June 1981.

The principal investigators were Mr. G. Gynn (Polymers and Composites) and Dr. R. N. King (ESCA and Surface Chemistry). Dr. S. F. Chappell was the Program Manager and Dr. M. L. Deviney was Program Co-Manager. Others contributing to the technical effort include Mr. Lyle Brostrom (Scanning Electron Microscopy), Dr. Paul J. Buscemi (Electron Microscopy), Mr. J. Milliner, Mrs. Becky Bushong, Mr. Lyle Miller, and Mr. Alan Lloyd.

This is the Final Report issued under Contract No. F33615-79-C-5060. It was submitted by the authors July 7, 1981.

iii/iv

Accession For

NTIS GRA&I	☑
DTIC TAB	☐
Unannounced	☐
Justification	

By

Distribution/

Availability Codes

Dist | Avail and/or Special

A

TABLE OF CONTENTS

TABLE OF CONTENTS (concluded)

I. INTRODUCTION

Graphite fibers are of increasing interest for construction of structural composites because of their very high strength to weight ratios; however, full utilization of their properties has not been attained because of weaknesses in the interphase bonding region between fiber and matrix. These weaknesses are evidenced by low interlaminar shear strengths for some matrices and loss of strength due to hydrothermal aging at high humidities and elevated temperatures.

The problem of obtaining good interlaminar shear strengths and other essential properties in epoxy resin composites, under many conditions, has been overcome, for the most part, by several fiber suppliers through proprietary surface treatments (believed to be mainly oxidative in type[1]). Fiber surfaces have been developed by suppliers which give good performance in epoxy composites which are being used in aircraft. Epoxy resins contain hydroxyl functionality and carboxylic acid functionalities, are thus highly polar, and consequently readily absorb water (up to about 6% by weight of the resin). As these structures absorb water they are plasticized with a loss in strength. This limits operating temperatures to about 265°F for epoxies. This strength is largely regained on drying. If, however, the composite part is subjected to high temperatures while wet, irreversible damage occurs. Aircraft encounter thermal conditions in flight sufficient to damage structures which have previously absorbed moisture at ground level. Newer aircraft designs require materials which will function with minimal strength losses at 450°F.

While the mechanisms of bonding and of bond degradation at the fiber/resin interface are only partially understood, it is evident that the

1

high polarity of the resin and the bonding interphase region leads to moisture intrusion into the matrix and interphase, setting up conditions for interfacial degradation. The work of Kaelble[2,3] and others[4] have demonstrated that polar interface bonds (mainly between fiber carboxylic acid groups and polymer amine, epoxy and hydroxy groups) are highly susceptible to irreversible hydrolytic degradation under hydrothermal aging or cyclic high temperature/high humidity service conditions.

Other recent papers which discuss mechanisms of fiber-matrix resin adhesion and bonding but not hydrothermal aging mechanisms include those by Donnet and co-workers[5,6,7], Fitzer and associates[8,9] and Thomas and Walker[1]. Ehrburger and Donnet[6] pointed out that the mechanical performance properties of a graphite fiber/resin composite depend mainly on the strength properties of the two materials, the surface of the fiber (which could lead to chemical or mechanical anchoring of the polymer), the nature of the fiber/resin bonding, and the mode of stress transfer at the interface. They classify interfacial modifications which could optimize fiber/resin interactions as chemical surface modifications of the fiber, deposition of sizing, and grafting of polymer onto the fiber. These authors discussed the influence of types of surface acidic functional groups upon the observed modes of failure in an epoxy composite. Strong acid groups (-COOH type), which were postulated to interact strongly with the resin producing good adhesion, appeared to lead to tensile (cantilever ILSS test) failure in the composite. Poor bonding or adhesion would lead to fiber "pull out" or shear failure. With weak surface acidic groups (-OH type), a mode of failure intermediate between shear and tensile failure was noted.

Fitzer and associates[8,9] have studied the influence of surface functional groups (produced by HNO_3 treatment of graphite fibers) upon bonding

2

and performance with both epoxy and phenolic resin composites (the latter as a precursor in the fabrication of carbon-carbon composites for high temperature or ablative applications). They postulated that the most probable chemical coupling mechanism between carboxylic acid functional groups and matrix precursors was a two-step process starting with hydrogen bonding between surface -COOH groups and amino groups in the resin, followed by formation of amide type coupling bonds. They carried out nitric acid oxidations on both Type II fibers (similar to Type AS-1 with a maximum temperature during manufacture of about 1500°C) and with Type I (Sigrafil HM, subjected to greater than 2500°C during processing). Suprisingly, they observed that the same interlaminar shear strengths (ILSS) were observed for epoxy composites reinforced with both fiber types, even though the concentration of reactive fiber surface groups on the Type I fiber was nearly one order of magnitude less in comparison to the Type II fiber. In addition to surface functionality their work shows the interplay of several other bonding mechanisms.

The surface functional groups or active sites on carbons and graphites and their chemical reactivity have been an area of much interest and research activity over the past 20 years. This area has been reviewed by Donnet[10,11], Boehm[12], Rivin[13], Puri[14], and Deviney[15], among others. McKee and Mimeault[16] have reviewed the general area of graphite fiber surface modifications and properties. In addition, surface treatments of carbon/graphite fibers and their effects on composites have been reviewed in a chapter of a recent book by Delmonte[17].

One approach to improving the hydrothermal aging properties is to change the matrix to types with lower moisture susceptibility, as the Air Force is attempting to do through the development of new resins such as HME-350 (an epoxy-modified polybutadiene), PBBI (a polybutadiene bisimide), and Thermid

3

600 (an acetylene terminated polyimide). Bonding of these new matrices, however, to current commercial fibers with polar surfaces must be improved. Thus a strong need exists for techniques to chemically modify graphite fiber surfaces so that good initial bonding is obtained with such low polarity resins, resulting in composites with good shear strengths and impact resistance which are retained under high temperature, high moisture conditions.

Interlaminar shear strengths in epoxy resin/graphite fiber composites have been shown to improve if the graphite surface is coated with certain polymers to form an interphase between fiber and matrix resin. Work reported by Subramanian et al.[18,19] on electro-polymerization of several monomers onto graphite fibers showed increases in interlaminar shear strength; however, no correlations could be made of the trend in shear strength with the chemical or mechanical properties of the polymer coating. Further work by Subramanian and other co-workers on electrodeposition of polymers onto graphite fibers[20] showed significant improvements in interlaminar shear strength and impact strength for epoxy resins using three copolymer systems containing maleic anhydride. This functionality has a high affinity for bonding to epoxy resins and there is some indication that interlaminar shear strength may be related to the maleic anhydride level in the deposited polymer. Impact strength for one system appears to be a function of molecular weight of the deposited polymer with flexural strength apparently related to co-monomer type (styrene, hexene, methyl vinyl ether). While no data were reported on the hydrothermal aging properties of these systems, this work did demonstrate opportunities for improved composite properties by design of a suitable polymeric interface. These authors discussed the possibility of grafting of the polymer to the graphit during ctrodeposition, an interaction which probably should be

4

beneficial to translation of stresses between the matrix resin and the reinforcing fiber.

A technical review and evaluation of the problem indicated that improvements in interfacial bonding of graphite fibers to high temperature, low-polarity, moisture-resistant resins, could be effected by a combination of the following criteria:

(1) lowering of the carboxylic acid functionality on the graphite surface;

(2) grafting of a polymeric adherend to the fiber to serve as a hydrolytically stable interphase;

(3) development of a low polarity interphase polymer with a strong affinity for the matrix resin through covalent and dispersion forces; this interphase polymer must be thermally stable and retain most of its modulus properties at composite performance temperatures, i.e., polymers with a glass transition temperature above 150°C for a composite performance temperature of about 450-500°F.

Ashland Chemical Company had underway, prior to this contract, basic research on the synthesis of co-polymers which include maleic anhydride in the backbone and which can be converted into imides by reaction with amines. Certain co-polymers of this type were likely ideal candidates to serve as a moisture-resistant interphase bridge between fiber and matrix. These maleic-type polymers can be electrodeposited in their amic acid form and subsequently thermally cyclized to the imide form.

The objectives of this program, as stated in Statement of Work Section of the Air Force RFP, were:

(1) To develop materials and processes for the treatment of high performance graphite fiber reinforcements to obtain a durable

5

(moisture resistant) high level of adhesion to selected matrix resins.

(2) The developed materials and processes shall result in strong, durable bonds between the fiber and matrix resins such as Thermid 600 (acetylene terminated polyimide), HME 350 (polybutadiene epoxy) and PBBI (polybutadiene bisimide). The latter two resins were later withdrawn from the program by the Air Force and were replaced by CON-4 (an epoxy modified polybutadiene) and an epoxy resin (Ciba Geigy MY720/DDS).

(3) To demonstrate the controlled durable adhesion obtained by single fiber and composite testing.

(4) To chemically characterize the fiber surface required to obtain the adhesive bond.

Ashland's original plan to meet these objectives placed primary emphasis upon obtaining an essentially low polarity fiber surface to form an interface with the polymeric matrix, or an interphase between fiber and matrix, containing covalent bonds between fiber and polymer along with strong dispersive (van der Waals) forces. As indicated above, a major aspect of our approach involved use of an electrodeposited interphase resin between the fiber and matrix resin. Initially our objective was to minimize carboxylic acid groups on the fiber surface and avoid polar bonding which could lead to moisture ingress at the interface. The expected resultant bonding in the composite should enhance interlaminar shear strength properties without significant sacrifice of "toughness" (impact resistance) properties and be resistant to hydrolytic degradation under long term service conditions.

6

II SURFACE CHARACTERIZATION OF COMMERCIAL GRAPHITE FIBERS

AS

STARTING MATERIALS

2.1 Introduction

Kaelble[21] attributes strength property losses from moisture degradation
in graphite fiber composites to irreversible changes directly related to
cumulative moisture degradation of the fiber/matrix interfacial bond. He
further states that surface treatments of commercial HTS and HMS graphite
fibers result in a highly polar surface character which would be expected to
have a pronounced susceptibility to degradation by moisture, and demonstrated
improvements in moisture resistance by modifying the graphite fiber surface to
make it less polar[3]. Steutz, et al.[22] reported that surface treatment of
Celion GY-70 fiber resulted in a highly polar surface, with a carboxyl-
phenolic hydroxy surface functional group mole ratio of 96/4. Clearly,
according to Kaelble's hypothesis, the highly polar nature of this surface
would also lead to moisture degradation susceptibility. The primary emphasis
of the Ashland program, therefore, was initially placed upon attempting to
obtain an essentially non-polar fiber surface which forms an interface with
the polymeric matrix (or an interphase between fiber and matrix) which
contains an optimum number of covalent bonds at the fiber/polymer interface.
An original objective then, was to minimize the carboxylic acid groups on the
fiber surface which are the mainstay for enhanced adhesion of many surface
treated fibers for conventional epoxy composites[23].

Since our approach involved surface modification of commercial graphite
fibers as starting materials, chemical characterization of the surface of the
"as received" and subsequently treated fibers was essential. Fortunately, the
surface chemistry of a variety of carbon types as analyzed by a variety of

7

techniques has been extensively studied and reviewed[10-17, 24-57]. It is generally believed that a variety of *carbon-oxygen functional* groups are present on carbon surfaces. Mattson and Mark[24] report that nearly every type of functional group known in organic chemistry has been suggested as being present on the surface of activated carbon. The nature and concentration of these groups varies with the type of carbon, and its processing history.

Carbon-oxygen reactions in particular appear to be crystallographically specific. Henning[25] has reported that molecular oxygen preferentially attacks graphite crystals at the edges of the layer planes at a rate nearly 20 times that of the atoms within the basal planes.

While a large number of oxygen-containing functional groups have been reported *on carbon surfaces, the most generally* accepted are carboxyls, hydroxyls, and quinone-like carbonyls. A variety of other carbon-oxygen groups have been suggested, including lactones, anhydrides, peroxides, ethers and esters[11,15]. These surface oxides have been studied by functional group reactions[11,14,16,26] heats of immersion[27-32], infrared[24,33], pyrolysis[34,35], chemisorption[26,36], and X-ray photoelectron spectroscopy[37-45].

The quinone-like carbonyl groups have received considerable attention in several electrochemical studies[24,37,46-50,53]. Such studies clearly show anodic and cathodic peaks which can be interpreted as arising from the formation and reduction of quinone-like groups on the surface. Similarly *quinones or quinone-like groups have been identified by* infrared studies[33] and by specific wet chemical reactions[37]. Studies of quinone-like groups on activated carbon surfaces[46] indicate such groups can participate as electron donors in donor-acceptor complexes with adsorbed molecules.[33,50]

8

Based on the work of these investigators, several analytical methods were selected to both directly or indirectly characterize the fiber surface chemistry: ESCA (X-ray Photoelectron Spectroscopy or XPS), programmed temperature devolatilization/mass spectrometry (PTDMS), surface energetics by contact angle methods[57,60], thermogravimetric analysis (TGA), and a radiochemical technique using a CH_2N_2 methylating reagent.

2.2 Surface Topography

Much of the data on various carbon surfaces can hopefully be correlated with the results on graphite fiber surfaces. Graphite fibers, however, present a difficult analytical problem because of their extremely low surface areas compared to carbon. Figures 1A-1D illustrate the general surface topographies of both sized and unsized commercial graphite fibers. Figures 1A and 1B are typical of both Hercules Magnamite AU-1 (unoxidized, unsized) and Hercules AS-1 (oxidized, unsized) fibers, with very little noticeable differences in surface topography for either fiber. Evidently the oxidative treatment does not significantly alter the fiber surface topography at the scale of magnification shown here. We have noted variations in fiber diameter, with an average of 8 µm normally observed for AS-1. The range, however, is considerable. Fibers as small as ~ 6 µm and as large as ~ 10 µm have been measured. In addition, we have occasionally observed what Hercules refers to as a 'monster' fiber within a tow. Some of these are as large as 26 µm in diameter. We have also noted that the relative depth, linearity, and extent of 'grooving' of the longitudinal striations on the AS-1 surfaces varies both within a roll and between lots. These variations probably account for the 4% variation in weight per unit length reported by Hercules.

9
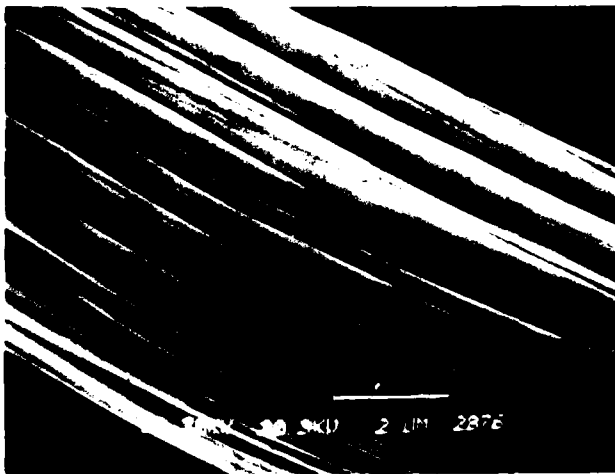
Figure 1A

'As-Received' AS-1 Graphite Fiber (10.3 KX)

Figure 1B

'As-Received' AS-1 Graphite Fiber (8.82 KX)

Figure 1C

Celion 3000 with 1.1% Epoxy Finish (7.72 KX)

Figure 1D

Celion 3000 with 1.1% Epoxy Finish (11.35 KX)

10

Figures 1C and 1D show a Celanese Celion 3000 tow with a 1.1% epoxy finish. The epoxy coating is quite evident in these photos and is considered a typical thickness for this level of coverage. Figure 1C shows a common observation, that of interfiber resin bridging. This is most likely due to a capillary effect caused by the close proximity of the fibers as they are withdrawn from the finishing solution. In Figure 1D, the finish shows a rippled texture which still reflects the underlying longitudinal striations on the fiber surface. Figures 1C and 1D are representative of the average coating found on all fibers within the Celion 3000/1.1% epoxy finish tow. The average diameter of the Celion fiber is ~ 5 μm, considerably smaller than AS-1. In the electrodeposition process we assigned a value of 1-2 wt.% pickup as an initial target value.

Aside from the longitudinal striations found on all the fiber surfaces we have examined, there are no other distinguishing topological features. Consequently the surface areas, and hence surface functional group concentrations, are quite low. Surface areas on the Hercules and Celion commercial fibers were determined using a three-point BET method with a calibrated He/N_2 mixture. Celion 6000, Hercules AU-1 and AS-1 all show values of 0.36 m^2/gm. Hercules AS-4 fiber showed 0.39 m^2/gm. These values are in relatively good agreement with similar measurements made by Drzal[61] on AU and AS type fibers calculated from krypton adsorption isotherms.

The lack of large scale 'surface roughness' on these fibers may not allow for strong adhesion via mechanical interlocking between the fiber and matrix resin. Hence, most of the adhesion is probably developed via interaction of the matrix resin component with the surface functional groups present on the fiber surface. Whether these interactions involve true chemical bonding across the interface region remains an open question.

2.3 XPS Analysis of Commercial Graphite Fibers

Several recent studies[1,44,62] have utilized XPS in analyzing the surface chemistry of graphite fibers. Hopfgarten[44] studied a number of graphite fiber surfaces both as received and after heating to 200°C in vacuum. His results indicate little adsorbed oxygen was present on the fiber and that heating produced a conversion in the carbon-oxygen bonding on the surface. Oxygen surface concentration for both Courtaulds and Torayca commercial fibers were in the range of 30-50 at.%. He speculated that the skewness in his C-1s spectra might originate from some carbonyl-type carbon on the fiber surface but that this alone could not account for the total skewness in the peak. In addition to carbon and oxygen, traces of sulphur, chlorine, nitrogen, and silicon were detected on these fiber surfaces, resulting from either the initial fiber fabrication process or subsequent oxidation.

Thomas and Walker[1] reported XPS results on a variety of Courtaulds fibers (HTU, HTS, HMU, HMS) and the Hercules AU-1 and AS-1 fiber used in the present study. They were unable to specifically assign carbon-oxygen functionalities from the C-1s spectra but did suggest the possibility of both N-O and C-O-N type functionalities as well as C-O and C=O containing groups. A portion of their quantitative elemental results, along with those of Hammer and Grant[62] on the same surfaces are listed in Table 1. The latter investigators also studied changes in surface elemental composition upon heating in vacuum at 300°C, 600°C, and 700°C and showed that after an initial increase in surface oxygen at 300°C, there is a rapid decrease in oxygen coverage at both 600 and 700°C. As shown in Table 1, for the elements analyzed there is general agreement (less than 10 at.% variation) between the two data sets. In particular, the oxygen concentration on the AS-1 fiber is over a factor of two larger than its unoxidized AU counterpart. Oxygen

12

coverage on AS-1 is very consistent (14.8-15%) but much less consistent (2.7-8.2%) on the parent AU-1 fiber surface. Both reports attribute traces of Na, S, and N to either the initial fiber preparation process or subsequent oxidation.

TABLE 1

QUANTITATIVE XPS RESULTS OF PREVIOUS INVESTIGATORS[1,62]
ON
GRAPHITE FIBER SURFACES

FIBER	Element (Atomic %)						
	C	O	N	Na	Cl	Si	S
AU*	85.5	8.2	4.1	1.0	0.1	0.5	0.3
AU**	88.0	6.1	-	5.3	-	-	-
AU**	91.0	2.7	1.0	5.3	-	-	-
AS*	73.2	14.8	9.5	2.1	0.4	0.3	0.4
AS**	79.0	15.0	3.0	2.8	-	-	-
AS**	77.0	15.0	5.4	2.4	-	-	-
HTU*	90.3	6.2	1.5	0.7	0.2	0.9	0.4
HTS*	81.0	11.2	5.7	1.3	0.2	0.5	0.2
HMU*	92.7	4.9	0.7	0.7	0.1	0.5	0.3
HMU**	97.0	2.5	-	-	NA	NA	NA
HMU**	97.0	3.1	-	-	NA	NA	NA
HMS*	87.5	8.2	1.6	1.7	0.2	0.4	0.4
HMS**	94.0	5.5	-	-	NA	NA	NA
HMS**	95.0	4.9	-	-	NA	NA	NA

* Thomas and Walker[1]
** Hammer and Grant[62]
NA - Not Analyzed

In the present study, X-ray photoelectron spectra were obtained with a Hewlett-Packard 5950B instrument utilizing monochromatic Al K$_{\alpha 1,2}$ radiation at 1487 eV. The samples were mounted in air, inserted into the spectrometer, and analyzed at ambient temperatures in a 10^{-9} torr vacuum. Power at the X-ray source was 800 watts. Instrument resolution in the spectrometer during this study was measured as 0.76 eV for the full width at half maximum of the C-1s peak from spectroscopic grade graphite. An electron flood gun operating

at 0.3 mA and 5.0 eV supplied a flux of low energy electrons to the carbon surface to minimize heterogeneous charging artifacts in the resulting spectra.

Wide scans (0 to 1000 eV) were performed for surface elemental analyses as well as detailed 20 eV scans of the C-1s, O-1s, N-1s, Na-1s, and S-2p regions. Several standards had been analyzed under the same scan conditions in order to obtain accurate chemical shift data for various carbon-oxygen functional groups[63]. These included poly(ethylene terephthalate), poly(ethylene oxide), and anthraquinone. The latter was run at -50°C in order to minimize volatility under the high vacuum conditions. All spectra were charge referenced to a C-1s line for an alkyl-like carbon at 284.0 eV.

Quantitative elemental results for the AU-1, AS-1, AS-4, and Celion 6000 fibers are listed in Table 2. Several features in these data are evident. The scans on AS-1 are very consistent in terms of surface elemental composition, with relatively high amounts of nitrogen noted on all AS-1 surfaces. Within the detectability limits of XPS, this would indicate a homogeneous surface composition for the AS-1 fiber, with very little variation within or among lots. The oxygen variation shown in this study on the AU-1 fiber was also exhibited in Table 1. Note that the oxidation step in going from AU-1 to the AS-1 fiber doubles the nitrogen content on the surface. This suggests several oxidation mechanisms, but most probably an electrolytic treatment. Such a treatment with nitric acid has also been reported to significantly increase the surface area of the fiber[64]. As noted earlier, however, we did not observe any significant topographical variation among these fibers by either SEM or BET analyses . This may indicate relatively mild reaction conditions are used by this manufacturer in oxidizing the fiber surface and that higher surface concentrations are possible.

The sodium levels decrease significantly on the AS-1 fiber, suggesting

14

that much of the original surface sodium is in a non-bonded state which is removed quite readily during the oxidation step. This sodium as well as the traces of sulphur (and possibly some nitrogen) reportedly result from either sodium sulphate[62] or sodium thiocyanate[1] used in the initial PAN precursor fiber processing.

From the data in Table 2, there also appear to be significant differences between the AS-1, AS-4, and Celion 6000. No sodium or sulphur were detected under comparable scan times for the AS-4 fiber indicating a different processing history for this fiber compared to AS-1. AS-1 and AS-4 do not originate from the same PAN precursor, however, so this is not unreasonable. Also note the relatively high level of surface oxidation of the Celion 6000 compared to both AS-1 and AS-4.

A careful examination of the C-1s and O-1s regions of the model oxygen-containing compounds listed in Table 3 allow us to estimate the nature of the carbon-oxygen functional groups on the graphite fiber.

The C-1s spectra of poly(ethylene terephthalate), poly(ethylene oxide), and anthraquinone are shown in Figure 2. All spectra were internally charge-referenced to an alkyl-like C-1s line at 284.0 eV. As shown in the figure, the oxygen-containing functional groups in these model compounds result in pronounced chemical shifts in the C-1s spectra.

Note also that the area ratios of the various carbon peaks shown in Figure 2 can be used to predict the structure of these compounds. For example, from Table 3 the structure of poly(ethylene terephthalate) shows two carbons in ether-like groups, two carbons in ester groups, and six carbons in an aromatic environment for a ratio of 1:1:3, respectively. In Figure 2, the C-1s spectrum of this polymer shows the predicted 1:1:3 ratio; the O-1s region (not shown) gives a 1:1 ratio of the oxygen atoms in ether and ester-type groups.

15
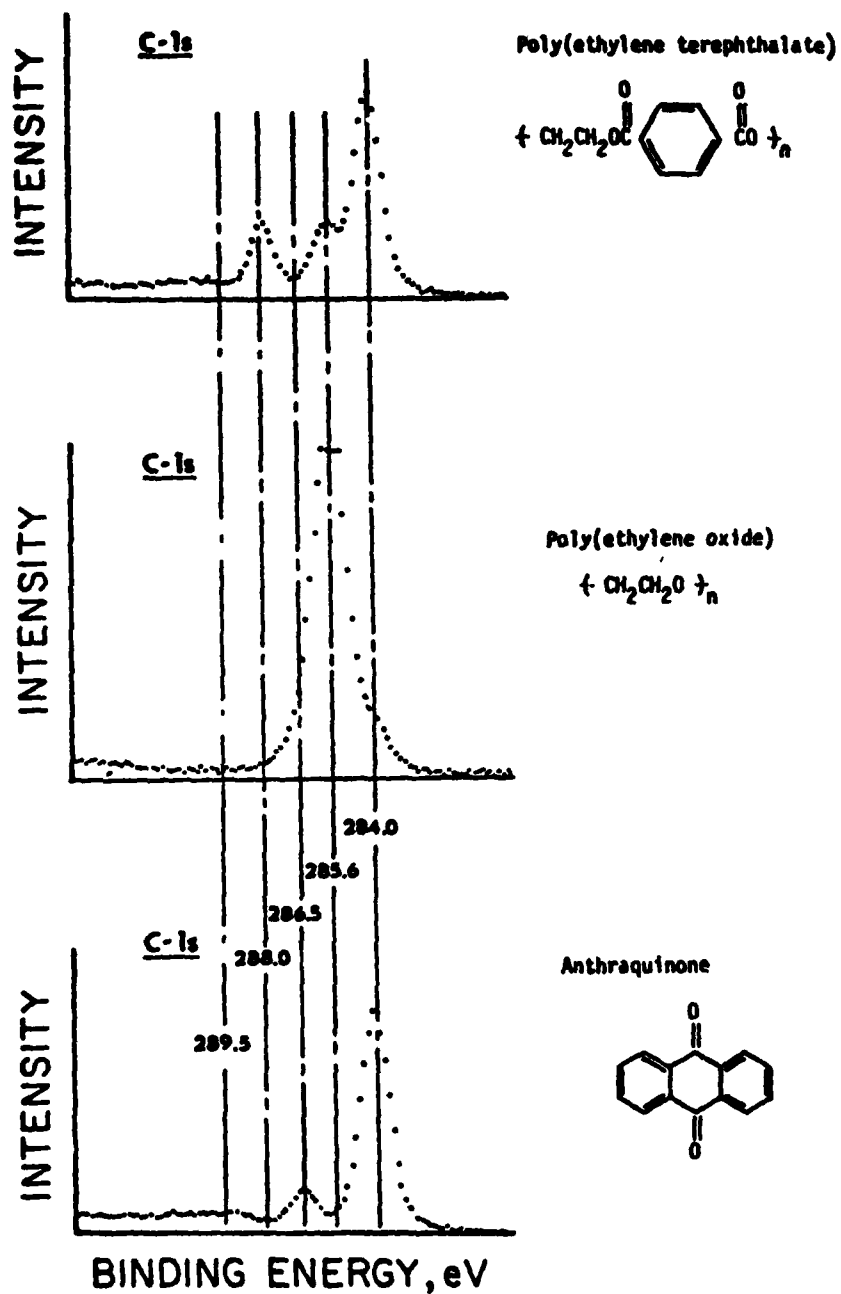
Figure 2. The C-1s XPS spectra of poly(ethylene terephthalate) (top), poly(ethylene oxide) (center), and anthraquinone (bottom). All spectra charge-referenced to alkyl-like C-1s at 284.0 eV.

16
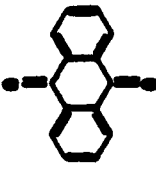
TABLE 2

OUANTITATIVE XPS RESULTS ON AU-1, AS-1,AS-4
AND
CELION 6000 GRAPHITE FIBER SURFACES

FIBER	Element (Atomic %)				
	C	O	N	Na	S
AS-1, oxidized unsized, Lot #130-2	82.7	8.9	7.9	0.6	trace
AS-1, oxidized unsized, Lot #130-2	82.5	10.5	6.4	0.6	trace
AS-1, oxidized unsized, Lot #145-3	84.0	10.0	5.4	0.5	trace
AU-1, unoxidized, unsized, Lot #145-2	92.4	2.7	3.5	1.5	-
AU-1, unoxidized, unsized, Lot #145-2	91.7	4.3	2.2	1.7	0.1
AU-1, unoxidized, unsized, Lot #145-2	88.1	6.8	2.2	2.9	trace
AS-4, oxidized, unsized, lot #3006 148-8	91.0	6.2	2.8	-	-
Celion 6000, oxidized, unsized, Lot #HTA-7-8521	81.1	17.6	0.9	0.4	-

Table 3 thus summarizes the chemical shift data of Figure 2 which were subsequently used to estimate the nature of the oxygen-containing functional groups found on the carbon fiber surfaces.

Figure 3 shows the C-1s spectra for the four commercial fibers examined in this study. The scale factors for the spectra have been increased by a factor of five compared to those in Figure 2 in order to enlarge the carbon-oxygen functional group regions. While distinct peak separations cannot be observed in the spectra due to the high intensity of the major alkyl or

17

TABLE 3

ORGANIC MODELS FOR DETERMINATION OF CARBON-OXYGEN
FUNCTIONAL GROUPS BY XPS: OXYGEN-CONTAINING
FUNCTIONAL GROUP DATA FROM THE C-1S LINE
OF POLY(ETHYLENE TEREPHTHALATE),
POLY(ETHYLENE OXIDE), AND ANTHRAQUINONE

Compound and Her Structure	Observed Binding Energy (eV)*	ΔE**	Fraction of Total Oxygen	Functional Group	
Poly(ethylene terephthalate)	284.0	0.0	--	-C-C-or ⬡	alkyl and/or aromatic
	285.6	+1.6	.5	-R-O-R-	ether-like
	288.0	+4.0	.5	R-C(=O)-O-R-	ester-like
Poly(ethylene oxide)	285.8	+1.8	1.0	-R-O-R-	ether-like
Anthraquinone	284.0	0.0	--	-C-C-or ⬡	alkyl or aromatic
	286.5	+2.5	1.0	[quinone structure]	quinone-like

* Charge-referenced to C-1s at 284.0 eV
** Binding Energy -284.0 eV = ΔE

18

-C-C-

-C-O-C-

AU-1

π→π*

AS-1

INTENSITY

AS-4

CELION
6000

284.0
285.6
286.5
288.0
289.5
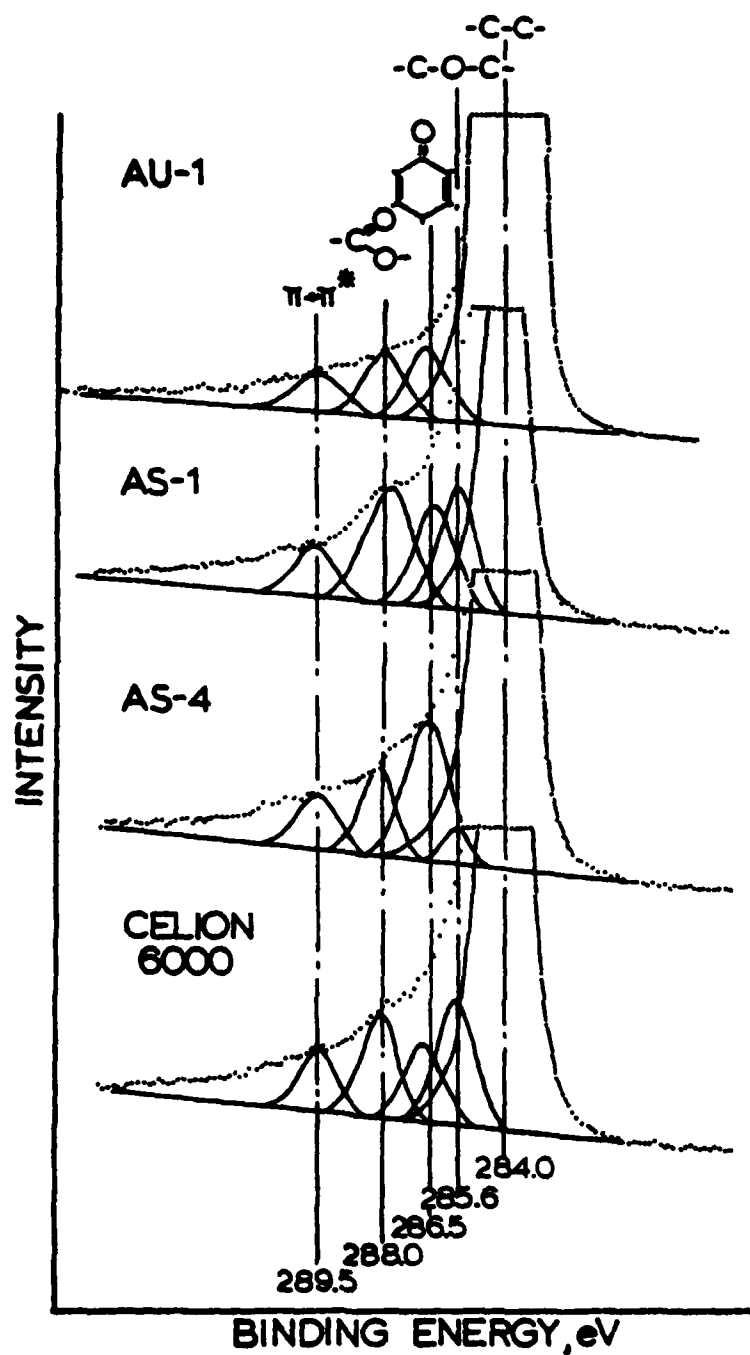
BINDING ENERGY, eV

Figure 3.   The C-1S XPS spectra of four commercial graphite fibers. All
spectra charge-referenced to alkyl-like C-1S at 284.0 ev.

19

aromatic C-1s line, the asymmetry evident on the high binding energy side of the peak is indicative of several additional carbon species, presumably chemically bound to oxygen. Using the chemical shift data of Figure 2 and Table 3, the carbon regions were roughly deconvoluted (by maintaining the same width at half-maximum peak intensity) to form the peaks superimposed on the spectra in Figure 3. For more information on deconvolution refer to Section 2.4, page 29.

In addition, a higher energy feature is noted in the C-1s spectra. If this is assigned to a carbon-oxygen group, it roughly corresponds to a carbonate-like carbon as reported by Clark[65]. However, Clark[66] has also demonstrated that low kinetic energy $\pi \rightarrow \pi^*$ shake-up transitions for aromatic polymers invariably lead to satellite peaks in the C-1s core level spectra located from 6 to 7 eV above the alkyl-like C-1s.

One would, therefore, expect to see such satellites in the C-1s spectra of poly(ethylene terephthalate), anthraquinone, and graphite fibers, since all exhibit varying degrees of aromaticity. Such peaks are suggested in Figures 2 and 3 and are shown to fall roughly within the same region for all of the C-1s spectra. Both explanations in this case are equally likely, and in fact probably both occur.

The deconvoluted peaks are shown to reasonably account for the asymmetry in the C-1s spectra of the carbon surfaces. Thus, to a first approximation the peaks correspond to the carbon-oxygen functional groups indicated in Table 3. Based on the deconvolution, the relative percentages of the various types of possible carbon-oxygen functionalities are given in Table 4. As shown in this data, from 35 to 50% of the surface oxygen species consist of highly polar ester or carboxylic acid-like functionalities. These can be expected to

20

play a significant role in terms of the moisture sensitivity of the final composite.

The nitrogen regions from the ESCA spectra of AU-1, AS-1, AS-4 and Celion 6000 were re-examined in an attempt to determine the nature of the nitrogen bonding on these surfaces. There appear to be two small peaks in the three AU samples analyzed, one at ~ 398 eV and one at ~ 400 eV (charge referenced to

TABLE 4

XPS ESTIMATIONS OF OXYGEN-CONTAINING FUNCTIONAL GROUPS
ON COMMERCIAL GRAPHITE FIBERS.

FIBER	APPROX % OF C-O FUNCTIONALITY	FUNCTIONAL GROUP
AU-1	--	ether-like
	52	quinone-like
	48	ester-like
AS-1	35	ether-like
	30	quinone-like
	35	ester-like
AS-4	14	ether-like
	53	quinone-like
	33	ester-like
Celion 6000	41	ether-like
	25	quinone-like
	34	ester-like

C-1s at 284 eV). In contrast, only one peak at 399 eV was observed for the three AS-1 samples and the AS-4 sample. The Celion 6000 showed one peak at 400.5 eV. The identification of these shifts has not yet been established, and we have no model compound reference spectra to compare to for functional group assignments. Nitrogen has been a nearly neglected element on the fiber

21

surface in terms of proposed interfacial bonding or bonding failure mecha-
nisms. This is surprising in that the nitrogen concentrations shown on the
AS-1 fibers are over 50% of the total oxygen surface concentrations.

2.4 $^{14}CH_2N_2$ Analysis of Commercial Graphite Fibers

For analysis of surface functional groups at very low surface concen-
trations, radiochemical methods appeared to offer a worthwhile approach with
suitable sensitivity. Puri[14] and Boehm[12] have provided a good review on
the use of diazomethane (CH_2N_2) as a specific chemical reagent for studying
the surface chemistry of carbon. Typical diazomethane reactions[67] and
subsequent cleavage reactions are shown in Table 5.

In 1978, Barton, and co-workers[68] published a paper in which good
agreement was obtained for values of surface carboxylic acid and phenolic
groups determined using the diazomethane methylation method in comparison with
values obtained using methyl Grignard reagent (CH_3MgI), and dilute (0.05N)
NaOH titration techniques. Their data were obtained on both a powdered
Acheson's Colloid graphite with a surface area of 163 m^2/gm and a channel-type
carbon black (Spheron 6), with a surface area of 116 m^2/g. In addition, these
researchers used diazomethane to characterize and follow the changes as the
acidic surface oxides were removed from the graphite sample as CO_2 at
increasingly higher temperatures. Again, agreement was good for values
obtained using the 0.05N NaOH titration and CH_3MgI methods. In the present
study, the use of $^{14}CH_2N_2$ followed by sequential hydrolysis of labelled
surface ester and ether groups[15,26,28,68,69] are of interest.

Approximately 0.6 gram samples of as-received AS-1 graphite fiber were
exposed to a diethyl ether solution of radiolabeled diazomethane made from
Diazald[R] (n-methyl-n-nitroso-p-toluenesulfonamide, CH_2N_2 precursor from

Aldrich Chemical). The diazomethane was generated using the method described by deBoer and Backer[70]. Solution concentrations were typically on the order of 5×10^{-3} to 2×10^{-2} molar. Isotope dilution analysis of the labeled diazomethane showed a specific activity of 0.67 mCi/mole. Approximately 50 ml. of solution was added to each fiber sample and allowed to stand 24 hours at room temperature. Following exposure the fiber was extracted for 48 hours in diethyl ether (two changes) followed by extraction in a 50/50 acetone/petroleum ether mixture. The extract was monitored via scintillation counting until background levels were reached. Each sample was then divided into two portions. One was treated with 3 ml of 1N HCl, and one with 3 ml of 57% HI in sealed glass containers at 100° to 120°C for 24 hours. The hydrolysis liquid was then scintillation counted in both cases. The liquid scintillation counting solution was prepared by mixing 100 gm. naphthalene, 5 ml H_2O and 5 grams of diphenyl oxazole (PPO) with one liter of dioxane (scintillation grade).

After hydrolysis, the fibers were washed to remove the hydrolysis products and acids. The fibers were then dried, separated into three portions, and weighed into scintillation vials fitted with specially-prepared silicon rubber septum caps. A small piece (5 mg) of carbon paper was included in each vial. Vials were flushed with O_2, closed, and injected with 10 ml. of O_2. The fibers and carbon paper were then burned by exposure to infrared. Scintillation cocktail was then injected and counted[69]. The scintillation counting solution used was prepared by mixing 100 ml. ethanolamine, 290 ml ethylene glycol monoethyl ether and 5 grams of diphenyl oxazole (PPO) with 500 ml. of toluene (scintillation grade).

As work in this area progressed, some concern developed over the possibility of methylene polymerization during the initial diazomethane

reaction with the surface functional groups of interest. Labeled dimer, trimer or larger tagged groups reacting with a single functional group on the surface would obviously lead to erroneous results. In addition, some side reactions are likely to occur.

As indicated in Table 5, the diazomethane may be expected to combine with carboxylic acids to form esters, and with alcohols and phenols to form ethers. Other reactions can potentially occur. For example, hydroquinone functionality can lead to ether formation and cyclic alkanes (cyclopropanes) could form via addition reactions with the α, β unsaturations of quinones and other olefinic carbon bonds. Carbon and hydrogen insertions are also potential side reactions. For the cleavage reactions, all of the esters are expected to be hydrolyzed by both HCl and HI. HI hydrolysis of ethers is also expected. C-14 labelled methylene added to α, β unsaturated bonds of quinones or other olefinic bonds, however, would not be removed by acid hydrolysis and would remain in the samples to be combusted. The same is true of carbon and hydrogen-inserted methylene.

To circumvent these problems an alternative approach was investigated. The methyl esters and ethers were cleaved as before and the cleavage products separated by gas phase chromatography[26]. The eluted material was passed into a combustion furnace as part of a gas proportional counter (Packard Inst. Co., Model 894 Gas Proportional Counter) where it was burned to carbon dioxide and counted as $^{14}CO_2$. The responses from the GC and gas proportional counter were traced on a dual pen recorder such that the radioactivity was matched with the material being eluted. In the case of carboxylic acid functionality, C-14 methanol was eluted, combusted and counted. For phenolics, C-14 methyl iodide was taken through the same sequence. The separation procedures used assure that only the cleavage products are counted, and interferences from

24

TABLE 5

FUNCTIONAL GROUP REACTIONS OF DIAZOMETHANE

AROMATIC CARBOXYLIC ACIDS

$$Ar\text{-}\overset{O}{\overset{\|}{C}}\text{-}OH + CH_2N_2 \xrightarrow[100\%]{\text{ETHYL ETHER}} Ar\text{-}\overset{O}{\overset{\|}{C}}\text{-}O\text{-}CH_3 + N_2 \uparrow$$

PHENOLIC

$$Ar\text{-}OH + CH_2N_2 \xrightarrow[CH_2Cl_2]{CH_3OH \approx 50\%} Ar\text{-}O\text{-}CH_3 + N_2 \uparrow$$

META CARBONYL

$$+ CH_2N_2 \xrightarrow[\approx 70\%]{\text{ETHYL ETHER}} \text{(ENOL)} + N_2 \uparrow$$

KETONES

$$+ CH_2N_2 \xrightarrow{\text{ETHYL ETHER}} + N_2 \uparrow$$

CLEAVAGE REACTIONS

$$Ar\text{-}\overset{O}{\overset{\|}{C}}\text{-}OCH_3 + H_2O \xrightarrow{OH^-} Ar\text{-}\overset{O}{\overset{\|}{C}}\text{-}OH + CH_3OH \quad \text{FIRST CLEAVAGE}$$

$$Ar\text{-}\overset{O}{\overset{\|}{C}}\text{-}OCH_3 + HI \longrightarrow Ar\text{-}\overset{O}{\overset{\|}{C}}\text{-}OH + CH_3I$$

$$Ar\text{-}O\text{-}CH_3 + HI \longrightarrow Ar\text{-}OH + CH_3I$$
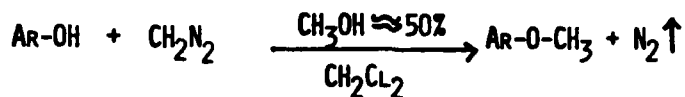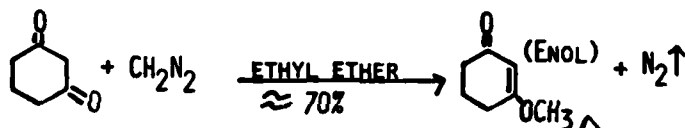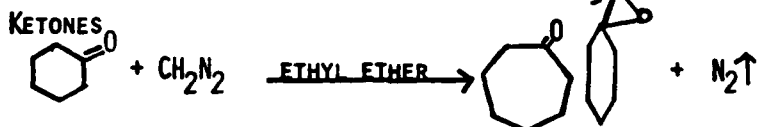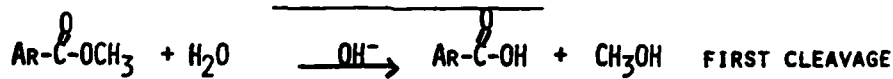
SECOND CLEAVAGE

TECHNIQUES

I. SCINTILLATION COUNTING
 A. LABELLING
 B. COMBUSTION

II. GAS CHROMATOGRAPHY
 A. LABELLING
 B. COMBUSTION
 C. GAS PROPORTIONAL
    COUNTING

quenching, most side reactions, and methylene polymerizations are minimized. In the case of the HCl hydrolysis of the CH_2N_2-treated fiber surface, the only radioisotope-labeled species observed by the GC procedure was the expected $^{14}CH_3OH$. Results from both methods are given in Table 6. For the purpose of rough correlation with the previous XPS data, the concentrations detected on the surface have been converted to atomic % using the following basis:

1. Assume close packing of carbon atoms (~ 0.8 Å radii) on the graphite fiber surface, i.e. roughly 80% of the surface area is occupied.

2. In terms of the surface density of atoms this amounts to:

$$\left[\frac{atom}{(0.8)^2 \pi Å^2}\right]\left[\frac{1 \times 10^{16} Å^2}{cm^2}\right][0.8] \quad \approx \quad 4 \times 10^5 \ atoms/cm^2$$

Hence 100% coverage (corresponding to 100 at.%) of the surface is equivalent to 4×10^{15} atoms/cm^2.

3. In terms of μmole concentrations on the fiber:

$$\left[\frac{n \ \mu mole}{gm \ fiber}\right]\left[\frac{6.02 \times 10^{23} \ atoms}{mole}\right]\left[\frac{10^{-6} \ mole}{\mu mole}\right] \approx \left[\frac{6n \times 10^7 \ atoms}{gm \ fiber}\right]$$

4. Since the measured fiber surface area corresponds to 4000 cm^2/gm:

$$\left[\frac{6n \times 10^{17} \text{ atoms}}{gm}\right]\left[\frac{gm}{4000 \text{ } cm^2}\right] \quad = \quad 1.5 \text{ } n \times 10^{14} atoms/cm^2$$

Hence, the atomic % conversion is given by:

$$\frac{1.5 \text{ } n \times 10^{14}}{4 \times 10^{15}} \times 100 \text{ where } n = \text{ \# } \mu moles \text{ } ^{14}C \text{ detected/gm fiber.}$$

As illustrated in Table 6, no usable results originated from the HI hydrolysis procedure because of severe color quenching by the iodine in solution. Similarly, the HI in the GC eluent damaged the column* (through adsorption or degradation) to such an extent that no data were obtained from this portion of the experiment. Consequently, we do not have a direct measure (following hydrolysis) of the alcohol and phenolic content of the surface. For comparisons drawn from Table 6, the phenolic content must be inferred by the difference between the combusted HI-hydrolyzed fiber and combusted HCl-hydrolyzed fiber.

The standard deviations on the data of Table 6 are quite large. This could either mean true heterogenity within the fiber itself or experimental errors within the technique. In the limited time devoted to this work we did not devise a procedure which would distinguish between these two sources of variability.

---

*These HI-related problems were encountered with stainless steel GC columns. It is possible that glass GC columns might be less susceptible to the adsorptive or degradative effects encounted when HI-containing samples are injected.

TABLE 6

$^{14}CH_2N_2$ RADIOCHEMICAL ANALYSES OF AS-1 GRAPHITE FIBER

Material Analyzed	Carbon-14 Detected		Functional Group Detected
	(μ mole/gm)	At.%*	
Hydrolysis liquid following 1N HCl hydrolysis	1.3 ± 0.4	4.8 ± 1.5	Carboxylic acid
Hydrolysis liquid following 57% HI solution hydrolysis	No data due to Iodine quenching		
Scintillation cocktail following combustion of HCl hydrolyzed fiber	0.6 ± 0.2	2.2 ± 0.8	Quinones, alcohols, phenols, carbon and hydrogen insertions
Scintillation cocktail following combustion of HI hydrolyzed fiber	0.4 ± 0.3	1.5 ± 1.1	Quinones, carbon and hydrogen insertions
GC eluent following 1N HCl hydrolysis	2.0 ± 1.0	7.5 ± 3.8	Carboxylic acid
GC eluent following 57% HI solution hydrolysis	No data due to GC column damage by HI		

* See text for calculation assumptions

Assuming that all the oxygen functional groups have been accounted for via the CH_2N_2 reaction, comparison of the total oxygen on the surface via the radiotracer method and the ESCA data (cf. Table 2) show both measurements agree quite well in terms of total oxygen. The relative ratios of functional groups on the surface, however, differ substantially as shown in Table 7. Several factors contribute to these discrepancies. While there is no doubt that the deconvoluted C-1s ESCA spectra account for all of the observed area shown in the peak, one must remember that the assignment of only three peaks is somewhat arbitrary. Other functional groups could be present, in particular nitrogen-carbon functionalities, which could easily result in a

28

different interpretation. The same can be said for the $^{14}CH_2N_2$ method, however. No reactions were considered nor devised for C-N functionality, and the assumption was made that the only groups present on the graphite fiber surface were carboxylic acids and phenols. This is obviously not an unreasonable assumption based on the literature evidence to date. However, a further assumption in the $^{14}CH_2N_2$ method is that the reaction yields for various functional groups are known. While this is generally true for homogeneous solution reactions with known compounds, the yield on a heterogeneous solid substrate cannot be considered equivalent. The relative conversions to esters and ethers via the diazomethane reaction are reportedly not equal even for the homogeneous case. Formation of methyl esters from carboxylic acids is reported to have a 100% yield[71] while formation of methyl aryl ethers from phenols has only a 49% yield[72]. It is thus possible that for a given reaction time the total oxygen content may be an underestimate, particularly if a large proportion of the surface contains phenolic groups. Reaction time also could play a role in the results. Barton, et al.[68] indicate higher total CH_2N_2 reactivity with acidic groups on Spheron 6 carbon black at longer reaction times.

In our work we independently measured the yields for diazomethane reactions with benzoic acid (an assumed model for -COOH) and phenol in order to at least provide data for the homogeneous case. Proton NMR results indicate a 100% yield with benzoic acid, but only a 69% yield with phenol. In both cases less than 1% C-H insertion was observed. We did not, however, analyze the quinone yield and consequently cannot fully correct the CH_2N_2 functional group data listed in Table 7. It is safe to say that the alcohol or phenol concentration is higher than the raw data presented in the table.

The ESCA data presented in Table 4 are considered closer to the actual surface concentrations shown on the AS-1 fiber.

TABLE 7

COMPARISON OF OXYGEN-CONTAINING FUNCTIONAL GROUPS
ON COMMERCIAL AS-1 GRAPHITE FIBERS BY XPS AND RADIOCHEMICAL METHODS

Functional Group	Approximate % of C-O Functionality	
	XPS	$^{14}CH_2N_2$
Carboxylic Acid (Ester-like)	35	69
Quinone	30	21
Alcohols, Phenols (Ether-like)	35	10

2.5 Thermal Desorption/Mass Spectrometer Analyses of Commercial Graphite Fibers

The objective of the initial Ashland surface modification plan was the optimization of alcohol and phenolic groups relative to the more polar carboxylic groups. The approach to achieve this result involved selective oxidation followed by controlled thermal devolatilization of oxygenated functional groups. Several investigators[13,38,73,74] have reported the use of thermal desorption/mass spectrometer analyses as a means of following the evolution of material from carbon and graphite samples as a function of temperature. The surface oxides reportedly desorb for the most part as CO and CO_2, with the relative amounts dependent on the devolatilization temperature. If it is assumed that the functional groups responsible for CO desorption are carbonyl-like and those for CO_2 desorption carboxylic-like, the thermal desorption method provides a monitor of the temperature at which these groups are preferentially removed from the surface.
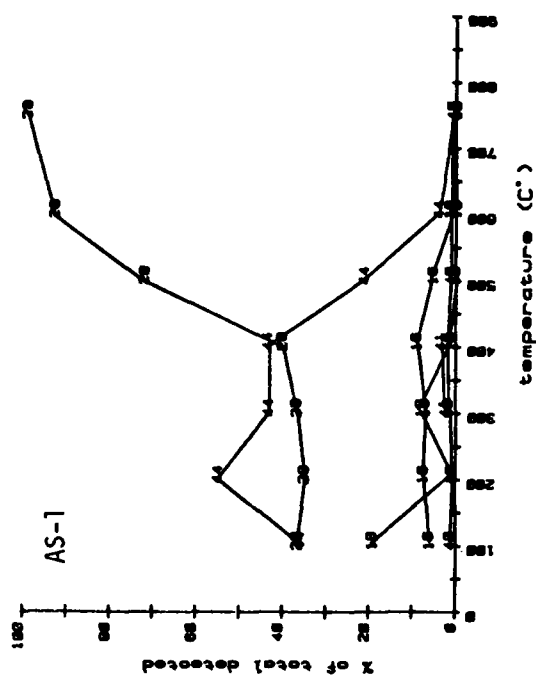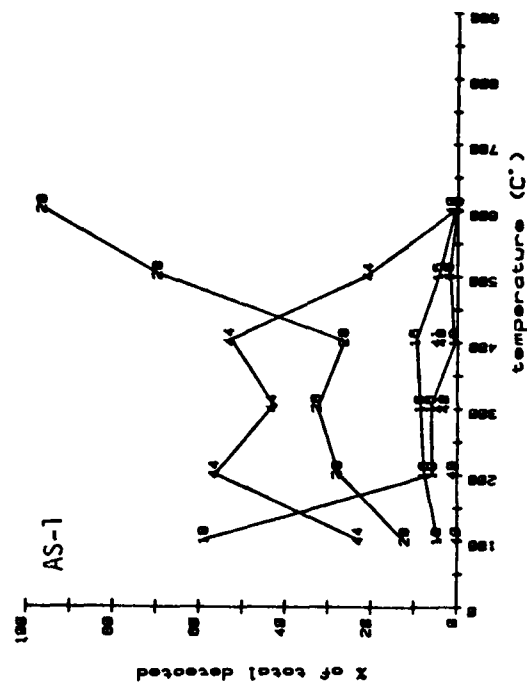
30
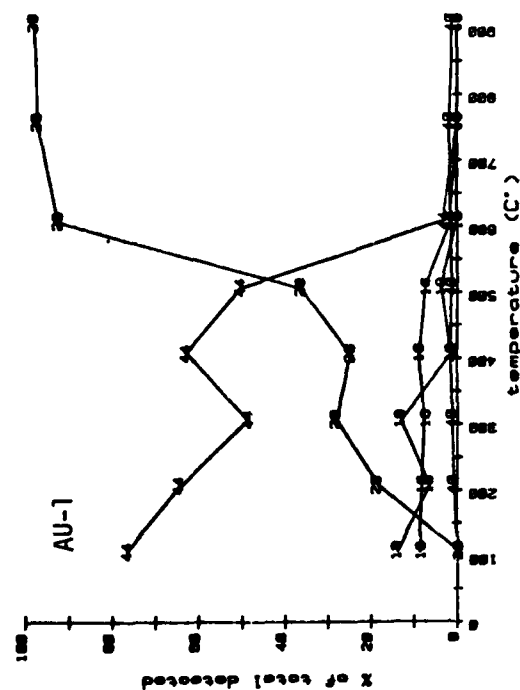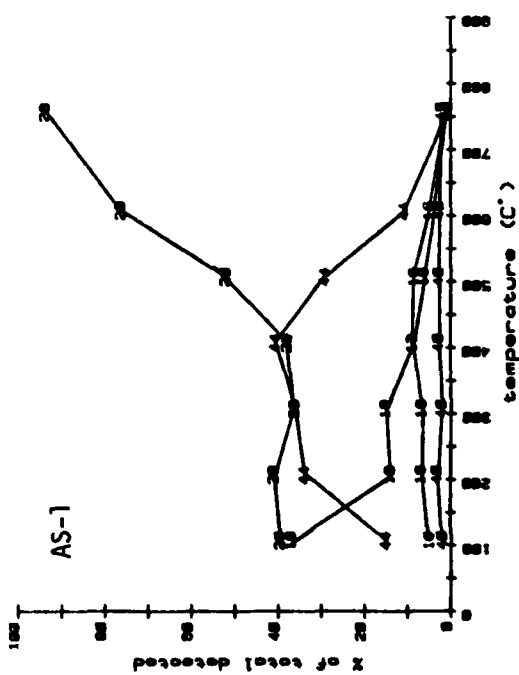
Figure 4. Thermal Desorption Data on AS-1 and AU-1 Fibers.

31

A UTI model 100C Quadrupole Mass Spectrometer was used to monitor the devolatilization products from the graphite fiber. Approximately 15 feet of fiber per run were placed in a high purity Al_2O_3 tube (McDanel Refractory Co., Beaver Falls, Pa.) and evacuated to the low 10^{-7} torr range via an ion pumped vacuum system. A background spectrum was taken, and the temperature then stepped in 100°C increments and equilibrated for 1 hour with the tube under static vacuum. Following this period the tube was opened to the mass spectrometer and the evolved gases sampled and analyzed. The system was then re-evacuated, the background analyzed, and then stepped to a new temperature to repeat the process. No attempt was made to quantitate the amount of desorbed product. Qualitative amounts of the species detected were corrected for background levels (which remained relatively constant throughout the run), normalized against total masses detected at a given temperature and plotted as a function of temperature.

Figures 4A-4D show the results of several thermal desorption runs on both AU-1 and AS-1 graphite fibers. The main variations noted in all of the plots are in H_2O (18), CO (28), and CO_2 (44) concentrations. On the AU-1 fiber (presumably not oxidized) a large CO_2 fraction is seen at low temperatures which rapidly drops off at over 500°C. At 600°-900° all of the measurable desorbed material is CO. From 5%-15% of the total desorbed material up to 300°C is water. The AS-1 plots are generally similar to the AU-1 with several exceptions. At 100°C. water comprises a much greater percentage of the desorbed species. Whereas CO_2 adsorption seems to predominate on the unoxidized AU surface, the oxidized (hence more polar) AS-1 surface shows a stronger affinity for water, as might be expected. In addition, the CO and CO_2 percentages at temperatures up to 425°-450°C are roughly equivalent for

32

AS-1. Beginning at 450°C, the CO evolution again dominates the total percentage of desorbed species.

Qualitatively, our results agree quite well with those of previous investigators, particularly with the work of Barton, et al.[34,73,75]. In their work with 'natural' graphite surfaces[34] they found an equivalent CO/CO_2 ratio in the 450-500°C range and an overall CO/CO_2 ratio for total amounts desorbed from 0 to 1000°C of over 4/1. The CO_2 desorption rate compared to CO desorption was only slightly higher in the 300°-400°C range. They found no preferential low-temperature desorption of CO_2 when oxygen had been chemisorbed on a clean graphite surface[28,75]. Perkins[74] showed a slight preference for CO_2 desorption on graphite fiber (Thornel 50) with a maxima near 300°C. Total production of CO, however, at temperatures from 475°C-500°C upwards far outweighed the amount of CO_2 evolved. Rivin[13] showed very similar behavior for a carbon black, with some evidence of physisorbed CO_2 as well. The picture thus evolves of a weakly associated (possibly predominantly physisorbed) CO_2-evolving species on the graphite fiber surface. Initially it would appear that the CO_2 concentration on the surface is considerably smaller than the amount of CO functionality present. However, as has been previously reported[13,74], at elevated temperature some CO evolution is due to carbon reduction of volatilized refractory oxides. While this was initially thought to involve only reduction of silica at temperatures in excess of 1000°C, we have noted reduction of quartz at temperatures as low as 600°C and of high purity (low SiO_2) Al_2O_3 below 900°C. Both of these materials have been used as vacuum enclosures for our devolatilization experiments. Consequently, the relative amount of CO desorption from the fiber surface, as has been reported in the literature, may be misleading, particularly with high surface area materials such as carbon

33

black where large amounts of desorbed species come in contact with the container walls.

Thus, if one were to attempt to minimize the CO_2/CO ratio of oxygen-containing functional groups on the AS-1 graphite fiber surface via thermal devolatilization, temperatures $\leq$ 400°C are in order. Both the literature results and our own work support this conclusion. Our data, however, were obtained nearly at the conclusion of our devolatilization work. As will be reported in those studies, the standard devolatilization temperature was 600°C (based on some earlier literature reports). Under such conditions the CO_2/CO ratio may have been minimized at an expense of some loss of CO functionality as well.

2.6 TGA Analyses of Commercial Graphite Fibers

Although not part of the original contract, a limited number of thermo-gravimetric analysis (TGA) measurements were run on both AU-1 and AS-1 fibers. The TGA data have potential use: (a) as a means of determining temperature/devolatilization conditions for graphite fibers, (b) as a means of following devolatilization kinetics, and (c) as a means of following the oxidation characteristics after devolatilization of oxygen species on the fiber surface.

Depending on the species devolatilized, the weight loss exhibited by the fiber should correlate with the quantities of oxygen detected on the surface via ESCA and the $^{14}CH_2N_2$ methods. Approximately 0.05 gm of continuous fiber was used in the experiments. Based on the $^{14}CH_2N_2$ results, total quantities for various oxygen functionalities on the surface are less than 10 μmole/gm. This corresponds to a total loss of around 0.5×10^{-6} to 5×10^{-6} gm. Thus, full devolatilization of all oxygen-containing surface functional

34

Figure 5   Thermogravimetric Analysis of AS-1 Fiber Under Flowing N_2
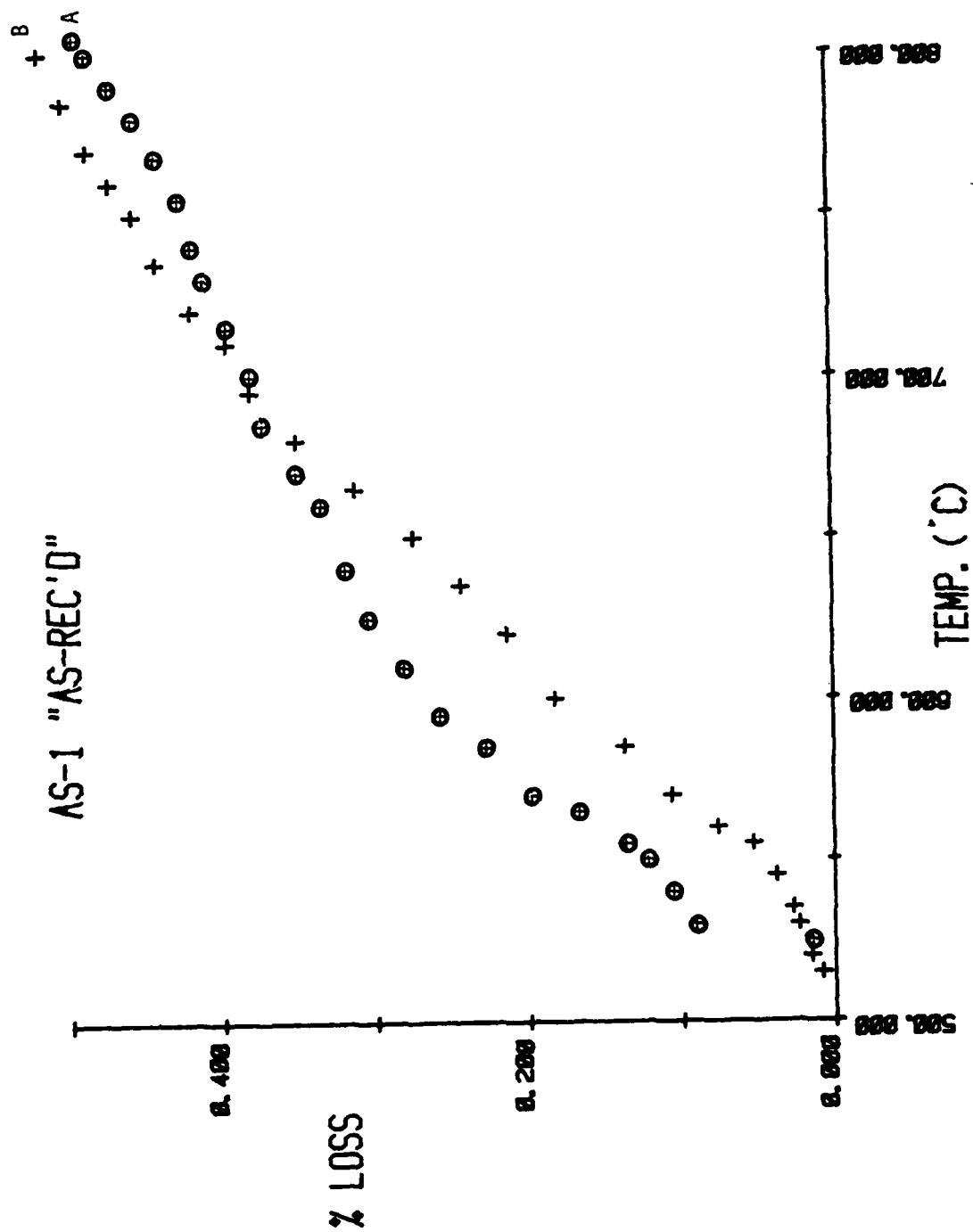
groups should correspond to a total weight loss of 10 µgm or less. For a 0.05 gm fiber this is approximately 0.001% to 0.01% of the total weight.

Figure (5) shows the devolatilization behavior of AS-1 under a presumably 'dry' nitrogen atmosphere. The temperature was linearly programmed from ambient to 800°C @ 267°/hr. for a 3 hour total run. Curve A is the initial run and Curve B is the same fiber taken through a successive run. Note particularly that the % loss on the fiber is significantly higher than was predicted, and that the second heating cycle on the same fiber produces a nearly identical curve. The data strongly suggest oxygen or water contamination in the carrier gas. The large losses exhibited result from extensive oxidative attack of the fiber structure itself in addition to the relatively small amounts desorbed from the surface.

The thermal oxidative stability of the AS-1 type fiber reportedly is quite poor[76,77]. Air exposure at 700°C of AS-1 fiber resulted in a 90% weight loss in less than 100 hours[76]. In contrast, Celion 3000 fiber showed less than a 5% loss under the same conditions. McMahon[77] reports an even more drastic loss for the AS-1 fiber. His data show a 98.7% weight loss after air exposure @ 500°C for three hours. He noted that sodium (present in measurable quantities on AS fiber surfaces) is known to catalyze air oxidation.

As will be discussed further in this report, the electrodeposition of the interphase resin requires a post-deposition imidization step at 300°C. We wished to test the stability of the fiber at this temperature in a flowing air environment to simulate these processing conditions. Using the TGA system, AS-1 fiber was heated to 320°C under room air flowing at 60 cc/min. through the system. From 0-320°C, the fiber tow lost weight at a rate of 0.04%/min. At a constant temperature of 320°C under these flow conditions the rate of loss was ~ 0.015%/min. Lowering the temperature to 300°C reduced the rate of

loss to ~ 0.006%/min. Considering that this loss occurs primarily from surface reactions, the overall loss rate is quite significant. The deposited resin may prevent oxidative attack, but we did not pursue this investigation further.

Judging from literature reports and the above results, selective air oxidation of AS-1 graphite fiber to enhance surface oxygen-containing functional groups was not considered a viable approach. The extreme sensitivity of AS-1 fiber to even small amounts of oxygen makes large scale high temperature surface modifications very difficult.

Several runs with AU-1 and AS-1 fiber were done under vacuum conditions (~ 10^{-3} torr) in hopes of avoiding the oxidation problems noted earlier. Two factors appeared in the vacuum runs, however, which were not apparent in the earlier results. For reasons we have not as yet fully determined (possible thermo-molecular flow), the gravimetric response of the electrobalance became thermally-dependent, with weight losses and gains associated with increases and decreases in temperature. In addition, a static charge effect became more evident, and more difficult to compensate. Consequently, only empirical observations could be made from these experiments. All weight losses exhibited by both AU-1 and AS-1 fiber under vacuum were shown to equilibrate rapidly under isothermal conditions at temperatures below 700°C. Between 700°-800°C, however, continual weight loss begins to occur, with the rate of loss increasing as the temperature increased. At 800°C weight loss in both fibers was 7 to 9 µg/hour. At 900°C, the rate loss increased to 21-23 µg/hour. Extensive attack on the interior surfaces of the quartz tube containing the fibers and the quartz hang-down fiber were noted following these runs. Clearly, evolved species from the fiber are responsible for the apparent reduction of the SiO_2 network. A similar effect is proposed for

37

reduction of the Al_2O_3 tubes. These added findings of relatively low temperature reduction by the carbon fiber devolatilization-products support our speculations that a portion of the CO measured via the mass spectrometer is a result of wall interactions rather than true surface species.

2.7 Surface Energetics of Graphite Fibers and Liquid/Solid Resins via Contact Angle Measurements

2.7.1 Graphite Fibers

The thermodynamic criteria for wetting of the graphite fiber by a resin is that the total surface free energy of the resin/solvent combination must be lower than that of the fiber surface. Hence, a study of the surface energetics of commercial graphite fibers (and in a later section surface modified fibers) is an important aspect in the characterization of the fiber surface chemistry.

Surface energetics of the commercial AU-1 and AS-1 fibers were determined by measuring the contact angles of liquids of known interfacial free energies with the fiber surface. The method of measurement is a micro-Wilhelmy plate technique[78] in which a single graphite fiber is immersed in the liquid and the force exerted on the fiber measured gravimetrically with a Cahn 2000 microbalance. The measured force on the balance is the sum of gravitational, buoyancy, and surface tension effects and is given by:

$$(\gamma_{LV}\cos \theta)C = (F - m + B)g$$

where: γ_{LV} = liquid/vapor surface tension
θ = contact angle at the solid/liquid/vapor interface

38

C = fiber circumference

F = balance force (mg)

m = weight of fiber (mg)

B = buoyancy force (mg)

g = gravitational acceleration

From the contact angle data and a knowledge of the surface free energy components of the liquids used, one can evaluate the dispersive (γ_s^d) and polar (γ_s^P) components of the solid surface using the relationship developed by Kaelble[79]:

$$\frac{\gamma_{LV}(1 + \cos\theta)}{2(\gamma_L^d)^{1/2}} = (\gamma_s^P)^{1/2}\left(\frac{\gamma_L^P}{\gamma_L^d}\right)^{1/2} + (\gamma_s^d)^{1/2}$$

where γ_{LV}, γ_L^d and γ_L^P refer respectively to the liquid surface free energy and its dispersion and polar components and θ is the measured contact angle between the liquid and solid surface. $(\gamma_s^P)^{1/2}$ and $(\gamma_s^d)^{1/2}$ are measured as the slope and intercept of the best straight line plot of:

$$\frac{\gamma_{LV}(1 + \cos\theta)}{2(\gamma_L^d)^{1/2}} \quad \text{vs.} \quad x\left(\frac{\gamma_L^P}{\gamma_L^d}\right)^{1/2}$$

Using this approach, a series of contact angle determinations were made on both "as received" AU-1 and AS-1 graphite fibers. The experimental method was equivalent to that developed by Drzal[80] and will not be expanded upon

here. Results are based on a minimum of 10 fiber measurements for each liquid. Five liquids were used in the analysis. A fiber diameter of 8 μm was assumed for all measurements.

The contact angle means and standard deviations for these samples are given in Table 8. Drzal's results[81] are included for comparison. The mean values obtained in our work are in quite good agreement. The larger standard deviations noted in our results are in large part due to our assumption of a uniform 8 μm fiber diameter on all samples. Drzal optically measured the diameter of each fiber tested.

Figure 6 shows the linear regression analysis plot used to determine the polar and dispersive components of the AS-1 and AU-1 fibers. Both the Ashland and Drzal data are included for comparative purposes. Both data sets are in very good agreement, and all four regressions have correlation coefficients of 0.95 or better. Based on these plots, Table 9 lists the surface free energy means for both AU-1 and AS-1 fibers. From our previous ESCA data, these surfaces differ less than 10 at.% in total oxygen. The sensitivity of the contact angle method is reflected by the 5-10 dyne/cm difference observed for the AS-1 and AU-1 polar components for this small variation in surface oxygen concentrations.

We have noted that both AU-1 and AS-1 fibers in distilled water and glycerol exhibit increases in force as a function of time of fiber immersion. In particular, AU-1 shows a substantial increase compared to the initial contact force before reaching equilibrium. This phenomenon is probably associated with the spreading pressure (π) of an adsorbed film of water or glycerol on the fiber surface. While values of π can be experimentally determined[82] little work has been done in this area for graphite surfaces.

TABLE 8

CONTACT ANGLES FOR GRAPHITE FIBER SURFACES

Liquid	Ashland		Drzal	
	AU-1	AS-1	AU	AS
Water	47 ± 7	29 ± 5	41 ± 4	29 ± 4
Glycerol	43 ± 11	21 ± 6	33 ± 7	25 ± 1
Bromonaphthalene	22 ± 3	22 ± 3	29 ± 3	26 ± 3
Polypropylene Glycol	17 ± 7	2 ± 2	3 ± 3	3 ± 3
n-Octane	12 ± 7	11 ± 8	---	---
n-Hexadecane	---	---	18 ± 8	22 ± 7

TABLE 9

POLAR AND DISPERSIVE COMPONENTS OF THE SURFACE FREE ENERGY OF AU-1 AND AS-1 GRAPHITE FIBERS

Fiber	Ashland		Drzal	
	γ^P	γ^d	γ^P	γ^d
AU-1	24.0*	25.3	27.0	26.7
AS-1	35.2	24.6	33.4	25.9

---

*All values in dynes/cm.
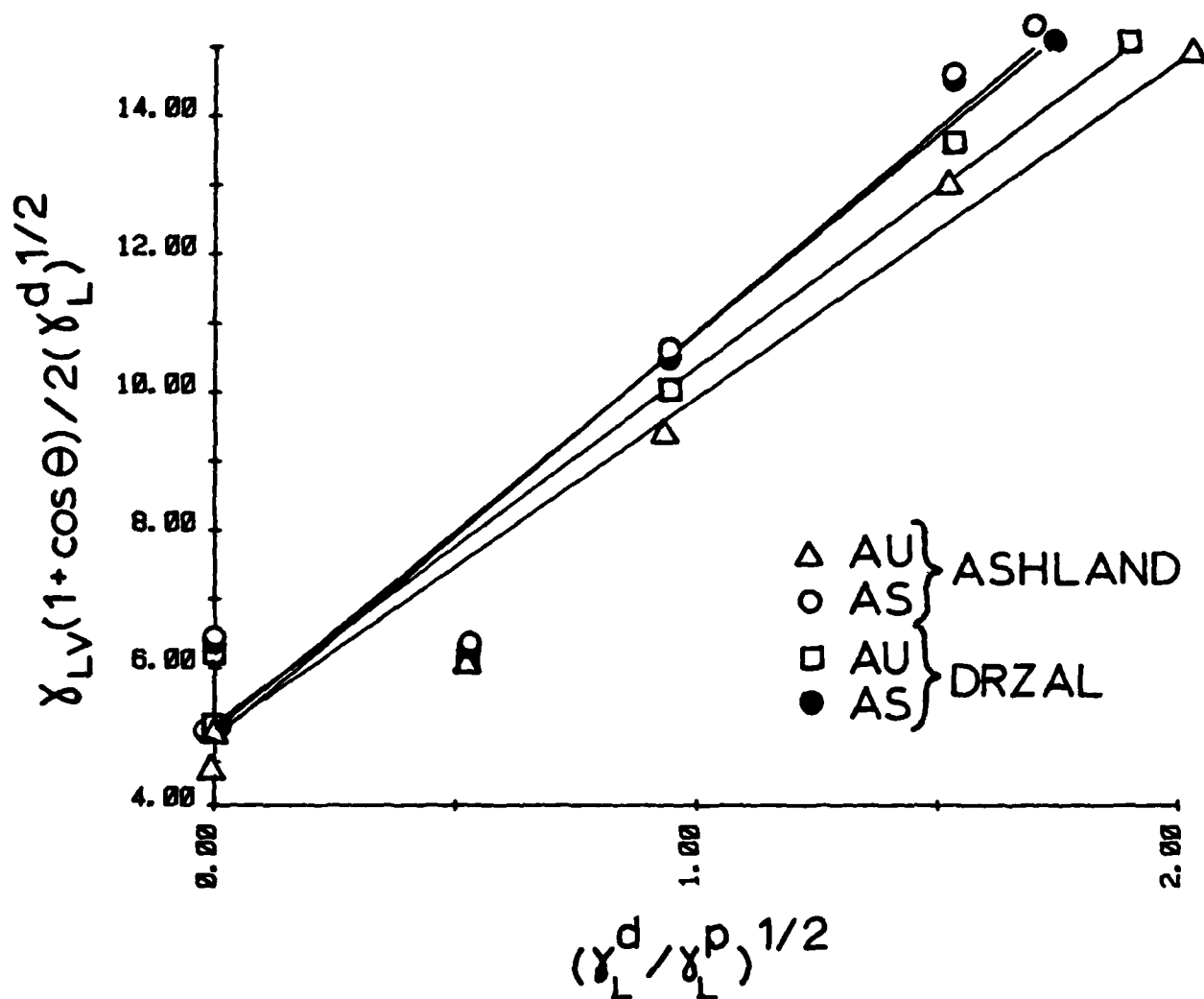
Figure 6. Linear Regression Plot for Determining Polar and Dispersion Components of AU and AS Graphite Fiber

42

The data listed in Tables 8 and 9 are based on measurements of the advancing contact angle only as a measure of the polar/dispersion components of the interfacial free energy. No attempt was made to measure the receding contact angle.

2.7.2   Liquid/Solid Resins

To determine the surface energetics of the final resin systems (MY720/DDS and CON-4; refer to Section 6.1 for resin details) surface tensions were run in air at room temperature on the liquid resin/solvent mixtures using a DuNuoy ring surface tensiometer. Obviously this is not indicative of the final cured solid resin surface free energy, but is more closely related to solution wetting of the fibers during the prepreg processing of the composites. Thus, the surface tension of the liquid system provides an estimate of the wetting behavior of the fiber/matrix combination during processing. To determine the resin solid surface free energy, the resins were dip-coated on 0.1 mm diameter Ni wire and cured according to the appropriate conditions for each resin. The micro-Wilhelmy method was then used to determine contact angles and the polar/dispersion components of the resin. Hence, the solid surface free energy provides a general measure of the solid resin/fiber interfacial free energy. Values for the resin systems are given in Table 10.

Clearly both resin/solvent systems satisfy the thermodynamic wetting criteria, with total surface free energies in excess of 15 dynes/cm lower than AU fiber and about 25 dynes/cm lower than AS fiber. From a work of adhesion standpoint, which is a measure of the interphase bonding, the relative

43

compatibility of the resin/fiber interface can be obtained. The work of
adhesion in our case is defined by:

$$W_{RF} = \gamma_R + \gamma_F - \gamma_{RF}$$

where the subscripts R and F refer to the resin and fiber respectively and
γ_R, γ_F, γ_{RF} represent the resin and fiber surface free energies and the
resin/fiber interfacial free energy. Fowkes[83] postulated that the
interfacial energy may be considered as a number of terms, each due to a
single type of intermolecular force:

$$\gamma = \gamma^{dispersion} + \gamma^{dipole} + \ldots$$

and then generally proposed that:

$$\gamma_{12} = \gamma_1 + \gamma_2 - 2\sqrt{\gamma_1^d \gamma_2^d} - 2\sqrt{\gamma_1^P \gamma_2^P} - \ldots$$

Using his expression for the interfacial free energy leads to total work of adhesion
values for CON-4/AS-1 interfaces of 87.7 dynes/cm and for MY720/DDS/AS-1
interfaces of 92.9 dynes/cm. The work of adhesion represents the
thermodynamic work required to part a unit area between the resin and fiber.
Consequently, the larger the work of adhesion, the stronger the interfacial
interaction. From our data the epoxy (MY720/DDS)/AS-1 interface exhibits
slightly stronger interfacial interaction which should translate into
comparatively better mechanical properties in the final composite. As will be

44

shown later in this report, the mechanical properties of the epoxy composite systems were generally higher.

TABLE 10

CONTACT ANGLES, SURFACE TENSION AND
POLAR/DISPERSION COMPONENTS OF COMPOSITE RESINS

A) Contact Angles

	Resin	
Liquid	MY720/DDS	CON-4
Water	72 ± 2	74 ± 1
Glycerol	64 ± 7	74 ± 2
Bromonapthalene	35 ± 4	27 ± 3
Polypropylene Glycol	20 ± 5	17 ± 6
n-Octane	23 ± 2	19 ± 2

B) Polar/Dispersion Components

	Surface Free Energy	
Resin	γ^p(dynes/cm)	γ^d (dynes/cm)
CON-4	10.0	25.6
MY720/DDS	11.0	29.1

C) Surface Tensions

Resin/Solvent Mixture	Surface Tension (dynes/cm)
CON-4/Acetone (60-65% solids)	35.5
MY720/DDS/Acetone (60-65% solids)	33.0

45

III. SELECTIVE OXIDATION AND DEVOLATILIZATION OF GRAPHITE FIBER SURFACES

3.1 Introduction

As was discussed earlier, one of the originally proposed surface treatment
approaches for selective modification of the surface chemistry of the graphite
fiber involved both oxidation and devolatilization of the fiber surface. The
objective of this approach was optimization of the concentration of surface
phenolic and alcoholic groups while minimizing surface carboxylic groups. The
use of selective surface oxidation techniques, followed by controlled partial
devolatilization of surface oxygenated functional groups, and by subsequent
hydrogen-capping (or other reaction to prevent oxygen pickup by unsatisfied
valences on the surface) was proposed as a means of providing this
optimization.

3.2 Devolatilization

The principal experimental apparatus for the devolatilization work on the
fiber consisted of a 4 ft. horizontal Lindberg furnace containing a 2 inch ID
quartz tube connected to both vacuum and gas handling equipment. This is
schematically shown in Figure 7. The system is configured for batchwise fiber
treatments. Exterior magnets are used to maintain fiber tension within the
tube. Devolatilization experiments using this system involved desorption of
AS-1 fiber at 600°C under vacuum followed by "capping" reactions with various
gases.

As required by the contract, the optimum surface treatment cannot
adversely affect the original mechanical properties of the fiber. In an
initial experiment to test this effect, a load of AS-1 fiber was treated at
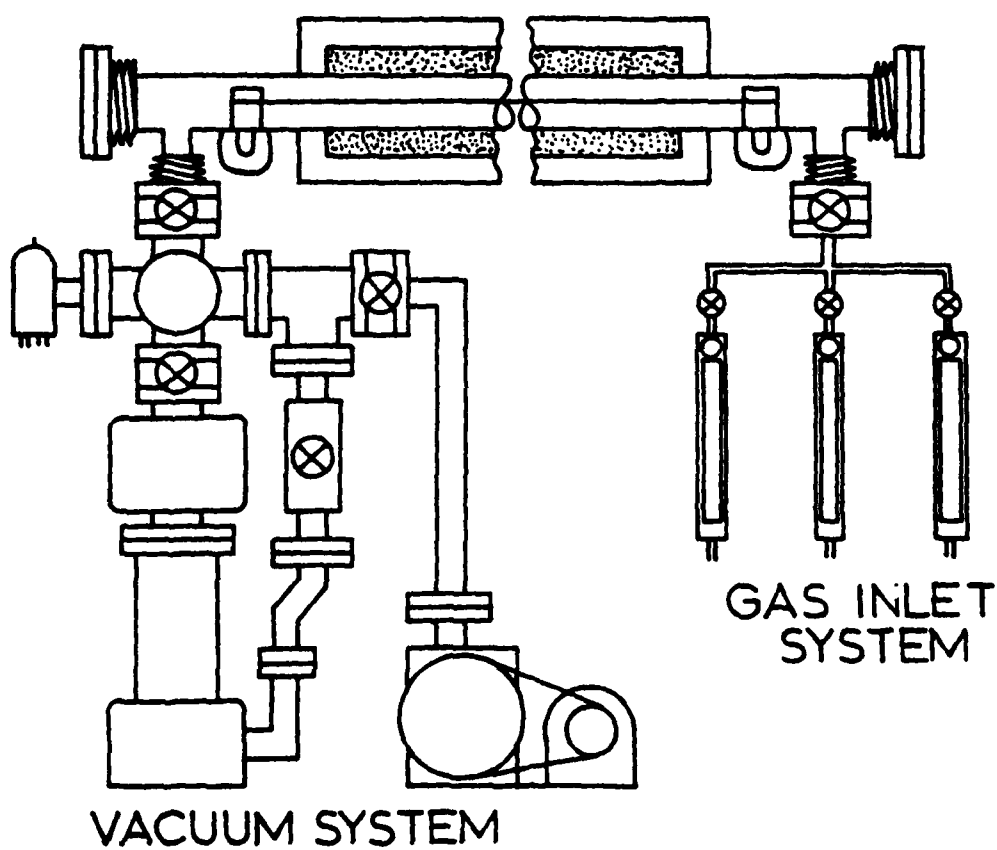
LINDBERG FURNACE/QUARTZ TUBE ASSEMBLY

GAS INLET
SYSTEM

VACUUM SYSTEM

Figure 7.   Schematic illustration of selective oxidation/devolatilization
furnace for surface modification of graphite fiber.

47

$600°C$ in a 1.5×10^{-7} torr vacuum for over 1 week (normal treatment at this stage is only a matter of hours). Following this step the furnace was cooled to ambient while still under vacuum, and molecular hydrogen was introduced in hopes of "capping" the free radials generated during the devolatilization process. Directly following removal from the furnace, a portion of the fibers were impregnated with Epon 815 for single strand tensile tests. Ten specimens of the treated fiber were compared to 8 control samples prepared at the same time. The average tensile strength and modulus of the treated samples were 2274 MPa ($330 \pm 29 \times 10^3$ psi) and 209 GPa ($30.28 \pm 0.69 \times 10^6$ psi) respectively. For the controls the values were 2687 MPa ($390 \pm 57 \times 10^3$ psi) and 206 GPa ($28.92 \pm 1.08 \times 10^6$ psi). While there does appear to be a slight decrease in the average for the treated fibers, the values overlap and cannot be considered significantly different. The batch-wise treated fibers were handled considerably more than the controls prior to pre-preg and this alone may be a significant factor in the results.

In addition, a series of experiments were run to optimize both the degree of surface oxidation and the efficiency of various capping reactions. Parallel experiments were conducted either under vacuum or argon blanketing in order to determine whether or not a hard vacuum was required for devolatilization. An argon atmosphere would be more desirable in the development of a continuous fiber treatment process. Reactions were carried out in air, nitrogen, hydrogen and oxygen as a function of temperature. XPS analyses were performed after each treatment using the University of Utah HP5950B ESCA system.

Elemental analyses for C, O, and N were obtained since these were the main elements suspected to vary as a result of these reactions. Other elements present, such as Na and S, were not included in the analyses.

48

Quantitative results are given in Table 11. The first two entries for AU-1 and AS-1 fiber are the average results for all our previous runs on the "as-received" fiber. The vacuum control was AS-1 fiber subjected to a 1×10^{-7} torr vacuum at ambient temperature for 6 hours, the normal time used in our devolatilization runs. 'Vac' refers to a 1×10^{-7} torr vacuum maintained at 600°C for 6 hours followed by the designated backfill gas at the temperature indicated. 'Ar' refers to atmospheric pressure argon maintained over the fiber at 600°C for 6 hours, again followed by the designated gas backfill at 600°C.

TABLE 11

ESCA RESULTS ON C, O, N ELEMENTAL CONCENTRATIONS FOR
VARIOUS DEVOLATILIZATION TREATMENTS ON AS-1 GRAPHITE FIBER

Fiber Treatment	Elemental Conc. (At %)		
	C	O	N
AU "As-Rec'd", Avg.	92.6 ± 2.3	4.7 ± 2.1	2.7 ± 0.8
AS "As-Rec'd", Avg.	83.0 ± 0.8	9.8 ± 0.8	6.6 ± 1.4
AS-1, Vacuum Control	82.9	12.0	5.1
AS-1, Vac - H_2 @ 600°C	81.4	13.7	4.9
AS-1, Ar - H_2 @ 600°C	83.4	14.5	2.1
AS-1, Vac - N_2 @ 600°C	76.9	19.8	3.2
AS-1, Ar - N_2 @ 600°C	82.0	15.2	2.8
AS-1, Vac - O_2 @ 390°C	84.5	12.0	3.5

From these data there appear to be no substantial changes in C, O, N surface concentrations as a result of the fiber treatment process, regardless of the backfill gas type. The oxygen levels are in fact higher than the average AS-1 fiber for all treatments. From the TGA and mass spectrometer work there is little doubt that material is removed from the surface at elevated temperature. The conclusion, therefore, is that the active sites created on the surface following devolatilization either do not specifically react with molecular H_2 or N_2, or that they recombine with oxygen (possibly through wall interactions) and are thus inactivated before the backfill gas was introduced in the system. In addition, the possibility exists for slow readsorption of atmospheric components during the 4-6 weeks before the ESCA analysis work was performed. Note that no protective atmosphere was provided during shipment of samples. Strongly physisorbed CO_2 or H_2O could lead to the observed results. It is also possible that not all of the oxidized surface region is removed within the time frame of our experiments. Regardless of a mechanism, we were unable to demonstrate that we either preferentially removed oxygen from the fiber surface or that we were successful in preventing oxygen re-adsorption or reaction with the devolatilized surface.

3.3 Oxidation

Experimental work on oxidation/devolatilization also included an investigation of the effects on graphite fiber surface functionality following exposure to the electrodeposition environment used in our fiber treatment process prior to resin pre-pregging. It was postulated that the surface might be oxidized by electrolysis in a triethylamine-water mixture similar to that used to dissolve the interphase resin. Fiber re-oxidation during the

electrodeposition process would directly affect the extent and type of surface modification used in pretreating the fiber prior to electrodeposition.

TABLE 12

ESCA RESULTS ON C, O, N ELEMENTAL CONCENTRATIONS FOR
VARIOUS TEA/H_2O TREATMENTS ON AS-1 GRAPHITE FIBER

Fiber Treatment	Elemental Conc. (AT %)		
	C	O	N
AU-1 - "As-Rec'd", Avg.	92.6 ± 2.3	4.7 ± 2.1	2.7 ± 0.8
AU-1 - TEA/H_2O	93.0	3.8	3.3
AS-1 - "As Rec'd", Avg.	83.0 ± 0.8	9.8 ± 0.8	6.6 ± 1.4
AS-1 - TEA/H_2O	87.3	8.3	4.3
Celion 6000 - "As Rec'd"	87.9	10.6	1.5
Celion 6000 - TEA/H_2O	89.2	8.6	2.2

Based on the data in this table, it does not appear, however, that the electrolytic treatment of the fiber under standard electrodeposition conditions leads to substantial changes in either the concentration or types of oxygen functionality on the surface.

Further work was done to determine the possibility of selectively oxidizing the fiber surface electrochemically. Because of the poor thermal oxidative stability of AS-1 fiber, it was hoped that electrochemical oxidation (as is probably commercially done) of the fiber would be a less destructive approach to surface modification. In addition, at the suggestion of Dr. L. T. Drzal (AFWAL/MLBM)[84] attempts were made to electrochemically reduce the surface by using the fiber as the cathode rather than the anode in solution.

Table 13
ELECTROCHEMICAL TREATMENT OF AS-1 FIBER

Run #	Fiber (a) Electrode	Electrolyte (b) Solution	Potential V.D.C. (c)	Current, Amps. Start	Current, Amps. End	Time In Cell, Sec. (d)	Observations
3802-93A	AU-Anode	1N-HNO$_3$	4 (max.)	0.75	0.75	30	
3802-93B	AS-Anode	1N-HNO$_3$	5.1(max.)	0.75	0.75	30	
3802-93C	Celion 6000-Anode	1N-HNO$_3$	5.2(max.)	0.75	0.75	30	
3893-86A	AS-Anode	1N-HNO$_3$	7.5(max.)	2.3	1.9	30	No inking, gas evolved at fiber
3893-86B	AS-Anode	1N-H$_2$SO$_4$	2.7(max.)	0.2	0.19	30	No ink; gas evolved at cathode and fiber
3893-36C	AS-Anode	0.05% Aq. AP	5.7	0.1	0.09	30	No ink; gas evolved at cathode
3893-86D	AS-Anode	0.05% Aq. AP	20	0.3	0.28	30	No ink; gas evolved at cathode
3893-86E	AS-Anode	1N KOH	5.7	1.69	1.4	30	Inking, gas evolved at cathode and fiber
3893-86F	AS-Anode	5% Aq. TEA	2.0	0.77.	0.72	30	No ink; gas evolved at cathode and fiber
3893-86G	AS-Anode	1N HNO$_3$	10.0	3.5	3.2	5	No ink
3893-88A	AS-Cathode	5% Aq. TEA	5.7	0.5	0.13	30	No ink; gas evolved at fiber
3893-88B	AS-Cathode	5% Aq. TEA	20.0	0.64	1.17	30	No ink; gas evolved at fiber and anode
3893-88C	AS-Cathode	1N H$_2$SO$_4$	5.7	1.25	1.65	30	No ink, sol. turned amber; gas at fiber
3893-88D	AS-Cathode	1N HNO$_3$	12.7	3.86	2.59	10	No ink, sol. turned amber; gas at fiber and anode
3893-88E	AS-Cathode	1H HNO$_3$	6.0	1.20	0.35	30	No ink, sol. turned amber; gas at anode
3893-88F	AS-Cathode	1N H$_2$SO$_4$	10.0	3.83	3.81	10	No ink, sol. turned amber; gas at fiber

(a) 316 stainless steel used for second electrode

(b) AP - Ammonium Persulfate; TEA - Triethylamine

(c) VIZ Model WP-705 D.C. Power Supply

(d) Tow was placed in cell; voltage applied for time shown; voltage turned off; specimen removed rinsed in deionized water and dried 18 hrs. r.t. and 2 hrs. 40°C (vac. 30 in. Hg.)

Electrolytes included nitric and sulfuric acids, ammonium persulfate, potassium hydroxide and triethylamine. The D.C. potentials applied ranged from 2.7 to 20 volts and the current from 100 ma to about 3.8 amps. Samples of the treated fiber were submitted for surface characterization by ESCA and SEM. The specific electrochemical treatments are shown in Table 13.

An interesting reaction was noted during the electrodeposition experiments. A dark cloudy liquid was always noted at the fiber/solution interface during the electrodeposition process in which a polymer was present in the electrolyte solution. We termed this "inking" and found it varied in degree with both electrodeposition resin type and electrodeposition conditions. We suspected the primary cause of "inking" was oxidation of the electrodeposition polymer during deposition. It is interesting to note, however, that the same "inking" behavior was exhibited in one case in a solution containing no polymer. Anodic oxidation in 1N KOH also showed "inking". This suggests that degradative attack of the fiber surface is occurring in this particular solution. SEM analysis of the surface showed a significant change in the number and depth of surface striations on this fiber. The mechanism behind this attack is unknown, but may be related to the presence of potassium. As was pointed out earlier in this report, thermal oxidation of graphite fibers is enhanced by the presence of Na and K in the fiber[77]. A similar enhancement may possibly occur with KOH in solution. With the exception of the KOH fiber, SEM analyses of the electrotreated samples showed little variation among the various treatments in terms of surface topography.

ESCA analysis of selected electrochemically-treated fibers showed significant variations in elemental concentrations and chemical functionalities on the surface. Table 14 lists the elemental concentrations

53

determined for several of the electrotreated series. Two main features are noted in these data. First, anodic oxidation of the fiber is generally independent of the electrolyte, with both acids and bases significantly increasing the oxygen content of the surface. Second, cathodic reduction of the fiber in either acid or base under various time and voltage/current conditions does not appear to significantly alter the fiber surface. In particular, oxygen concentrations do not show appreciable decrease under conditions comparable to the anodic oxidations. Note, however, that significant variability may be present. Compare, for example, results of the HNO_3-5 sec. vs. HNO_3-30 sec. treatments run at different times. Oxygen concentrations are significantly higher on the 5 sec. run. This may be a result of true treatment differences or incomplete rinsing following electrolytic oxidation. The nitrogen levels are comparable, however, suggesting that no residue differences are present on both fibers. Many repetitions would be required to determine the source of these variations and time did not permit further investigation in this area.

Thus, while we have shown substantial increases in surface oxygen via electrolytic methods, regardless of fiber treatment we have not been able to demonstrate any reduced level of oxygen on the AS-1 fiber surface beyond that exhibited by the 'as-received' fiber. Consequently, for our preliminary electrodeposition work, the decision was made to investigate the use of interphase resins on AS-1 fiber supplied without organic sizing and without any added surface modification.

In addition to the elemental analyses, the C-1s spectra of several of these samples were roughly deconvoluted as was previously done with the commercial graphite fibers. The results are shown in Figure 8. The predominant trend shown with all anodic oxidations is a significant increase

54

TABLE 14

ELEMENTAL CONCENTRATIONS ON FIBER SURFACES BY ESCA, AFTER VARIOUS ELECTROCHEMICAL TREATMENTS

Fiber Treatment (See Table 13)	Elemental Concentration (At %)				
	C	O	Na	S	N
AS-1 Fiber H_2SO_4 - 30 sec. Fiber as Anode	63.7	29.6	0.1	3.1	3.5
AS-1 Fiber $(NH_4)_2S_2O_8$ - 30 sec. Fiber as Anode	73.4	23.3	0.2	-	3.1
AS-1 Fiber KOH - 30 sec. Fiber as Anode	76.9	16.5	0.4	1.0	0.9 (K=4.3)
AS-1 Fiber HNO_3 - 5 sec. Fiber as Anode	72.9	23.8	0.2	-	3.1
AS-1 Fiber TEA - 30 sec. Fiber as Cathode	89.0	8.1	0.2	-	2.7
AS-1 Fiber H_2SO_4 - 30 sec. Fiber as Cathode	85.7	9.9	0.1	0.8	3.5
AS-1 Fiber HNO_3 - 10 sec. Fiber as Cathode	88.6	7.9	trace	-	3.5
AU-1 Fiber HNO_3 - 30 sec. Fiber as Anode	84.1	11.0	not scanned		4.9
AS-1 Fiber HNO_3 - 30 sec. Fiber as Anode	81.3	14.8	not scanned		3.9
Celion 6000 Fiber HNO_3 - 30 sec. Fiber as Anode	69.2	29.5	not scanned		1.3
AS-1 'As-Received'	83.0 ± 0.8	9.8 ± 0.8	not scanned		6.6 ± 1.4

in the more polar -COOH and quinone-like functionalities relative to the -COH surface species. Note that the cathodically reduced fibers show very little oxygen functionality at comparable scale factors. The latter spectra are very similar to 'as-received' AS-1.

In addition to the ESCA analyses on these surfaces, contact angles were measured for fiber electrolytically oxidized in 1N H_2SO_4 for 30 sec. Although treated identical to Run #3893-86B in Table 14, the fibers analyzed were not from the same treatment batch. Consequently some differences in total oxygen (as was seen for the HNO_3 treatments) may exist. Using the Wilhelmy technique described earlier in this report, the polar component (γ^p) of this fiber was 37.4 dynes/cm and the dispersion component 22.7 dynes/cm. The correlation coefficient for these data was 0.96. While the polar component is slightly higher than AS-1 'as-received' and the dispersion component slightly less, it is interesting that total surface free energy of this fiber (60.1 dynes/cm) is nearly identical to AS-1 commercial fiber (59.8 dynes/cm). Drzal[81] has proposed a linear relationship between total oxygen on the fiber surface and surface free energy.

As was done earlier for the thermally-treated AS-1, the tensile strength of the electrolytically-oxidized fibers was determined. Table 15 lists these results. No major differences in fiber strength were noted for either the standard electrodeposition treatment conditions or for the electrolytic oxidation process for the specific conditions indicated. These data are thus in keeping with the requirement of < 10% strength loss following fiber treatment.

From the ESCA data and contact angles determined for the H_2SO_4-treated fibers, we have shown that oxidation of graphite fibers above commercially-obtainable levels can be accomplished via electrochemical methods without a

56
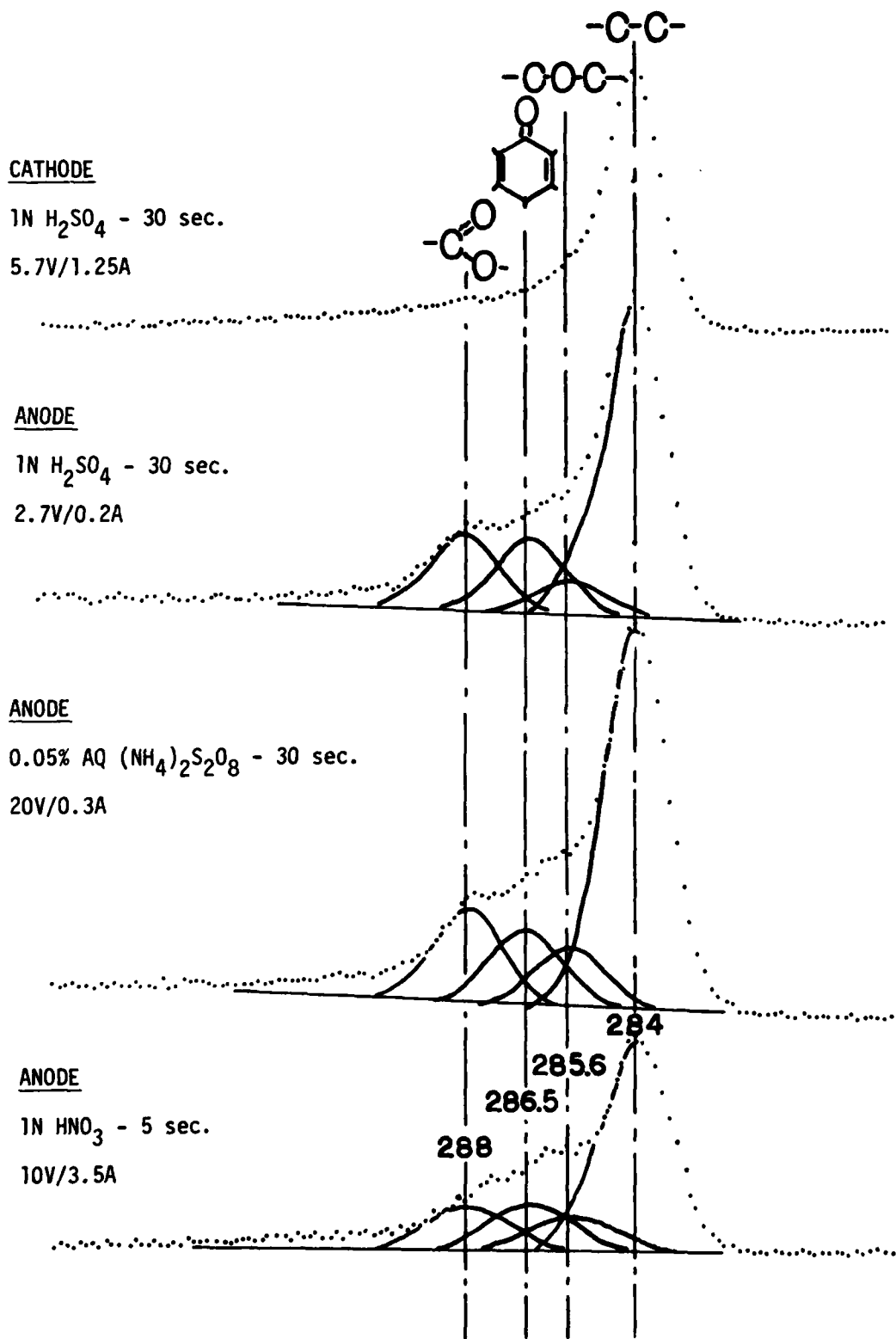
Figure 8. C-1S Regions from Various Electrotreatments (See Table 13 for Details). Charge-Referenced to Alkyl-like C-1S at 284 eV.

detectable loss in fiber tensile strength. Selective oxidation, i.e.
production of specific oxygen functional groups on the fiber surface, was not
demonstrated although there is a strong trend towards more polar
functionalities following the electrolytic treatment.

TABLE 15

EFFECT OF ELECTRODEPOSITION ENVIRONMENT ON FIBER

Fiber Type	Electrolyte	Volts	AMPS	Fiber Strength MPA	(KSI)	E.D. Polymer Pickup, % (1)
AS-1	None	-	-	2,551	(370±48)	2.7
AS-1	1% TEA	11.3-12.7	0.75	2,882	(418±24)	2.3
AS-1	1N HNO$_3$	3.5- 5.1	0.75	3,027	(439±26)	0.7
AU-1	None	-	-	2,923	(424±31)	0.5
AU-1	1% TEA	10.8-12.7	0.75	2,896	(420±43)	0.6
AU-1	1N HNO$_3$	3-4	0.75	2,875	(417±32)	1.7
C-6000	None	-	-	2,027	(294±22)	1.4
C-6000	1% TEA	15.1-16.6	0.75	2,413	(350)	1.2
C-6000	1N HNO$_3$	4.3- 5.2	0.75	2,372	(344±28)	1.1

(1) SMA/Aniline Amic Acid Polymer deposited on fiber polymer conc. = 2.5%;

pH = 9.1-9.3 (TEA); time = 30 sec.; D.C. volts = 5.7; Amps = 0.2.

IV. GRAPHITE FIBER SURFACE MODIFICATIONS VIA OLEFIN CYCLOADDITION REACTIONS

As . been discussed earlier, it would be very desirable to produce a graphite fiber surface essentially free of polar, oxygenated functional groups such as carboxylic acid and phenolic types. Even more desirable would be a fiber surface with very little (or no) oxygen, which was capable of forming a limited number of covalent bonds with the matrix resin.

Recently Mazur and coworkers[56,57] reported that carbon surfaces, freed of surface oxygen groups by high vacuum (10^{-5} torr) pyrolysis at 1020°C would, after cool down to 25°C in the absence of oxygen, undergo cycloaddition reactions when contacted with certain olefins. This reaction is shown schematically below with cyclopentadiene as an example.
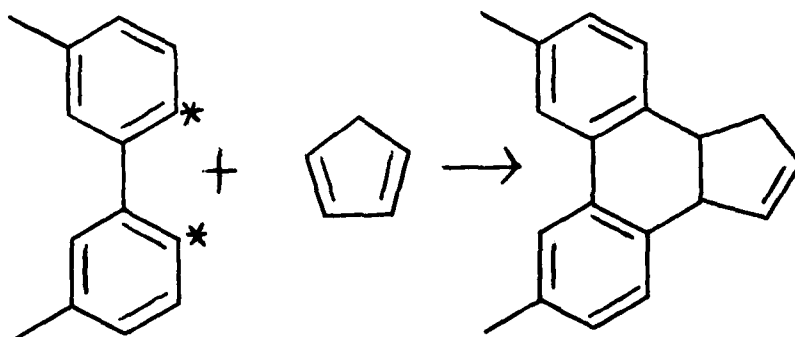
With this reaction scheme, it is possible that one double bond of cyclopentadiene could survive after cycloaddition and thus might be available for reaction (probably free radical type) with the matrix resin.

Mazur's data, however, showed that the cycloaddition reaction of cyclopentadiene with the devolatilized carbon surface (Union Carbide VYB carbon yarn with a BET surface area of $240m^2/gm$) was not quantitative, since oxygen was found to chemisorb in significant amounts on heat treated carbon surfaces previously reacted with cyclopentadiene. Other olefins, when used in

the cycloaddition reaction, appeared to be much more effective than cyclopentadiene in blocking subsequent oxygen uptake by the carbon surface.

The initial experiment for the cycloaddition work was again aimed at establishing the tensile strength of the fiber following high temperature treatment. The fiber tensile strength was tested following a 6 hour, 1050°C vacuum devolatilization at 10^{-7} torr. The results are given in Table 16. Again, no loss in tensile properties as a result of thermal treatment of the fiber was indicated.

For the initial cycloaddition run, following 1050°C devolatilization for 8 hrs. under vacuum (10^{-6} torr), the fiber was cooled to room temperature and vapor from a refluxing system of cyclopentadiene was introduced in the vacuum chamber. Approximately $\frac{1}{2}$ hour under these conditions produced a condensate on the inner surfaces of the quartz tube indicating near saturation. Following this reaction a portion of the fiber was directly analyzed via contact angle measurements. A second portion was Soxhlet extracted overnight in n-octane. A brown residue was noted in the Soxhlet thimble following extraction suggesting excess (non-bonded) cyclopentadiene on the fiber surface. Results are given in Table 17. As seen in the table, the polar component of the extracted fiber shows a significant increase relative to the unextracted data. This would be expected if excess cyclopentadiene had been removed. Note, however, that the value is still within the expected statistical range of AS-1 fiber. Since the cyclopentadiene reaction with the fiber surface is not stoichiometric, some residual oxygen should remain on the surface. The extracted fiber results support these observations.

Since unbonded excesses of cyclopentadiene were detected on the surface, subsequent experiments used controlled amounts (2 monolayers or less) introduced through a manometer metering system. In addition, allene was also introduced in the

60

TABLE 16

TENSILE STRENGTH OF VACUUM (10^{-7} TORR) DEVOLATILIZED
AS-1 FIBER AT 1050°C - 8 HR.

Fiber	Tensile Strength		Modulus	
	(MPa)	(KSI)	(GPa)	(MSI)
AS-1/As Received	2,972	(431 ± 26)	191	(27.73 ± .4)
AS-1/1050°C	2,896	(420 ± 37)	262	(38.02 ± .6)

TABLE 17

POLAR AND DISPERSION COMPONENTS OF AS-1 FIBER
FOLLOWING CYCLOADDITION REACTION WITH CYCLOPENTADIENE

Fiber	γ^p (dynes/cm)	γ^d (dynes/cm)
AU-1	24.0	25.3
AS-1	35.2	24.6
AS-1/Cyclopentadiene	5.0	32.0
AS-1/Cyclopentadiene, Octane Extracted	21.6	26.0

system following cyclopentadiene in hopes of 'capping' most of the active
sites (~ 40%) which remain following the cyclopentadiene reaction. Again,
attempts were made to introduce controlled amounts of allene into the reaction
chamber. Allene reportedly has an efficiency of about 85% for the
devolatilized graphite surface. This particular reaction (cyclopenta-
diene/allene) was carried through to composite testing since it was the only
case which suggested a lowering of the polar functionality on the surface.
Four batch wise treatments of approximately 70ft. to 80ft. of tow per run were
used in preparing the fiber for prepreg and composite fabrication. Testing of
these composites in described in Section 6.5.

Programmed temperature/mass spectrometer measurements were run on the cyclopentadiene/allene treated fiber using the method and equipment described earlier in this report. Figure 9 is a plot of the data from this experiment. The data are considerably different than either the AU or AS plots of Figure 4. The overwhelming majority of all evolved species is AMU-28 (CO or C_2H_2, etc.) with very little CO_2 exhibited at any temperature. Ncte also that considerable CH_4 are evolved between 400°-500°C. The CH_4 and H_2O evolution probably reflects devolatilization of either an allene or cyclopentadiene component, probably as a result of an incomplete reaction with the surface. We have no explanation for a strong water component in the 400°-500°C range. An alternative prospect could be NH_4, possibly a result of a strong interaction of the nitrogen species on the fiber surface with either of the dienes. This mechanism, however, is totally speculative.
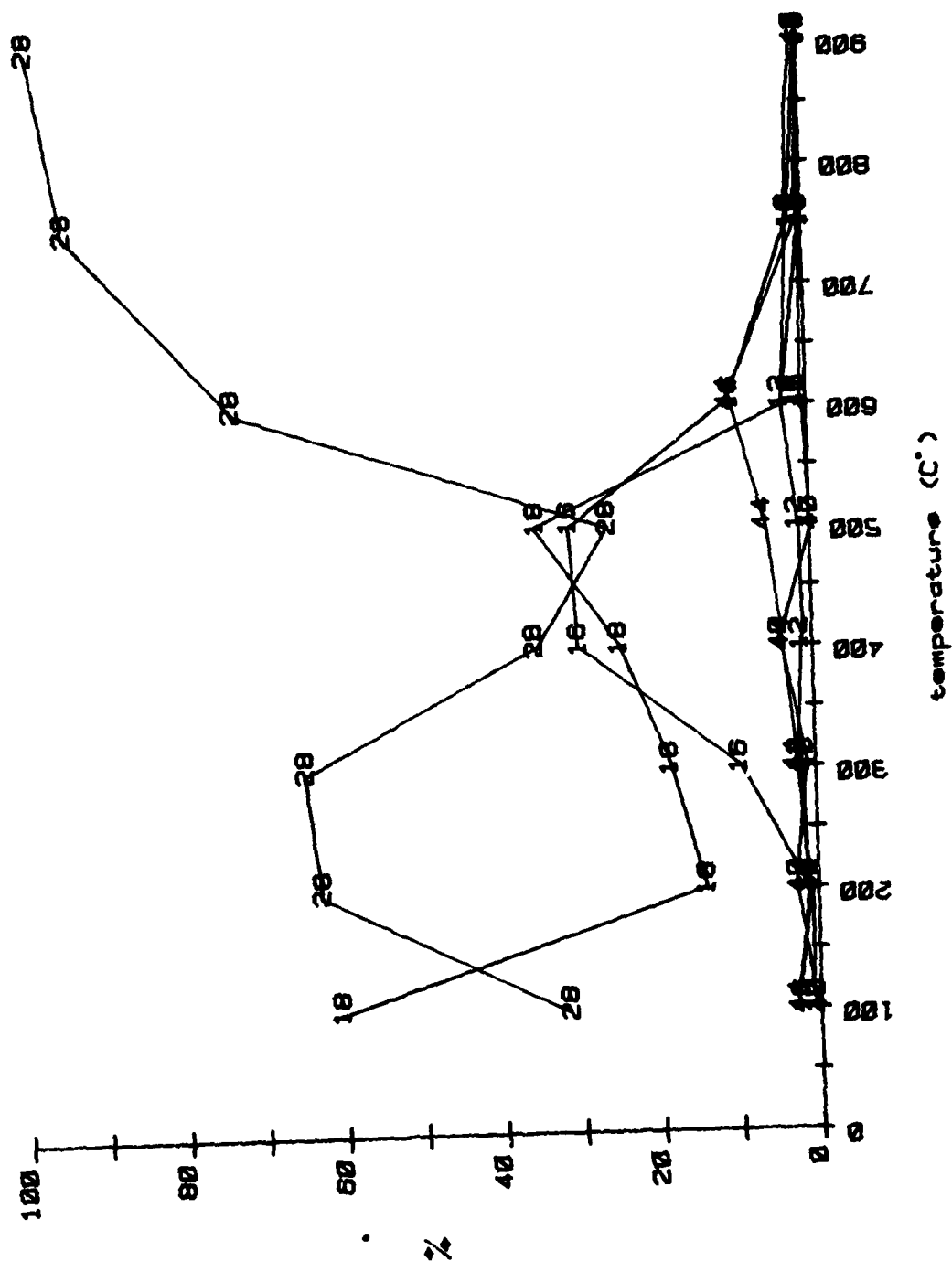
Figure 9   Thermal Devolatilization Mass Spec. Data for Cyclopentadiene/Allene-Treated AS-1 Fiber.
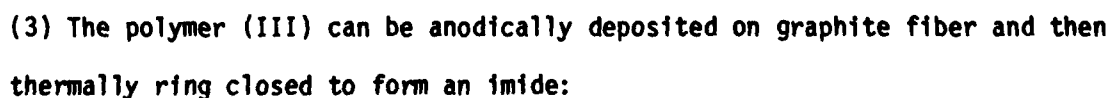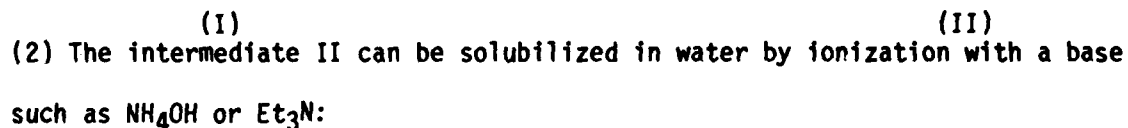
63

V. FIBER MODIFICATION BY ELECTRODEPOSITED INTERPHASE RESINS

5.1 Introduction

Electrodeposited coatings systems are widely used as primers to provide uniform, thin films that yield excellent adhesion and corrosion protection. Electrodeposited polymers have also been investigated as primer coatings for adhesive joints between metals[85]. Work reported by Subramanian, et. al.[20] has shown that mechanical properties of graphite fiber-epoxy composites can be improved by electrodepositing selected resins on the surface of the fibers to form an interphase layer between the fiber and matrix resin. Improvements in interlaminar shear, impact, and flexural strengths were observed. The polymers used in that work were maleic anhydride copolymers with styrene, methyl vinyl ether, and olefins. The maleic anhydride provided the functionality needed to solubilize the polymer in water, to provide for transport by an applied potential, and to react with epoxy matrix resins in the composite. Some of the deposited polymers were not easily washed from the fiber suggesting that they were bonded to the fiber during the electrodeposition process. In an investigation of hydrothermal aging effects, Kaelble, et. al.[86] applied a thin coating of a methyl vinyl ether/maleic anhydride copolymer to HTS graphite fiber from a methyl ethyl ketone solution. It was found that the presence of the moisture sensitive polymeric layer resulted in an increase in water gain during hydrothermal aging (100°C) in water, and a decrease in interlaminar shear strength in epoxy composites. The results were compared to those obtained with HTS fiber which had been heat treated for 120 minutes at 1030°C in a 90/10 hydrogen/nitrogen atmosphere to give a relatively low moisture sensitivity interface.

It was proposed for this program that interphase resins be developed that could be applied by the anodic electrodeposition process to achieve bonding to

the fiber, be convertible to a structure of low moisture sensitivity, and have pendant functional groups capable of forming moisture-resistant bonds with three matrix resins. Further, it was proposed that the resins be applied to fibers whose surface had been modified to minimize moisture sensitivity. The synthesis of the interphase resins was carried out under an independent Ashland-funded program. The basic chemistry of the resins is described below:

(1) reaction of a maleic anhydride copolymer (I) with selected amines to form an amic acid intermediate (II):

$$+ R'NH_2 \longrightarrow$$

(I)   (II)

(2) The intermediate II can be solubilized in water by ionization with a base such as NH_4OH or Et_3N:

$$(II) \quad + \quad Et_3N/_{H_2O} \longrightarrow$$

(III)

(3) The polymer (III) can be anodically deposited on graphite fiber and then thermally ring closed to form an imide:

$$(III) \longrightarrow$$

65

It was postulated that tne imide form would be relatively moisture insensitive, and depending on the choice of comonomer (R) could have a high Tg. Further, the R or R' groups could be selected to provide pendant olefinic, acetylenic, or phenolic functionality capable of reacting with HME, Thermid, PBBI, or epoxy matrix resins.

Early in the program two changes were made. The interphase resin compositions were modified by the addition of low levels of diamines to control the solubility of the resins. Also, as indicated in a previous section of this report, a decision was made to investigate the use of the interphase resins on AS-1 fiber supplied without organic sizing and without any added surface modification.

5.2 Interphase Resin Selection

Two maleic anhydride copolymers were selected as base materials, including a commercial styrene maleic anhydride copolymer obtained from ARCO Chemical Company (SMA-1000) and an experimental copolymer prepared from 2-allyl phenol. A large variety of primary, mono and diamines were reacted with the two copolymers to form amic acid intermediates. Table 18 lists many of the materials prepared for investigation. The aniline half-amide acid derivative of SMA-1000 and the corresponding imide were selected as "model compounds" for many experiments.

The intermediates and imidized polymers were characterized by acid number, solubility, infrared spectroscopy, and in selected cases by proton NMR and thermal analysis.

In general, proton NMR was found to be of limited use in characterizing the materials. Efforts to determine the mole ratio of reacted amine were not successful for the model system. Polymers prepared with 3-aminophenyl

66

Table 18
INTERPHASE RESINS

Anhydride Copolymer Type	AMINES Type(a)	Mole %	Product Acid No.	AMIC-ACID SOLUBILITY						IMIDE POLYMER(c)				
				AC	MEK	NMP	ETOH	HEP	H₂O(b)	AC	MEK	NMP	ETOH	HEP
SMA	AN	100	213	S	S	S	S	I	S	S	S	S	I	I
SMA	AN/MDA	94/6	232	S	S	S	S	I	S	P	P	P	I	I
SMA	AN/AA	80/20	267	S	P	S	S	I	S	S	S	S	I	I
SMA	AN/AA/MDA	74/20/6	-	P	I	S	P	I	S	I	I	I	I	I
SMA	AN/AA/DDA-S	74/20/6	235	P	P	S	S	I	P	P	P	P	P	I
SMA	p-CAN	100	-	S	P	S	S	I	S	S	S	S	I	I
SMA	p-HAN/MDA	92/8	255	P	S	S	S	I	S	P	P	P	I	I
SMA	AN/3APA/MDA	73/20/7	227	S	S	S	S	I	S	I	I	I	P	I
AP/MAN	AN/AA	80/20	261	S	P	S	S	I	S	S	S	S	I	I
AP/MAN	AN/AA/DDS	75/20/5	233	S	S	S	S	I	S	P	P	P	I	I
AP/MAN	AN/AA/MDA	75/20/5	-	S	S	S	S	I	S	P	P	P	P	I
AP/MAN	AN/DDS	96/4	229	S	S	S	S	I	P	S	S	S	I	I
AP/MAN	AN/MDA	92/8	229	S	S	S	S	I	S	I	I	I	I	I
AP/MAN	AN/3APA/DDS	75/20/5	227	S	S	S	S	I	S	P	P	P	P	I
AP/MAN	AMDAPA/MDA	75/20/5	264	S	S	S	S	I	S	P	P	P	P	I

(a) AN = aniline; MDA = methylene dianiline; AA = allylamine; DDS = diaminodiphenyl sulfone; p-CAN = p-chloro aniline; pHAN = p-hydroxy aniline; 3APA = 3-aminophenyl acetylene

(b) pH adjusted to 8-10 with triethylamine

(c) Amic acid polymers converted to imides by heat

67

acetylene (3APA) and aniline (AN) could not be quantitatively analyzed by proton NMR because the acetylenic proton overlaps with the resonances of the polymer backbone protons.

Proton exchange with deuterated solvent was observed with polymers made with the 3APA and allylamine. In theory, this latter composition can be determined by proton NMR, however, it was not possible with this sample because of the appearance of broad resonance signals of unknown origin in the allylic region. It was found that the allylic resonances became prominent after the addition of deuterium oxide to the sample solution. It appears that there were molecular associations which were disrupted by D_2O. This spectrum did qualitatively establish that the allyl amine had been incorporated in the derivative.

Infrared (IR) spectra have been of particular use in preparing and characterizing the polymers. The disappearance of absorption bands for anhydride (1850 cm^{-1} and 1780 cm^{-1}), the formation of free acid functionality from opening the anhydride ring (free acid hydroxyl at 3500-2500 cm^{-1} and position of acid carbonyl at 1710 cm^{-1}), along with formation of secondary amide (1500 cm^{-1}) were observed. Low levels of anhydride were suspected in most products (1850 cm^{-1} and 1780 cm^{-1}). The presence of some unreacted anhydride was also suggested by acid numbers in excess of theory.

IR absorption spectra for the aniline half-amide acid and converted imide (by heating 1 minute at 300°C) are shown in Figs. 10 & 11, respectively. These spectra are typical of ones obtained on each polymer. The formation of the imide was followed by the disappearance of the amide band and formation of carbonyl bands characteristic of the imide structure.

Thermal analytical procedures (thermogravimetric analysis) coupled with IR analysis indicated that the amic acid derivatives thermally ring close to
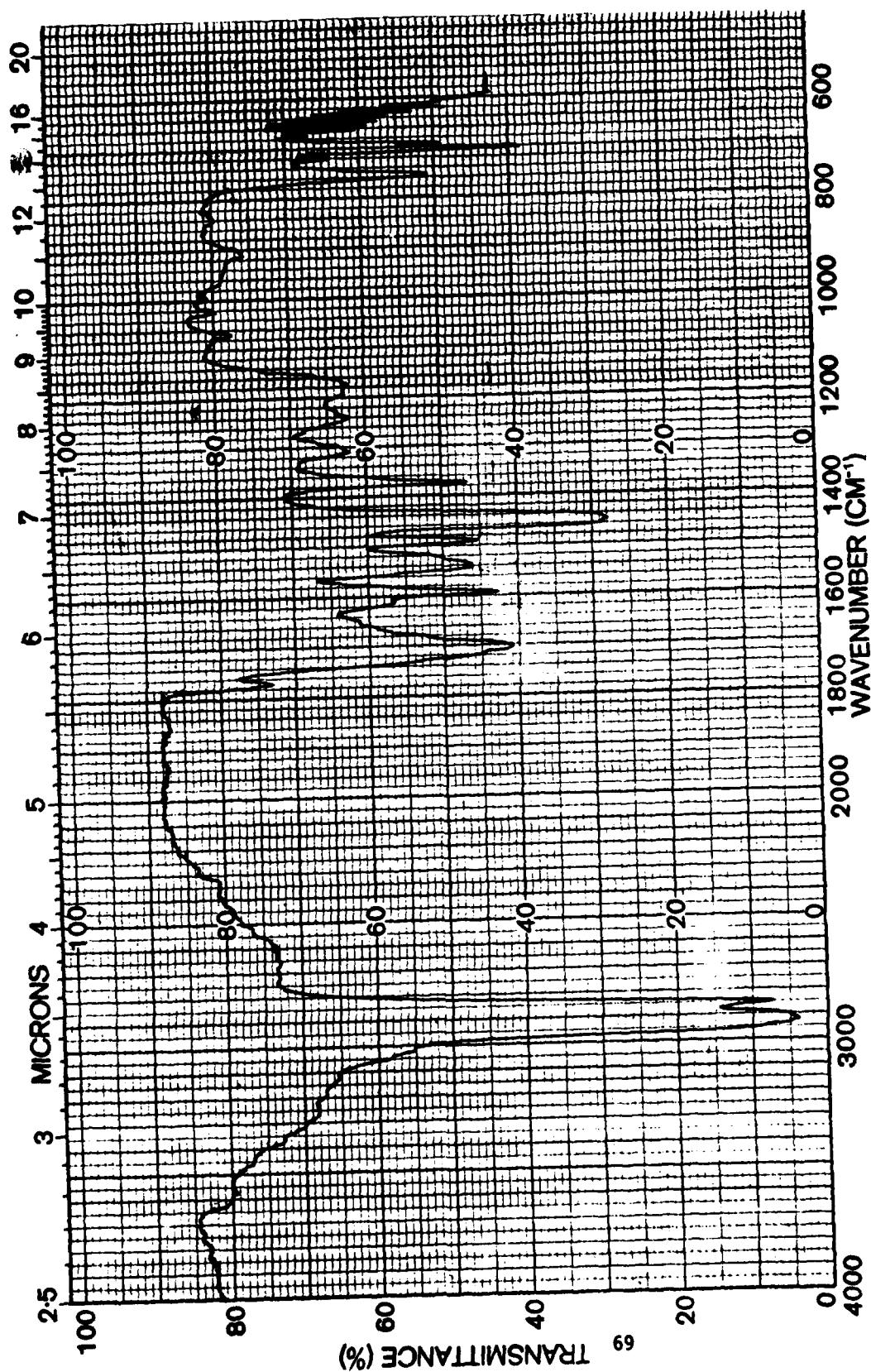
68

Figure 10 IR Spectra for SMA:AN Amic Acid Interphase Polymer.
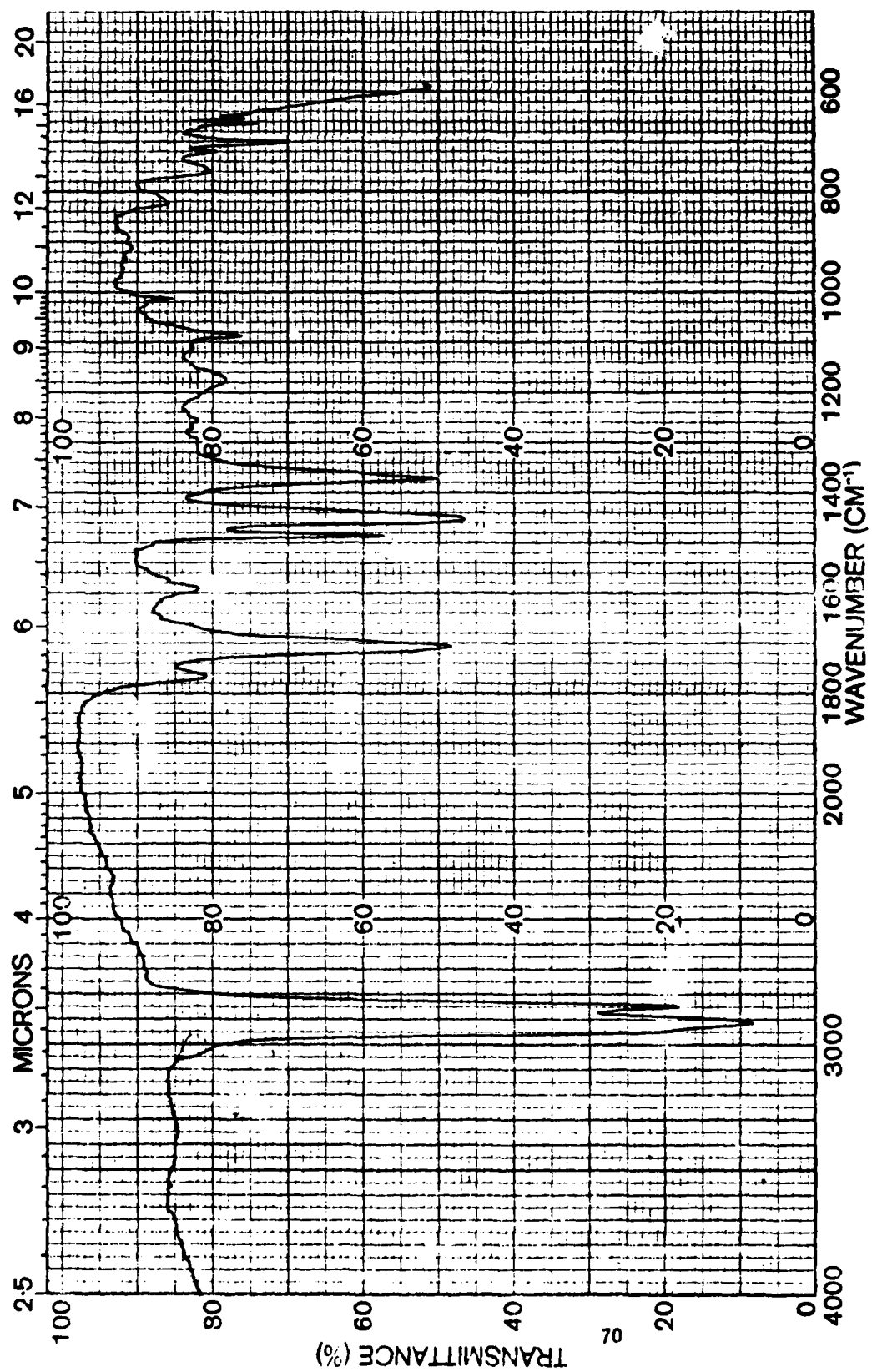
69

Figure 11   IR Spectra for Imidized SMA:AN Interphase Polymer.

form imide structures when heated above 200°C. The rate is highest (2 minutes) at 300°C. Both programmed and isothermal TGA tests were run under N_2 on the model system. The results as shown in Table 19 suggest that some decomposition occurs in addition to the loss of water which would account for ~ 6% weight loss. Because of the relatively slow heating rate compared to that used in practice to convert the material to the imide structure, no further TGA work was done.

TABLE 19

TGA DATA ON AMIC ACID POLYMER

Programmed Run, 10°C/min.		Isothermal	
Temperature, °C	% wt. Loss	Temperature, °C	% wt. Loss
75	4	200	24
175	17	250	31
395	75	-	-
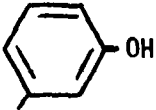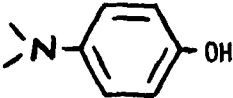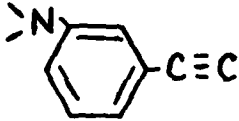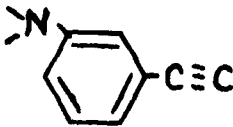
The solubilities of the amic acids were determined in several solvents and in a water-triethylamine mixture (pH 8-10). With two exceptions, all the amic acid polymers prepared were soluble in the aqueous media. The amic-acid derivatives were heated for 2 minutes at 300°C to cyclodehydrate the polymer to form the corresponding imide. The solubilities were determined in several common solvents.

The primary purpose was to determine if the polymers would be removed from the fiber during the preparation of prepreg by solution techniques. As indicated in Table 18, the use of a low level of a diamine MDA or DDS significantly reduced the solubility of the imide resin, thus permitting the

71

use of solution impregnation techniques. It is believed that the low
solubility of the resins also help reduce the tendency for them to be
dissolved in matrix resins.

Based on solubility characteristics, functionality, availability, and ease of
preparation, 7 polymers were selected for screening as shown in Table 20.

TABLE 20

INTERPHASE RESIN/MATRIX RESIN MATCH-UPS

Interphase Resin	Functional Groups	Matrix Resin
SMA-AN	None	CON-4
SMA-AN/MDA	None	CON-4
SMA-AN/AA/MDA	$-CH_2-CH=CH_2$	CON-4
AP/MAN-AN/MDA	OH	Epoxy
SMA-HAN/MDA	$>N$—⬡—OH	Epoxy
AP/MAN-AN/APA/DDS	$>N$—⬡—$C\equiv C$	Thermid 600
SMA-AN/APA/MDA	$>N$—⬡—$C\equiv C$	Thermid 600

5.3   Electrodeposition of Resins - Batch Process

Preliminary experiments were run to determine conditions (current, potential, time solution concentration, pH, etc.) that would be required to electrodeposit the amic acid copolymers on AS-1 fiber. A coating weight of about 1-2% was set as an objective. Short lengths of tow (4-inches) were suspended as the anode in a small cell. Stainless steel cathodes were placed on opposite sides of the tow. A low voltage regulated D.C. power supply was used to provide the potential. Initially, the polymer solutions were made with the SMA:AN amic acid polymer solubilized in water by the addition of ammonium hydroxide (pH=8.5). It was found that the polymer was easily deposited under mild conditions. Weight gains of about 3 percent were measured on specimens after only 15 seconds at 200 ma. using a 2.5 percent solution. Investigations on the chemistry of ring closure by thermal methods carried out under the Ashland program indicated that triethylamine (TEA) is preferred over ammonium hydroxide to solubilize the resins. The electrodeposition conditions were then explored using the TEA salt of the aniline half-amide of SMA-1000 as a 2.5% solution in water (pH-8.8). The resin was deposited using a voltage of 5.7 v.D.C., at a current of .2 amps. Time of deposition was varied from 10 to 30 seconds. After deposition, the strands were washed with water or a solution of TEA in water and then dried. The results are summarized in Table 21.

As expected, the TEA/H_2O rinse was more effective than water for removing unbonded resin. Because extended soaking in the 1% TEA solution did not remove the resin, it appeared that the resin was bound by grafting. However, in subsequent experiments it was found that the deposited amic-acid polymer could be quantitatively extracted by using a stronger TEA solution (5%) than used originally to solubilize the polymer. Also, it was found in later work

TABLE 21

EFFECT OF ELECTRODEPOSITION CONDITIONS - BATCH PROCESS

Deposition Time, sec.	Water rinse, wt % pick up	TEA/water Rinse, wt % pick up	TEA/water Rinse Soak wt %pick up, after hrs. 17 hrs.	41 hrs.	65 hrs.
10	2.7	1.5	1.73	-	-
20	8.3	2.4	-	3.4	-
30	14.6	4.8	-	-	4.5

that the imide form of the SMA:AN polymer could be extracted from the fiber with an organic solvent. Although that extraction also appeared quantitative by weight measurement, it does not preclude the possibility that a very thin layer of interphase resin remains on the fiber surface. Another series of batch experiments included the deposition of other interphase polymer compositions including the mixed amic acid derivatives of SMA-1000 and the 2-allyl phenol/maleic anhydride AP/MAN copolymer. The various polymers gave some variations in pick-up under the same deposition conditions. However, pick-up weights in the range of 1 percent could be obtained with most systems using a solution concentration of 2.5 percent, and a deposition time of 10 seconds at 5.7 v. DC and 200 ma.

In addition to establishing preliminary conditions for electrodeposition, the batch work was expanded to include the investigation of related parameters. To investigate possible effects of the fiber surface chemistry, the aniline and aniline/allylamine derivatives of SMA-1000 were deposited on Hercules AU-1 and AS-1, and Celion 6000 fibers. The fibers represent three levels of surface oxygen. The polymers were deposited using a voltage of

5.7v. and current of about 200 ma. for 10-30 seconds. Following deposition, the fibers were rinsed for 10 sec. in a 5% TEA solution, 10 seconds in deionized water, then dried 1 min. at 110°C. It was found that the AU-1 and Celion 6000 fibers both had lower resin weight gains than the AS-1 under the same conditions. The AU-1 was particularly low with a weight gain of only 0.5 percent after 30 seconds compared to 1.4% for the Celion and 2.7% for the AS-1.

Experimental work on this task also included an investigation of the effects of exposure to electrodeposition environment upon the surface functionality of graphite fiber. It was postulated that the surface could be oxidized by electrolysis in a triethylamine-water mixture similar to that used to dissolve the interphase resins. For comparative purposes, fibers were also exposed to electrolysis in an oxidizing medium ($1N$ HNO_3). Hercules AU-1, AS-1 and Celion 6000 graphite fibers were treated. Voltage was varied to maintain a constant current density. To detect changes in fiber strength properties, single strand tensile strength measurements were made on treated fiber. To detect possible changes in the surface chemistry of the fiber, a polymer was electrodeposited on the fiber. To characterize further possible changes in surface chemistry, the fibers were examined by ESCA. The ESCA results are give in Table 22. As shown in the table, the TEA/H_2O electrotreatment did not significantly alter the elemental surface concentrations compared to the 'as received' fibers. We have not, however, done the detailed ESCA comparisons on changes in the functional group chemistry in the C-1s spectra, which requires high resolution (monochromatic Al K_α X-ray source techniques). It is suspected that few differences would be found. The HNO_3 electrolysis of the fibers, on the other hand, resulted in large increases in surface oxygen concentrations, particularly in AU-1 and Celion 6000 fibers. Note that nitrogen did not exhibit the same relative increase as oxygen, and that AS-1

75

exhibits a much smaller relative increase in oxygen compared to AU and Celion 6000. The mechanism behind these differences in oxygen uptake has yet to be explained, but oxygen functionality which exists on AS-1 prior to further electrolytic oxidation may lead to this effect, as could the substantial difference in the local surface morphology of this fiber relative to AU-1 and Celion 6000.

TABLE 22

ESCA RESULTS ON C,O,N ELEMENTAL CONCENTRATIONS
AFTER
VARIOUS ELECTROTREATMENTS ON AS-1 GRAPHITE FIBER

Fiber Treatment	Elemental Conc. (At %)		
	C	O	N
AU-1 'As Rec'd.' Avg..	92.6 ± 2.3	4.7 ± 2.1	2.7 ± 0.8
AU - TEA/H_2O	93.0	3.8	3.3
AU - 1N HNO_3	84.1	11.0	4.9
AS-1 - 'As Rec.d.' Avg.	83.0 ± 0.8	9.8 ± 0.8	6.6 ± 1.4
AS - TEA/H_2O	87.3	8.3	4.3
AS - 1N HNO_3	81.3	14.8	3.9
Celion 6000 - 'As Rec'd'	87.9	10.6	1.5
Celion 6000 - TEA/H_2O	89.2	8.6	2.2
Celion 6000 - 1N HNO_3	69.2	29.5	1.3

As shown in Table 23, the strength of the fibers was not degraded by the electrochemical treatment in either triethylamine or nitric acid solutions. Electrochemical treatment in the triethylamine solution did not appear to affect the level of pick-up of resin. However, the resin pickup appears to

76

increase for AU-1 and decrease for AS-1 and Celion 6000 after prior treatment in nitric acid solution.

TABLE 23

EFFECT OF ELECTRODEPOSITION ENVIRONMENT ON FIBER

Fiber Type	Electrolyte	Volts	Amps	Fiber Strength		E.D. Polymer Pick-up, %
				MPa	(KSI)	
AS-1	None	-	-	2550	(370 ± 48)	2.7
AS-1	1% TEA	11.3-12.7	0.75	2882	(418 ± 24)	2.3
AS-1	1 N. HNO$_3$	3.5- 5.1	0.75	3027	(439 ± 26)	0.7
AU-1	None	-	-	2923	(424 ± 31)	0.5
AU-1	1% TEA	10.8-12.7	0.75	2896	(420 ± 43)	0.6
AU-1	1 N. HNO$_3$	3-4	0.75	2875	(417 ± 32)	1.7
C-6000	None	-	-	2027	(294 ± 22)	1.4
C-6000	1% TEA	15.1-16.6	0.75	2413	(350)	1.2
C-6000	1 N HNO$_3$	4.3- 5.2	0.75	2372	(344 ± 28)	1.1

SMA/Aniline amic acid polymer deposited on fiber, polymer conc. = 2.5%; pH-9.1-9.3 (TEA); time=30 sec.; D.C. volts=5.7; Amps = 0.2.

In one series of experiments, ammonium persulfate was added to the electrodeposition bath in an effort to promote grafting of the polymer to the fiber. A large increase was observed in the amount of polymer deposited (6.5% compared to 2.7%). However, the deposited polymer was removed by 19 hours soaking in a 5% TEA solution. Although grafting does not appear to occur to any appreciable extent during electrodeposition, it was postulated that bonding to the fiber could result during the imidization step. In one experiment the aniline derivative of SMA-1000 was deposited on AS-1 fiber and

77

was thermally ring closed by heating 3 minutes at 300°C. The resin pick-up after imidization was 0.9%. One specimen was then extracted with acetone for several days. Gravimetric analysis showed that most if not all the resin was extracted, indicating that the polymer was not grafted to the fiber. This does not account for the possibility of a monolayer.

SEM analysis of an SMA 1000 (styrene/maleic anhydride) copolymer, electrodeposited on AS-1 graphite fiber as the amine salt, showed a relatively smooth, uniform coating which appeared to completely cover the fiber and bridged several fibers in some areas of the tow. Rinsing the fiber in a 5% TEA solution for 10 sec., however, proved very destructive to this smooth integral film. As shown in Figure 12A, the rinsed fiber coating is very rough and uneven on the fiber surface. Clearly areas of the film have been essentially completely removed as a result of the TEA rinse, suggesting at this level of detection no bonding of the interphase resin to the fiber surface.

Effort was made to reduce the pickup during electrodeposition, by varying conditions, so that a washing step would not be required. Reducing voltage, current, time and batch concentration all helped to reduce polymer pickup. The lowest level of pickup (2.2%) was still above the desired level of 1%. However, based on these results, initial work on determining conditions for continuous electrodeposition was done using a polymer concentration of 1%. The current used (~ 100 ma.) corresponds to $4.48A/m^2$.

5.4 Electrodeposition of Interphase Resins - Continuous Process

A treating line was constructed for the continuous electrodeposition of interphase resins on graphite fiber tow. The basic features of the line are shown in Figure 13. The tow was pulled through the bath and then through an

Figure 12A.

Electrodeposited, Washed AS-1 Fiber,
0.6 wt.% Pick-up (8.3 KX)

Figure 12B

Electrodeposited, 7.3 wt.% Pick-up (3.37 KX)

Figure 12C.

Electrodeposited, 4.6 wt.%
Pick-up (2.45 KX)

Figure 12D.
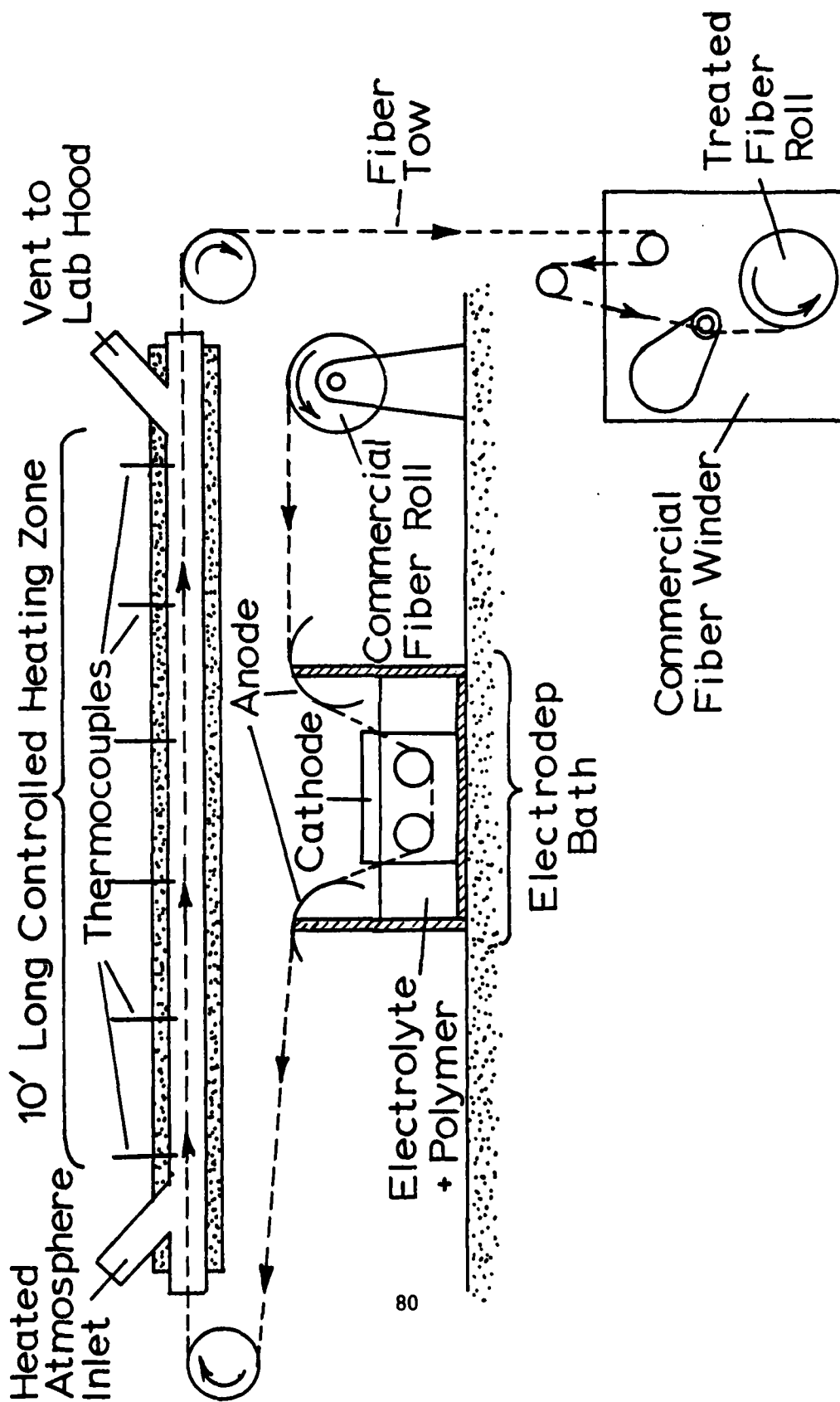
Electrodeposited, 1.3 wt.%
Pick-up (8.28 KX)

Figure 13   Schematic Illustration of Continuous Electrodeposition System

80

electrically heated tube having a controlled temperature gradient. The
temperature at the inlet was maintained at ~ 100°C to start drying the coated
fiber. The inlet zone was followed by a transition zone, a 4-foot zone controlled
at 300°C, and a short transition zone at the exit. The fiber speed (2 ft./min.) was
maintained by a Bouligny 503 re-winding machine. Residence time in the
electrodeposition bath was about 17 seconds. As shown in Figure 13 electrical
contact with the fiber was maintained by passing it over stainless steel
plates at each end of the bath. Stainless steel cathodes were placed on each
side of the fiber. The bath was circulated by means of a magnetic stirrer.

Initial trial runs were made using the aniline amic acid derivative of
SMA-1000 (1% in TEA/H$_2$O). Attempts were made to develop a current pickup
curve by measuring weight/unit length changes. However, the results were not
reproducible because of the variation in the weight/unit length of the base
fiber. Specimens cut from the coated fibers were examined by SEM.

The sequence illustrated in Figs. 12B, C, and D is representative of the
topography of the coatings produced by the continuous electrodeposition system
for various pickup levels. In 12B, representing the heaviest (7.3 wt%) level
of pickup, a pattern is seen similar to that exhibited for the sized Celion
6000 fiber of Figures 1C and D. The high, ridged areas represent broken
interfiber bridges. Note that even at this level the underlying fiber
striations are often reproduced, indicating that the resin intimately
replicates the surface. At 4.6 wt% (Fig. 12C) little difference is noted in
most areas compared to 12B. At 1.3 wt%, however, which is in the targeted
pickup range, some question exists as to coverage, as illustrated in Fig.
12D. It should be noted that in all samples, regardless of the pickup, areas
such as those shown in Fig. 12D were common. The p-chloraniline (CAN)
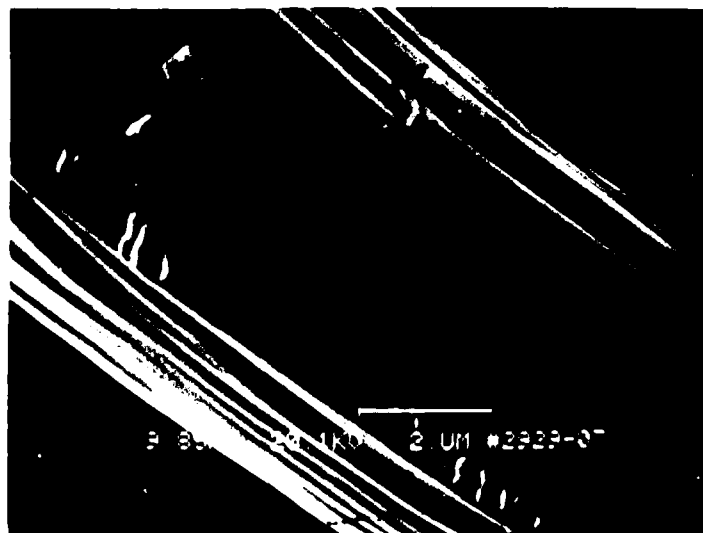interphase polymer was prepared and electrodeposited in hopes of mapping the

81

Figure 14A

Electrodeposited CAN Resin on AS-1 Fiber,
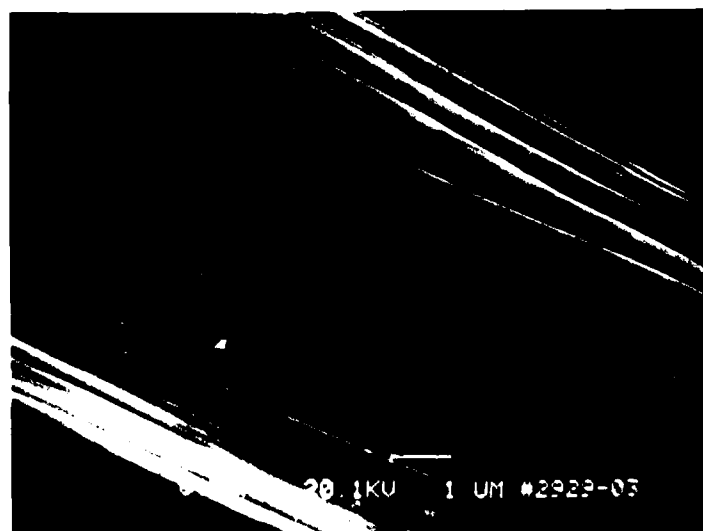Cl Observed in EDAX Scan (9.85 KX)

Figure 14B

Same Tow as in A, Different Region
Shows no Cl in EDAX Scan (8.56 KX)

Cl levels on the fiber surface via SEM/X-ray fluorescence (EDAX). Figs. 14A and 14B show the CAN electrodeposited surface at 1.8 wt% pickup. EDAX of 14A, with an obvious coating shows a strong chlorine signal. Fig. 14B, however, shows no chlorine over an equivalent accumulation of 100,000 K counts. We conclude from these analyses that at low levels of deposition there is a strong possibility of heterogeneous and/or spotty resin distribution on the fiber surface. There is an outside possibility that the Cl concentrations are below the EDAX detection limits. However, higher pickup levels were targeted in initial runs in hopes of insuring full coverage of the individual fiber surface.

Another series of experiments were run on the continuous electro-deposition line to determine the effect of current density on resin pickup using AS-1 fiber and the aniline half amide derivative of SMA-1000 as the interphase resin. The current, measured at the power supply, was varied from 0.1 to 0.3 ampere by changing the amine-water mixture and the fiber was processed at a rate of 2 ft./min. Although there was some variability in the weight per unit length of the untreated fiber which affects the calculated pickup level, the results clearly demonstrated the expected trend of increasing weight gain with increasing current.

Specimens cut from untreated and coated fibers were also examined by SEM. At all current levels, variability in the overall resin pickup was noted. Areas of high pickup, particularly between fibers, were observed as well as areas on individual fibers where coverage is questionable. Even at the highest current levels (corresponding to the highest pickup levels) there were fiber surfaces which visually do not appear to be covered. It is possible, however, that several undetectable monolayers may exist on the surface. Further increases in current density generally lead to greater resin bridging between fibers rather than increased coating on individual fibers.

83

Since the coating weights were in the desired range at 0.3mA and SEM observations showed a reasonably homogeneous coating, this value was selected for the initial preparation of fiber for evaluation. This value (0.3mA) corresponds to a calculated current density of $5.3A/m^2$ based on a 7-inch immersion length, a fiber weight of 0.2422 gm/ft., and a fiber surface area of $0.4m^2/gm$.

Because of the difficulties experienced in determining weight pickup by weight/unit length measurements, attention was given to developing an extraction method. It was found that a procedure often used to determine the resin contents of laminates worked quite well; that is, digestion of the resin with hot sulfuric acid followed by the addition of hydrogen peroxide. The acid digestion method was used during the rest of the program.

During some initial runs under the selected conditions, it was observed that there was a slight drift in the polymer solution conductivity with time. Adjustments in voltage were made to compensate for that change. In an effort to minimize that drift, and possibly improve the penetration of the solution into the middle of the tow, a pre-wet bath containing the interphase resin solution was inserted in the treating line ahead of the electrodeposition bath. This addition might also reduce the amount of material removed from the E.D. bath during a run. The results indicated that the pre-wet bath did improve the stability of the electrodeposition bath and it was included as a part of the treating line.

Table 24 summarizes the runs made to prepare coated fiber for evaluation. In most runs 360-400 ft. of fiber was coated. This was sufficient fiber to prepare 8.3 feet of 6" wide prepreg tape. Resin pickup measurements made at the start and finish of the run showed only a small decrease in deposition with time. The current was held constant by

84

controlling the voltage. Small increases in voltage were required. Occasional cleaning of the anode contact plates was also required.

TABLE 24

CONTINUOUS ELECTRODEPOSITION ON AS-1 FIBER

Interphase Resin*	No. of runs	Voltage D.C.	Current Amps	Resin Pickup, %
SMA:AN	3	17.9-18.5	0.30	1.3-2.3
SMA:AN	1	12.4	0.20	1.1
SMA:AN	1	6.1	0.10	0.4
SMA:AN	1	0	0	0.8
SMA:AN/MDA	1	13-15	0.20	0.9
SMA:AN/AA/MDA	2	17.6-24	0.30	1.5-2.7
SMA:AN/AA/MDA	8	12-16	0.20	0.8-1.0
SMA:PHAN/MDA	2	13-14	0.20	0.9-1.0
SMA:3APA/MDA	1	19.3	0.30	1.8
SMA:3APA/MDA	1	13.2-14.8	0.20	0.9
AP/MAN:AN/MDA	1	21	0.30	2.9
AP/MAN:AN/MDA	1	22-26	0.25	2.3
AP/MAN:AN/MDA	1	18.5	0.20	1.7
AP/MAN:AN/MDA	3	12.3-15.1	0.15	1.2-1.5
AP/MAN:AN/MDA	7	5.8-9.1	0.10	0.5-1.0
AP/MAN:AN/3APA/MDA	1	18-22	0.30	2.1

*Interphase resin solution concentration = 1%; Fiber rate = 2 ft./min.

Specimens cut from the coated fiber were examined by SEM. Areas of resin bridging and densely covered fibers were observed in most cases. There did appear to be a distinct difference between the SMA/AN resin and the resins containing MDA (methylene dianiline). The former coatings appeared less uniform and more segregated into the bridging areas between fibers. Many fractures were noted in the SMA/AN systems. In contrast, those systems containing MDA seemed to show much smoother, more uniform coatings with less fracture. This may reflect the fact that the molecular weight of the SMA/AN polymers is lower, and that the film-forming quality of the electrodeposited polymers requires a higher molecular weight such as offered by MDA additions.

The tensile strength of tow coated with an interphase resin (SMA:AN) was found to be 3675 MPA (533 ± 17 ksi) compared to 3620 MPA (525 ± 27 ksi) for AS-1 tow from the same lot. The modulus was also not affected with values of 227 GPA (32 ± 10^6 psi) and 214 GPA (31 ± 9 x 10^{-6} psi) for the control. Contact angle measurements were done on the SMA:AN electrodeposited fiber in order to determine the surface free energy of this electrodeposition resin. The polar component (γ^p) was 26.6 dynes/cm and the dispersion component (γ^d) was 14.0 dynes/cm.

VI. COMPOSITES

6.1 Introduction

It was originally proposed that the surface modified fibers would be evaluated in composites utilizing HME-350, PBBI, and Thermid 600[R] as matrix resins. However, at the request of the project officer the HME-350 was replaced late in the program by CON-4 and the PBBI by an epoxy resin. The CON-4 resin is prepared by chain extending a carboxy terminated polybutadiene (C-1000) with a diepoxide (See Appendix A). The resulting structure has pendant vinyl unsaturation which may be crosslinked by a free-radial mechanism. The highly unsaturated CON-4 polymer can also react with unsaturation present on the reinforcing fiber such as that associated with the allylic functional electrodeposited interphase resin. The epoxy resin formulation selected was the tetraglycidylether of p'p'-diaminodiphenyl methane (Ciba Geigy MY-720) cured with 36 phr diaminodiphenyl sulfone (Ciba-Eporal). The Thermid 600, an acetylene terminated polyimide resin, was purchased from Gulf Oil Chemicals Co. Both the LR-600 (a pre-imidized form of Thermid 600 dissolved in NMP) and AL-600 (an alcohol soluble type) were used.

6.2 Prepreg Preparation

Prepreg tape 6-12" wide were prepared by conventional drum winding techniques from solutions of the resins. The fiber was passed through a dip bath of resin and wound onto a 32" drum and collimated to form a sheet. Tension on the fiber was maintained at 150-200 gm. during winding. The resin solids in the dip bath were adjusted to give a pickup on the fiber of 38-42% by weight. The prepreg tape, supported by a backing sheet (generally Mylar) was

87

removed after partial drying from the drum and cut into convenient lengths to be dried in an air circulating oven or vacuum oven at elevated temperatures (80-110°C). After drying, the prepreg was placed in polyethylene bags sealed, and stored in a freezer until use.

6.3 Molding of Panels

Panels were molded from the CON-4 and epoxy resin prepregs using vacuum bag-autoclave curing techniques employing Mini-Clave (Tetrahedron Associates, Inc.) equipment. Typical molding conditions for these systems are given in Appendix A. The time-temperature cure cycle profiles were controlled with a Micricon Process Control System (Research Inc.). Panels made from the Thermid 600 resin were compression molded.

Considerable effort was made to prepare quality panels having the desired fiber volume fraction (60%), low void contents, and uniform fiber distribution. Considerable difficulty with cracking was experienced with the CON-4 type resins. Longitudinal cracks such as shown in Figure 15 developed during molding. High fiber volume fractions emphasized the problem. However, it was found that the cracking could be nearly eliminated by reducing the transverse panel dimension from 6 inches to 3 or 4 inches as shown in Figure 16. We believe that the high shrinkage of the resin (exhibited in clear castings made for density measurements), combined with rather weak interfacial strength as exhibited by interlaminar shear strength measurements, caused the crack problem. Variations in resin flow out during molding were also a problem. The flow behavior was influenced by the surface treatment used.

Difficulty was experienced in preparing low void content panels using the epoxy matrix resin. As shown in Figure 17, interply voids were the primary problem. These voids are associated with the residual solvent, methyl ethyl
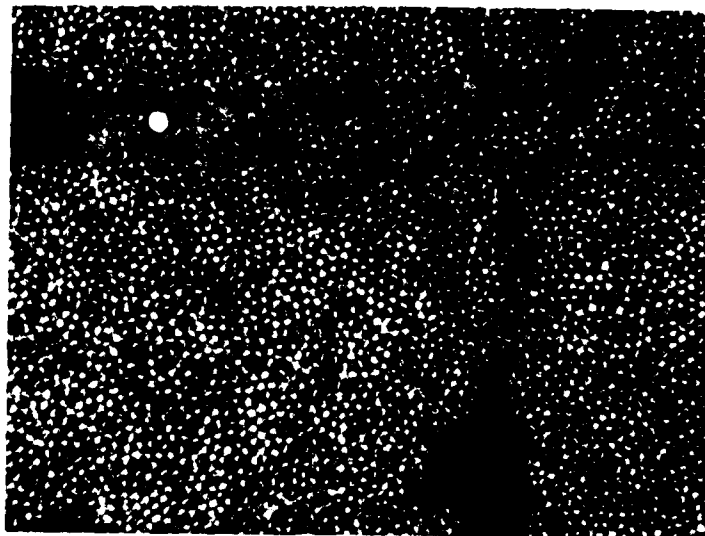
Figure 15.

Cracking in a 10 Ply CON-4/AS-1 6" x 6" Panel,
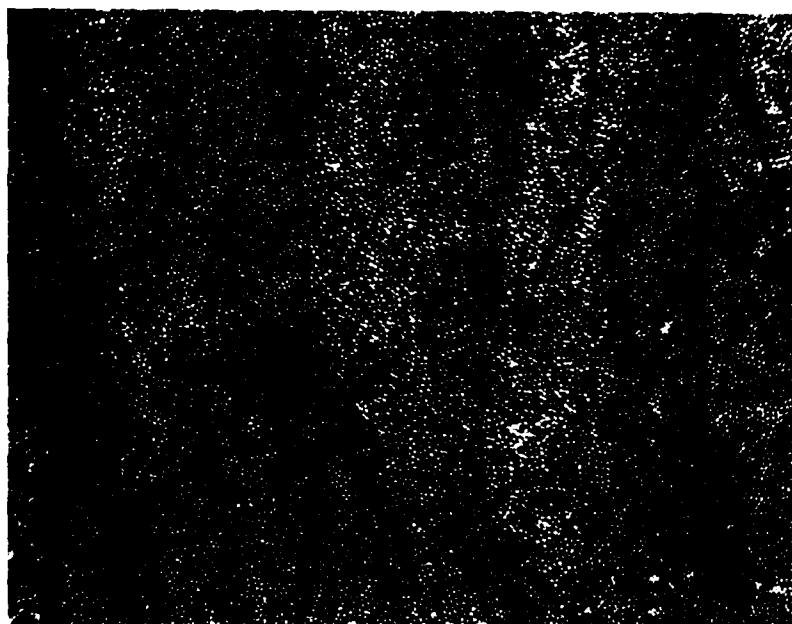Fiber Content is 62.9% (100X).

Figure 16.

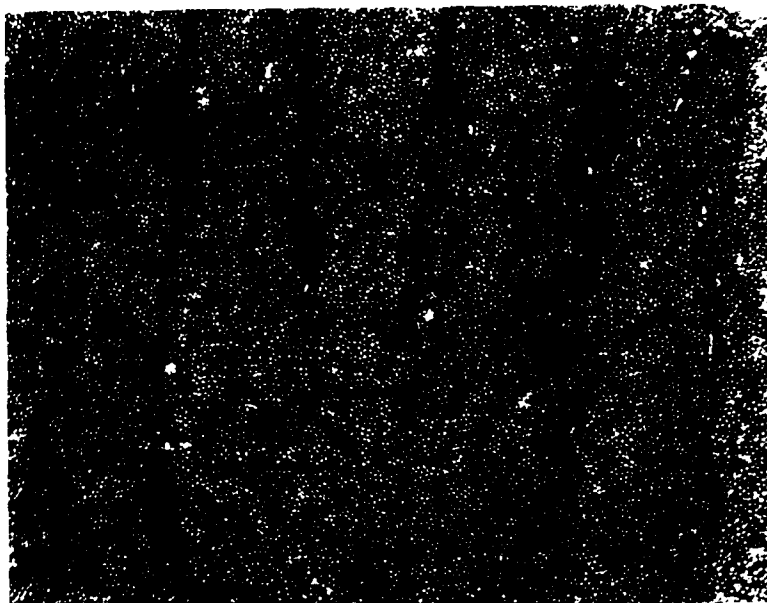Absence of Cracking in a 10 Ply CON-4/AS-1 3" x 6" Panel (75X).

89

Figure 17.

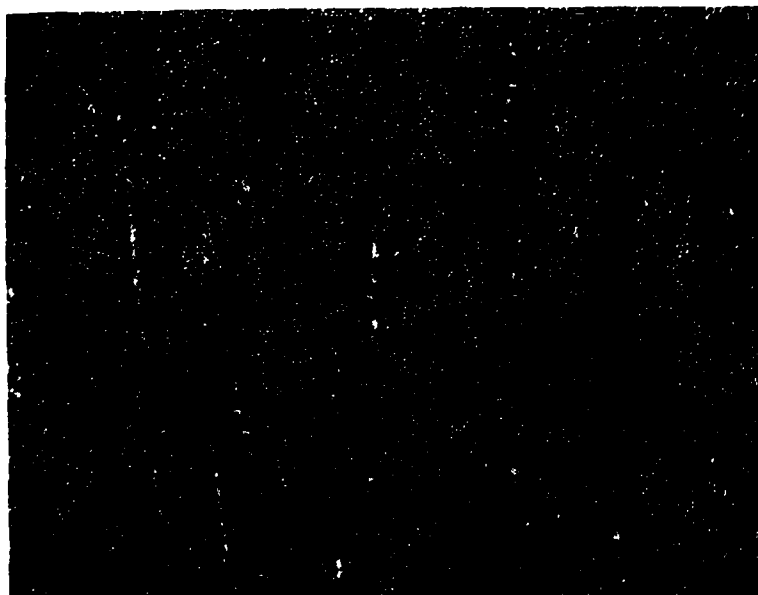Interply Voids in Epoxy/AS-1 Composite Cross-Section (75X).

Figure 18.

Reduced Void Content in Epoxy/AS-1 Composite by
Varying Drying of the Prepreg (75X)

90
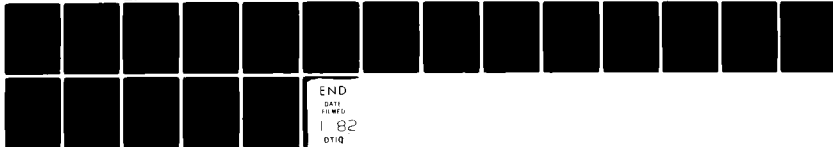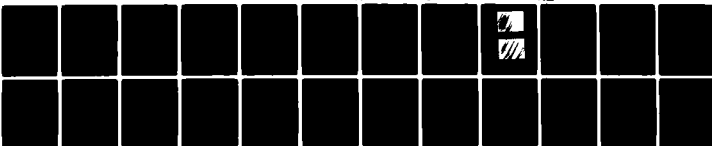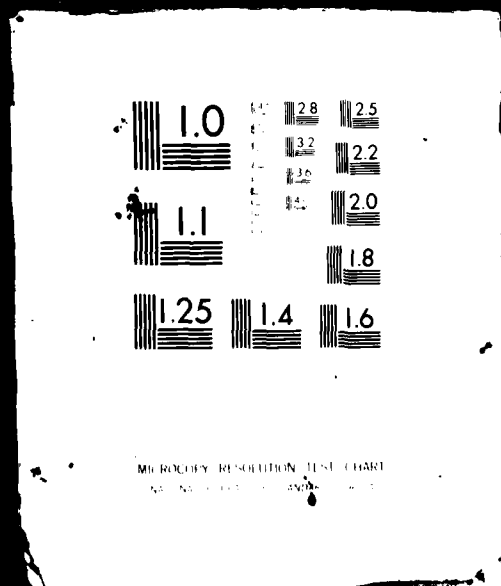
ketone (MEK), trapped in the prepreg. It was found that the voids often could be reduced by air circulating drying followed by a secondary drying of the prepreg in a vacuum oven (Figure 18). To help minimize the moisture sensitivity of the epoxy resin system, no accelerator such as BF_3MEA was used. However, the lack of an accelerator is believed to have caused variations in gel time, affecting resin flow out.

We were not successful in preparing satisfactory panels from Thermid 600. Attempts were made with both the LR-600 and AL-600 versions. Hydroquinone and phenolic modified resins were also tried. The prepregs made ranged from extremely boardy and non-tacky to loose individual tows. The panels made from the best prepregs were not useful because of high void contents. Arrangements were made through the project officer to have the treated fiber prepreged and molded at the University of Dayton Research Institute. They were able to prepare prepreg and moldings. However, one molding cracked during post cure and the others had excessive voids.

6.4 Composite Testing of Electrocoated Fibers

6.4.1 Initial Systems - Hydrothermal Aging Effects on ILSS

It was proposed that the modified fibers would be screened for hydrothermal aging effects using a new "H pull" shear test being developed in the Ashland laboratories. The test requires only a few feet of tow which would permit rapid screening as well as multiple specimens for statistical control. Initial test results obtained on composites made with AS-1 fiber and a bisphenol-A type epoxy matrix resin cured with Eporal were promising in that hydrothermal effects were observed. However, efforts to employ the test in this program were not successful. Changes in room temperature properties as a result of hydrothermal aging were not observed, while changes in elevated

temperature properties after aging were masked by the effects of elevated temperature. Because of those difficulties, that test was abandoned in favor of an interlaminar shear strength test (ILSS). The test employed was a 4-point load, bending test using a span to depth ratio of 16:1 as recommended by the project officer[87]. Four test conditions were used to evaluate the effects of hydrothermal aging:

1) Specimens stored over Drierite[R] and tested at room temperature (R.T.).

2) Specimens stored over Drierite[R] and tested at elevated temperature (E.T.).

3) Specimens immersed in 71°C (160°F) water for about 30 days and tested at R.T.

4) Specimens immersed in 71°C (160°F) water for about 30 days and tested at E.T.

The elevated temperature tests were run at 93°C (200°F) for the CON-4V based composites and 121°C (250°F) for the epoxy composites.

Magnamite AS-1 fiber was treated by the electrodeposition of the seven interphase resins described in the previous section (Table 20). Prepreg was prepared from untreated and coated fibers using the CON-4D, CON-4V, epoxy, and Thermid 600 resins. Ten ply, 0° panels were molded. It should be noted that adjustments in prepreg and molding procedures and conditions were necessary with each material system to compensate for changes in resin flow resulting

92

from the surface treatments. Per ply thickness in the composites varied between systems because of variations in the strand integrity which in turn affected the spread of the tow as it was collimated in the drum. It is believed that many of the effects observed were related to variations in the resin distribution in the prepreg from system to system. As previously indicated, the surface energetics were altered by the presence and type of interphase resin, and likely affected the tow wettability and saturation.

6.4.1.1. CON-4 Matrix

Shear strengths obtained by the 4-point beam test for the CON-4V composites are summarized in Table 25. The value for the control panel, 49.4 MPa, is in the range expected for the CON-4 system based on data reported by the AFML. The deposition of an interphase resin on the fiber resulted in some decrease in the room temperature strength under dry conditions. A reduction in the room temperature strength was observed in each system after hydrothermal aging. Moisture gain was also somewhat higher for the composites made with the coated fiber. The shear strengths (dry specimens) were reduced in most cases at elevated temperature (93°C).

The decrease was significantly greater for the specimens tested at 93°C after hydrothermal aging. The data do not reveal any improvement in hydrothermal aging resulting from the use of an interphase resin.

6.4.1.2 Epoxy Matrix

Shear strengths for the epoxy based composites are summarized in Table 26. It was observed that the moisture gain for the epoxy system during hydrothermal aging is higher than that measured for the CON-4 materials; in fact, the values are higher than expected[88]. It is believed that the high

93

TABLE 25

SHEAR STRENGTH OF CON-4V COMPOSITES

System No.	2	6	5	4
Interphase Resin				
Type	None	SMA:AN/MDA	SMA:AN/AA/MDA	SMA:AN/AA/MDA
Level, %	0	0.85	0.84	1.5
Fiber Volume, %	65-66	67	65	58
Exposure Time, $\sqrt{Hrs.}$	29.4	29.4	29.4	29.4
Weight Gain, %	0.47	1.1	0.73	1.7
Shear Strength, MPa (KSI)				
R.T. Dry	49.4 (7.2)	34.2 (5.0)	48.3 (7.1)	36.2 (5.3)
R.T. Wet	32.0 (4.6)	26.6 (3.9)	33.7 (4.8)	20.8 (3.0)
E.T. Dry	42.7 (6.2)	37.1 (5.4)	36.1 (5.2)	27.6 (4.0)
E.T. Wet	21.6 (3.1)	22.3 (3.2)	19.9 (2.9)	15.0 (2.2)

TABLE 26

SHEAR STRENGTH OF EPOXY COMPOSITES

System No.	3	8	7	9
Interphase Resin				
Type	None	AP/MAN:AN/MDA	AP/MAN:AN/MDA	SMA:PHAN/MDA
Level, %	0	0.74	1.7	1.0
Fiber Volume, %	67-69	68-71	65	63
Exposure Time, $\sqrt{Hrs.}$	29.4	31	29.4	29.4
Weight Gain, %	2.6	2.4-3.3	3.1	3.1
Shear Strength, MPa (KSI)				
R.T. Dry	45.3 (6.6)	44.8 (6.5)	41.3 (6.0)	44.8 (6.5)
R.T. Wet	41.6 (6.0)	37.9 (5.5)	38.8 (5.6)	39.7 (5.8)
E.T. Dry	39.3 (5.7)	32.4 (4.7)	35.2 (5.1)	36.2 (5.3)
E.T. Wet	27.6 (4.0)	24.1 (3.5)	25.9 (3.8)	25.7 (3.7)

values were related to the relatively high (2-3%) void content of the panels as can be observed in Fig. 17. The voids were minimized but not entirely removed from some panels by vacuum drying the prepreg suggesting that the voids were related to residual solvent. The high void content is also reflected in the relatively low interlaminar shear strength values (45.3mPa) for the dry specimens tested at room temperature. A comparision of the data obtained on the four systems evaluated under the four test conditions does not reveal any significant differences relating to the use of the interphase resin. All systems showed a deleterious effect by hydrothermal aging.

6.4.2 Final Composites

The systems listed in Table 27 were selected for final composites testing and for delivery to the Air Force.

TABLE 27

FINAL COMPOSITE SYSTEMS

Matrix Resin	Interphase Resin	4-Pt ILSS	Flex Prop.	90°C Tensile	Izod Impact
CON-4V	None	X	X	X	X
Epoxy	None	X	X	X	X
CON-4V	SMA:AN/AA/MDA	X	X	X	X
Epoxy	AP/MAN:AN/MDA	X	X	X	X
Thermid 600	SMA:AN/3APA/MDA	No	No	No	No

Hydrothermal aging effects were investigated by 4-point interlaminar shear strength as indicated in the previous section and by flexural strength properties. Indications of changes in interface properties were also

95

investigated by transverse tensile strength and Izod impact strength measurements.

6.4.2.1 Flexural Strength Properties

The flexural strength and modulus values for the CON-4V matrix composites are give in Table 28. The moisture gain for the treated fiber composites was slightly higher than for the control. The dry, room temperature flexural strength of the treated fiber composite was lower than that obtained for the control. However, the former appears to retain a greater percentage of strength on aging. It is not known if this effect is significant or if it reflects differences in panel preparation. The treated fiber panels had a significantly higher fiber volume fraction than the controls. Both thermal and hydrothermal effects on flexural strength are apparent. Modulus values also reflect both thermal (test temperature) and hydrothermal aging effects. Similar to the flexural strength, the retention of modulus appears higher for the experimental system than for the control. Data for the flexural properties of the epoxy resin composites are listed in Table 29. The room temperature dry strength (1848 MPa) of the control was found to be in line with published data for epoxy - AS-1 composites and is considerably higher than that obtained with the CON-4 system. Two levels of interphase resin were investigated in this series. As indicated in Table 13, the moisture gain was higher for the system using the interphase resin modified fiber than the control. The moisture gain also increased with the higher level of interphase resin. The flexural strength and modulus values decreased with the use of interphase resin treated fiber. Both thermal (test temperature) and hydrothermal aging effects were obvious. No advantage was apparent for the treated fiber.

96

TABLE 28

FLEXURAL PROPERTIES OF CON-4V COMPOSITES

System No.	2	5
Interphase Resin		
Type	None	SMA:AN/AA/MDA
Level, %	0	0.84
Fiber Volume, %	51-55	60-64
Exposure Time, Hrs.	28	28
Weight Gain, %	0.42-.43	0.57-.58
Flexural Strength*, MPa(KSI)		
R.T. Dry	1131 (164)	1069 (155)
R.T. Wet	1069 (155)	1048 (152)
E.T. Dry	758 (110)	951 (138)
E.T. Wet	476 (69)	669 (97)
Flexural Modulus, GPa(MSI)		
R.T. Dry	111.7 (16.2)	97.9 (14.2)
R.T. Wet	104.8 (15.2)	106.9 (15.5)
E.T. Dry	99.3 (14.4)	96.5 (14.0)
E.T. Wet	88.9 (12.9)	92.4 (13.4)

6.4.2.2 Transverse Tensile Strength

Transverse tensile strength measurements were obtained on composites made with the two matrix resins, and treated and as received AS-1 fiber. The data listed in Table 30 indicate that higher interfacial strengths were obtained with the epoxy resin system. In both systems the strengths were lower for composites made with the treated fiber than for the control. Examination of the fracture surfaces by SEM was very revealing. The epoxy control specimens failed cohesively (Fig. 19) while the remaining three materials failed adhesively at the interface Figs. 19 and 20. One can conclude that the CON-4

*Flexural strength and modules were determined according to ASTM D790 method I. Values are average for 5 specimens.

97

system has poorer interfacial bond strength than the epoxy (also indicated by interlaminar shear data), and that the interphase resin layer reduces the bond strength. It suggests that if an interphase resin layer is used it must be well bonded to the fiber or interfacial properties will be degraded.

TABLE 29
FLEXURAL PROPERTIES OF EPOXY COMPOSITES

System No.	3	8	7
Interphase Resin			
Type	None	AP/MAN:AN/MDA	AP/MAN:AN/MDA
Level, %	0	0.84	1.2
Fiber Volume, %	65-79	62-63	62-63
Exposure Time, $\sqrt{\text{Hrs.}}$	28	28	28
Weight Gain, %	1.6-2.6	2.5-2.7	3.4-3.6
Flexural Strength, MPa(KSI)			
R.T. Dry	1848 (268)	1579 (229)	1310 (190)
R.T. Wet	1420 (206)	1317 (191)	1282 (186)
E.T. Dry	1558 (226)	1193 (173)	1020 (148)
E.T. Wet	1145 (166)	855 (124)	731 (106)
Flexural Modulus, GPa(MSI)			
R.T. Dry	121.3 (17.6)	105.5 (15.3)	97.2 (14.1)
R.T. Wet	126.9 (18.4)	106.2 (15.4)	97.2 (14.1)
E.T. Dry	115.1 (16.7)	104.8 (15.2)	95.1 (13.8)
E.T. Wet	113.8 (16.5)	102.0 (14.8)	86.2 (12.5)

TABLE 30
TRANSVERSE TENSILE STRENGTH

Matrix Resin	Interphase Resin Type	Level %	Composite Fiber Vol.%	Strength* MPa	(KSI)
CON-4V	None	-	55-57	25.5	(3.7 ± .9)
CON-4V	SMA:AN/AA/MDA	1.0	59-62	15.9	(2.3 ± .4)
Epoxy	None	-	65-66	30.3	(4.4 ± .5)
Epoxy	AP/MAN:AN/MDA	1.5	58-60	17.2	(2.5 ± .5)

* ASTM D 3039; gauge length = 1.5 inches, specimen width = 1 inch; cross-head rate = .02 inches/minute.
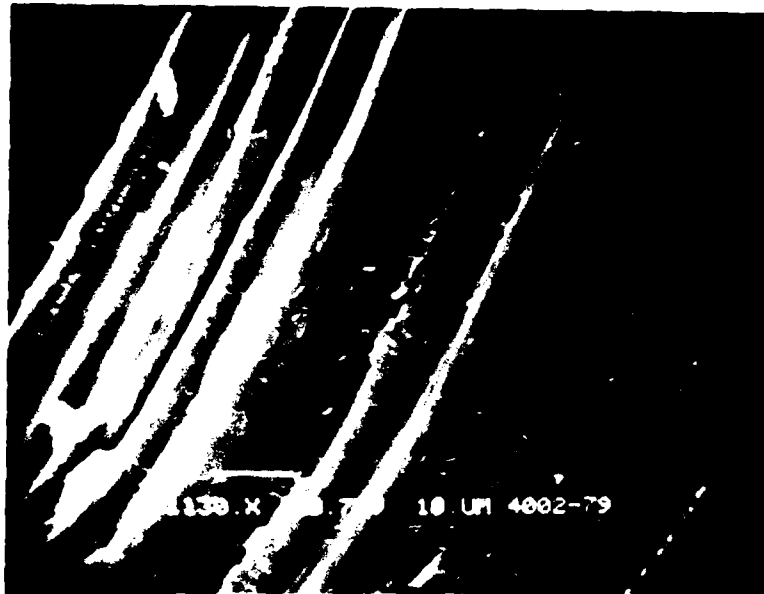
Figure 19.

Cohesive Failure in Epoxy/AS-1 Fiber
Composite 0° Tensile Specimen (1.13 KX)

Figure 20.

Adhesive Failure in CON-4/Interphase-treated Fiber
Composite 0° Tensile Specimen (1.78 KX)

99

6.4.2.3 Impact Properties

Effort was made to determine the effect of the electrodeposited interphase resin on impact strength properties. Izod type specimens were used in this work. The transverse specimens were unnotched while the longitudinal epoxy based specimens were notched. The results of the impact tests as given in Table 31 are quite similar to results obtained with the transverse tensile strength measurements in that the treated fiber composites had lower values than the controls. However, the value obtained for the CON-4 control system was slightly higher than that obtained for the epoxy control (0.96 vs. 0.80). The values obtained in the longitudinal tests are questionable in value because of the variety of the type of failures observed (hinge, broom, partial break, etc.).

TABLE 31

IMPACT STRENGTH PROPERTIES

Panel Number	Matrix Resin Type	Fiber Treatment Type	Level, %	Vol. %/m Fiber	Impact Strength, (ft.lbs./in.) Transverse	Longitudinal
4002-83	CON-4V	None	0	52	51 (0.96 ± .21)	1,810 (33.9 ± 6.9)
4002-88	CON-4V	SMA:AN/AA/MDA	0.80	56	27 (0.50 ± .05)	3,044 (57.0 ± 1.8)
4002-90	Epoxy	None	0	62	43 (0.80 ± .06)	3,818 (71.5 ± 7.4)
4002-92	Epoxy	AP/MAN:AN/MDA	1.39	61	27 (0.51 ± .07)	2,969 (55.6 ± 5.8)

6.5 Composite Testing of Other Fiber Surface Treatments

In addition to the composites prepared from fiber coated with the various electr deposition resins of Table 20, a limited amount of physical testing was

performed on laminates containing fibers with several surface modifications. Four point loaded beam shear specimens were prepared from panels of electrolytically oxidized AS-1 (1N H_2SO_4 = 30 sec.) fiber/epoxy matrix resin and from cyclopentadiene/allene treated AS-1/CON-4 matrix resin combination using the standard lay-up and curing procedures. Results of these measurements are given in Table 32.

Based on the limited data available, all of the panels exhibit the same trends noted in the electrodeposited fiber composites. Interlaminar shear strength losses occur due to both temperature and water effects. Water pickup is equal to or significantly greater than that exhibited in the control panels prepared with commercial AS-1. In the case of the cyclopentadiene-treated fiber, the room temperature unaged composite shows a significant loss in shear strength, presumably due to either lack of bonding or lack of bonding sites between the fiber and matrix resin. With the H_2SO_4 electro-oxidized fiber, the epoxy composite shows a significantly greater elevated temperature, dry strength than even the room temperature, dry control. This possibly means that the dry properties of epoxy composites can be significantly enhanced by increasing the surface oxygen levels on the fiber. Water, however, is still shown to drastically lower the shear strength of this laminate. This illustrates that the problem of moisture susceptibility at the interface still remains a significant hurdle to improvements in composite properties.

TABLE 32

EFFECTS OF SURFACE TREATMENT ON SHEAR STRENGTH

Matrix Resin	Fiber Treat.	Fiber Vol. %	Exp. Time, $\sqrt{hrs}$	Weight Gain, %	Shear Strength, MPa (KSI)			
					R.T. Dry	R.T. Wet	E.T. Dry	E.T. Wet
Epoxy	None	65	21	2.0	57.9 (8.4)	51.0 (7.4)	-	-
Epoxy	None	69	28	2.5	-	-	39.3 (5.7)	27.6 (4.0)
Epoxy	H_2SO_4 Oxid.	53	21	2.1	-	-	62.1 (9.0)	33.1 (4.8)
CON-4	None	66	29.4	0.47	49.4 (7.2)	32.0 (4.6)	42.7 (6.2)	21.6 (3.1)
CON-4	Cyclo-pentadiene Allene	60	21	1.8	32.4 (4.7)	26.2 (3.8)	23.4 (3.4)	20.0 (2.9)

VII. SAMPLES OF MATERIALS DELIVERED

As requested by the AFML Project Engineer, selected samples of materials developed in the program were prepared and delivered to AFML. The samples included composite panels made from electrocoated AS-1 fiber (SMA:AN/AA/MDA and AP/MAN:AN/MDA) and CON-4 and epoxy resin matrices. Control panels made with "as received" AS-1 fiber and the two matrix resins were also delivered. In addition, 400 ft. samples of the two electrocoated fibers used for preparing the selected composites and a 1000 ft. sample of fiber electrocoated with an interphase resin (SMA:AN/3APA/MDA) designed for use with an acetylene terminated polymer such as Thermid 600 were delivered.

VIII. CONCLUSIONS AND RECOMMENDATIONS

Summarized below are the conclusions reached during this program to develop materials and processes to obtain moisture-resistant high-level adhesion between carbon fibers and selected matrix resins. Based on these findings, recommendations are given for further studies in this area.

8.1 Conclusions

8.1.1. As determined from a variety of surface analysis techniques, the oxygen-containing functional groups on commercial AS-1 graphite fiber are predominantly carboxyls, quinones, and phenolics. As determined by ESCA analysis, these groups are present in approximately a 1/1/1 ratio on the surface.

8.1.2. Cycloaddition reactions following high temperature (1050°C) vacuum devolatilization of the AS-1 fiber were conducted with cyclopentadiene and allene. Tensile properties of the fiber were unchanged by this treatment. Composites prepared from the cycloaddition-treated fiber did not have improved interlaminar shear strengths compared with untreated AS-1 fiber.

8.1.3. Additional attempts aimed at altering the oxygen levels on the AS-1 fiber by capping reactions following thermal (600°C) vacuum devolatilization showed no reduction in total surface oxygen. This is most likely due to oxygen or water readsorption or reaction with the devolatilized surface.

8.1.4 Substantial increases in surface oxidation were obtained on AS-1 fiber by electrochemical methods. ESCA analysis showed that most of the added functionality was carboxyl-like and quinone-like. Thermal

104

the fiber integrity. The ILSS of composites prepared from electrochemically oxidized fiber increased relative to control values.

8.1.5 Electrodeposition of a large variety of interphase resins on the surface of AS-1 fiber was successfully accomplished in accordance with the primary program goal. Large scale, continuous processing of entire spools of AS-1 fiber was demonstrated.

8.1.6 The physical properties of composites prepared from electrodeposited AS-1 fiber were not improved as a result of these fiber treatments. Moisture susceptibility and deleterious hydrothermal effects were not decreased by the electrodeposition process. This is likely due to lack of adhesion or grafting between the interphase resin and fiber or the interphase resin and matrix resin.

8.2 Recommendations

8.2.1 Emphasis for future work with interphase materials should be to develop strong adhesion to the fiber through covalent bonding. Techniques to obtain grafting to the graphite fiber surface should be developed.

8.2.2 Matrix resin modification to obtain higher levels of surface free energy but with lower levels of moisture susceptibility should be investigated. Matching the surface free energy of a low moisture susceptible matrix resin more closely to a high surface energy fiber may offer a route to high levels of adhesion with improved moisture resistance.

8.2.3   Further work to obtain specific chemical modifications of a Type A (or equivalent) fiber should be done on an unsized fiber which has been shown to be relatively resistant to thermal oxidation.

8.2.4   Several surface characterization techniques which proved useful or promising in this study are recommended for use in future investigations. These techniques include high resolution ESCA, surface energetics, programmed temperature devolatilization, TGA and possibly radiotracer techniques using a gas chromatography-radiochemical detector combination.

8.2.5   Further work on the use of microscopy techniques for determining the mode of composite failure (adhesive, cohesive, intermediate) should be done. SEM/XRF and SAM (Scanning Auger Microprobe) are promising techniques.

IX. REFERENCES

1. C. R. Thomas and E.J. Walker, "Effects of PAN Carbon Fiber Surface in Carbon - Carbon Composites," _Proc. 5th London Carbon Graphite Conf._, 520 (1978). Society of Chemical Industry, London.

2. D.H. Kaelble, P.J. Dynes and L. Maus, "Hydrothermal Aging of Composite Materials, Part 1. Interfacial Aspects, "_J. Adhesion, 8_, 121 (1976).

3. D.H. Kaelble and P.J. Dynes, "Hydrothermal Aging of Composite Materials, Part 2: Matrix Aspects, "_J. Adhesion, 8_, 195 (1977).

4. P.W.R. Beaumont and B. Harris,"Effect of Environment on Fatigue and Crack Propagation in Carbon Fiber-Reinforced Epoxy Resins, "_J. Comp. Matl., 7_, 1265 (1975).

5. J.B. Donnet and Pierre Ehrburger, "Carbon Fiber in Polymer Reinforcement," _Carbon, 15_, 143 (1977).

6. P. Ehrburger and J.B. Donnet, "Interface in Composite Materials," _Phil. Trans., R. Soc. Lond._, A 294, 495 (1980).

7. P. Ehrburger, J.J. Herque and J.B. Donnet, "Recent Developments in Carbon Fiber Treatments," in _Petroleum Derived Carbons_, M.L. Deviney and T.M. O'Grady, eds., ACS Symposium Series No. 21, Am. Chem. Soc;, Washington (1976).

8.   E. Fitzer, K.H. Geigl, W. Huttner, and R. Weiss, "Chemical Interactions between the Carbon Fiber Surface and Epoxy Resins," Carbon, 18, 393 (1980).

9.   E. Fitzer, K.H. Geigl and W. Huttner, "The Influence of Carbon Fiber Surface Treatments on the Mechanical Properties of Carbon/Carbon Composites," Carbon, 18, 265 (1980).

10.   J.B. Donnet and A. Voet, "Carbon Black," (esp. Chap. 4), Marcel Dekker, New York (1976).

11.   J.B. Donnet, "The Reactivity of Carbons," Carbon, 6, 161-176 (1968).

12.   H.P. Boehn, "Chemical Identification of Surface Oxides," in Advances in Catalysis, Vol. 16, Academic Press, New York (1966).

13.   D. Rivin, "Surface Properties of Carbon," Rubber Chem. Technol., 44, 307 (1971).

14.   B.R. Puri, "Surface Complexes on Carbons," in Chemistry and Physics of Carbon, P.L. Walker, Ed., Marcel Dekker, New York, 6, 191 (1970).

15.   M.L. Deviney, "Surface Chemistry of Carbon Black and Its Implications in Rubber Chemistry," Adv. Colloid & Interface Sci., 2, 237 (1968).

16.   D.W. McKee and V.J. Mimeault, "Surface Properties of Carbon Fibers,"
        in Chemistry and Physics of Carbon, P.L. Walker and P.A. Thrower,
        eds., Marcel Dekker, New York, 8, 151-249 (1973).

17.   J. Delmonte, Technology of Carbon and Graphite Fiber Composites, Van
        Nostrand Reinhold Company, New York (1981).

18.   R.V. Subramanian, J.J. Jakubowski and F.D. Williams, "Interfacial
        Aspects of Polymer Coating by Electropolymerization," J. Adhesion, 9,
        (1978).

19.   R.V. Subramanian and J.J. Jakubowski, "Electropolymerization on
        Graphite Fibers," Polym. Eng. Sci., 18, 590 (1978).

20.   R.V. Subramanian, V. Sundaram and A.K. Patel, "Electrodeposition of
        Polymers on Graphite Fibers: Effects on Composite Properties, " Proc.
        33rd Ann. Conf. Reinforced Plastics/Compos. Int., Soc. Plast. Ind.
        1978, Section 20-F, pp. 1-8.

21.   D.H. Kaelble, P.J. Dynes and L. Maus, "Interfacial Mechanism of
        Moisture Degradation in Graphite-Epoxy Composites," J. Adhesion, 1,
        25 (1974).

22.   D.E. Steutz, et al., "Effects of Moisture on Chemical Interactions at
        a Polymer-Fiber Interface," AFML-TR-77-214, December, 1977.

23.   K. Horie, H. Murai and I. Mita, "Bonding of Epoxy Resin to Graphite
        Fibers," Fiber Science and Technology, 9, 253 (1976).

24.   J.S. Mattson and H.B. Mark, Jr., <u>Activated Carbon-Surface Chemistry and Adsorption from Solution,</u> Marcel Dekker, New York (1971).

25.   G.R. Henning, "Surface Oxides on Graphite Single Crystals," <u>Proceedings of the 5th Conference on Carbon</u>, Pergamon Press, New York, <u>1</u>, 143 (1962).

26.   M.L. Deviney and L.E. Whittington, "Radiotracer Studies of Carbon Black Surface Interactions with Organic Systems. I. Experimental Approach and Initial Results from Chemisorption and Vinyl Polymerization Studies," <u>Rubber Chem. Technol.</u>, <u>41</u>, 382 (1968).

27.   S.S. Barton, G.L. Boulton and B.H. Harrison, "Surface Studies on Graphite: An Estimation of the Average Polarity of the Oxygen Complexes," <u>Carbon</u>, <u>10</u>, 391-393 (1972).

28.   S.S. Barton, D. Gillespie and B.H. Harrison, "Surface Studies on Graphite," <u>Nat. Phys. Sci.</u>, <u>234</u>, 134-135 (1971).

29.   S.S. Barton and B.H. Harrison, "Surface Studies on Graphite: Immersional Energetics," <u>Carbon</u>, <u>10</u>, 245-251 (1972).

30.   S. Hagiwara, K. Tsutsumi and H. Takahashi, "Surface Polarity of Carbon Blacks," <u>Carbon</u>, <u>16</u>, 89-93 (1978).

31. W.H. Wade and M.L. Deviney, "Adsorption and Calorimetric Investigations on Carbon Black Surfaces. I. Immersional Energetics of Heat Treated Channel and Furnace Blacks," Rubber Chem. Technol., 44, 218-229 (1971).

32. W.H. Wade, M.L. Deviney, W.A. Brown, M.H. Hnoosh and D.R. Wallace, "Adsorption and Calorimetric Investigations on Carbon Black Surfaces. III. Immersion Heats in Model Elastomers and Isosteric Heats of Adsorption on C-4 Hydrocarbons," Rubber Chem. Technol., 45, 117-128 (1972).

33. J.S. Mattson, L. Lee, H.B. Mark, Jr., and W.J. Weber, Jr., "Surface Oxides of Activated Carbon: Internal Reflectance Spectroscopic Examination of Activated Sugar Carbons," J. Colloid Interface Science, 33, 284-293 (1970).

34. S.S. Barton, G.L. Boulton, and B.H. Harrison, "Surface Studies on Graphite: Acidic Surface Oxides," Carbon, 10, 395-400 (1972).

35. R.C. Bansal, T.L. Dhami and S. Parkash, "Surface Characteristics and Surface Behavior of Polymer Carbons - I. Associated Oxygen and Hydrogen," Carbon, 15, 157-160 (1977).

36. P.J. Hart, F.J. Vastola and P.L. Walker, Jr., "Oxygen Chemisorption on Well Cleaned Carbon Surfaces," Carbon, 5, 363-371 (1967).

37. C.M. Elliott and R.W. Murray, "Chemically Modified Carbon Electrodes," Anal. Chem., 48, 1247-1253 (1976).

38.   H. Marsh, A.D. Foord, J.S. Mattson, J.M. Thomas, and E.L. Evans,
       "Surface Oxygen Complexes on Carbons from Atomic Oxygen: An Infrared
       (IRS), High Energy Photoelectron Spectroscopic (XPS), and Thermal
       Stability Study," J. Colloid Interface Science, 49, 368-382 (1974).

39.   M. Fujihira, A. Tamura and T. Osa, "Organo-Modified Carbon
       Electrode. I. Studies of Modified Layer via Amide Bonds by
       Capacitance Measurements and ESCA," Chem. Letter, 361-366 (1977).

40.   M. Yamada, I. Ikemoto and H. Kuroda, "Surface Oxidation of the Thin
       Films of Polycyclic Aromatic Hydrocarbons Studied by X-ray Photoelectron
       Spectroscopy," Bull. Chem. Soc. Japan, 50, 2262-2265 (1977).

41.   J.F. Evans, T. Kuwana, M.T. Henne and G.P. Royer, "Electrocatalysis
       of Solution Species Using Modified Electrodes," J. Electroanal Chem.,
       80 409 (1977).

42.   S. Evans and J.M. Thomas, "The Chemical Nature of Ion-Bombarded
       Carbon: A Photoelectron Spectroscopic Study of "Cleaned" Surfaces of
       Diamond and Graphite," Proc. R. Soc. Lond., 353, 103-120 (1977).

43.   E. Papirer, E. Guyon and N. Perol, "Contribution to the Study of the
       Surface Groups on Carbons. II. Spectroscopic Methods," Carbon, 16,
       133-140 (1978).

44.   F. Hopfgarten, "Surface Study of Carbon Fibers with ESCA and Auger
       Electron Spectroscopy," Fiber Sci Tech., 11, 67-79 (1978).

45.   H.S. Borovetz, "Scanning Electron Microscopic and Surface Analytical Study of an Isotropic Vapor Deposited Carbon Film on Microporous Membranes," _SEM_, _2_, 85-93 (1978).

46.   V.A. Garten and D.E. Weiss, "The Quinone-Hydroquinone Character of Activated Carbon and Carbon Black," _Aust. Chem. Soc. J._, _8_, 68-95 (1955).

47.   J.V. Hallum and H.V. Drushel, "The Organic Nature of Carbon Black Surfaces," _J. Phys. Chem._, _62_, 110-117 (1969).

48.   I.F. Jones and R.C. Kaye, "Polarography of Carbon Suspensions," _J. Electroanal. Chem._, _20_, 213-221 (1969).

49.   B.D. Epstein, E. Dalle-Molle and J.S. Mattson, "Electrochemical Investigations of Surface Functional Groups on Isotropic Pyrolytic Carbons," _Carbon_, _9_, 609-615 (1971).

50.   J.S. Mattson, H.B. Mark, Jr., M.D. Malbin, W.J. Weber, Jr. and J.C. Crittenden, "Surface Chemistry of Active Carbon: Specific Adsorption of Phenols," _J. Colloid Interface Science_, _31_, 116-144 (1969).

51.   L.A. Mashkovich, "Oxidation Resistance of Pyrolytic Carbon in a Liquid Medium," _Inorg. Materials_, _6_, 56-69 (1977).

52. B.D. Epstein and E. Dalle-Molle, "Surface Charge Behavior of Pyrolytic Carbon in Saline and Blood Plasma," *Trans. Amer. Soc. Artif. Int. Org.,* 17, 14-21 (1971).

53. K.F. Blurton, "An Electrochemical Investigation of Graphite Surfaces," *Electrochem. Acta,* 18, 869-876 (1973).

54. J.P. Randin and E. Yeager, "Differential Capacitance Study on the Edge Orientation of Pyrolytic Graphite and Glassy Carbon Electrodes," *J. Electroanal. Chem.,* 58, 313-322 (1975).

55. T.J. Fabish and M.L. Hair, "The Dependence of the Work Function of Carbon Black on Surface Acidity," *J. Colloid Interface Science,* 62, 16-23 (1977).

56. S. Mazur, T. Matusinovic and K. Cammann, "Organic Reactions of Oxide-Free Carbon Surfaces, and Electroactive Derivative," *J. Am. Chem. Soc.,* 99, 3888-3890 (1977).

57. S. Mazur "Studies of the Structure and Reactivity of Oxygen-Free Carbon Surfaces" *Technical Report DAHCO-75-G-0054* July 27, 1976. U.S. Army Research Office, Research Triangle Park, N.C.

58. E. Papirer and E. Guyon, "Electrochemical Response of the Surface Oxygenated Groups on Carbons," *Fuel,* 57 123-124 (1978).

59.   A.W. Adamson, _Physical Chemistry of Surfaces,_ Wiley Interscience, N.Y., 1976.

60.   D.H. Kaelble, _Physical Chemistry of Adhesion,_ Wiley Interscience, N.Y. 1971.

61.   L.T. Drzal, "The Surface Composition and Energetics of Type A Graphite Fiber," _Carbon,_ _15,_ 129-138 (1977).

62.   J.T. Grant ad G.E. Hammer, "Electron Spectroscopic Studies of Surfaces and Interfaces for Adhesive Bonding," AFML-TR-79-4220, August, 1979.

63.   R.N. King, "Surface Characterization of Synthetic Polymers for Biomedical Applications," Ph.D. Dissertation, University of Utah, June, 1980.

64.   B. Rand and R. Robinson, "Surface Characteristics of Carbon Fibers from PAN", and "A Preliminary Investigation of PAN Based Carbon Fiber Surfaces by Flow Microcalorimetry," _Carbon,_ _15,_ 257 and 311 (1977).

65.   D.T. Clark, "Some Chemical Applications of ESCA," in _Molecular Spectroscopy,_ A.R. West, Ed., Heydon and Sons, New York (1977).

66.   D.T. Clark, "The Investigation of Polymer Surfaces by Means of ESCA," in _Polymer Surfaces,_ D.T. Clark and W.J. Feast, eds., John Wiley and Sons, New York (1978).

67.   Technical Information Bulletin No. AL-103 Aldrich Chemical Co., 940
        W. St. Paul Ave., Milwaukee, Wis. 53233.

68.   S.S. Barton, D.J. Gillespie and B.H. Harrison, "The Structure of
        Acidic Surface Oxides on Carbon and Graphite-II, Carbon, 16, 363-365
        (1978).

69.   M.L. Deviney, L.E. Whittington and B.G. Corman, "The Migration of
        Extender Oil in Natural And Synthetic Rubber. V. Dependence of
        Diffusion Rates on Oil Concentration and Elastomer Blend Ratios in a
        Simulated Tire During Service," Rubber Chem. Technol. 44, 87 (1971).

70.   T.J. deBoer and H.J. Backer, Organic Synthesis, Coll. Vol. 14, J.
        Wiley and Sons, N.Y., N.Y. (1963).

71.   F. Arndt, Org. Synthesis, Coll. Vol. 2, Wiley, New York (1943).

72.   M. Neeman and Y. Hashimoto, "The Structure of Estriol
        Monoglucosiduronic Acid from Human Pregnancy Urine," J. Am. Chem.
        Soc., 84, 2972 (1962).

73.   S.S. Barton, B.H. Harrison and J. Dollimore, "Surface Studies on
        Graphite: Desorption of Surface Oxides," J. Chem. Soc. Faraday I,
        69, 1039 (1973).

74.   J.S. Perkins, D.S. Smith and D. Rivin, "Pyrolytic Analysis of Carbon
      Fibers," Ext. Abstracts of Papers, 11th Biennial Conf. on Carbon,
      Gatlenburg, Tn., June 4-8, 1973. American Carbon Committee, Oak
      Ridge National Labs, Pubs.

75.   S.S. Barton, B.H. Harrison, and J. Dollimore, "Surface Studies on
      Graphite. Desorption of Surface Oxides Formed on the Clean Surface
      at 300°K," J. Phys. Chem., 82, 290-294 (1978).

76.   C.B. Delano, J.D. Dodson and R.J. Milligan, "High Temperature Resins
      for Composites," AFML TR-77-188, Part II, Acurex Corp., (1977).

77.   P.E. McMahon, "Oxidative Resistance of Carbon Fibers and Their
      Composites," Advanced Composite Materials - Environmental Effects,
      ASTM STP 658, J.R. Vinson, ed., 254-266 (1978).

78.   R.T. Bendure, "Dynamic Adhesion Tension Measurement," J. Colloid
      Interface Sci., 42, 137-144 (1972).

79.   D.H. Kaelble and P.J. Dynes, "Surface Energy Analysis of Treated
      Graphite Fibers," J. Adhesion, 6, 239 (1974).

80.   L.T. Drzal, J.A. Mescher and D.L. Hall, "The Surface Composition and
      Energetics of Type HM Graphite Fibers," Carbon, 17, 375-382 (1979).

81.   G.E. Hammer and L.T. Drzal, "Graphite Fiber Surface Analysis by X-ray
        Photoelectron Spectroscopy and Polar/Dispersive Free Energy
        Analysis," <u>Appl. Surface Sci.</u>, <u>4</u>, 340-55 (1980).

82.   R. Aveyard and D.A. Haydon, <u>An Introduction to the Principles of
        Surface Chemistry,</u> Cambridge Press (1973).

83.   F.M. Fowkes, "Attractive Forces at Interfaces," in <u>Chemistry and
        Physics of Interfaces,</u> ACS Publications, Wash., D.C. (1965).

84.   L.T. Drzal, Personal Communication, present Address: AFWAL, Wright-
        Patterson Air Force Base, Ohio.

85.   S.L. Diener, "Development of Improved Electrodeposited Corrosion
        Inhibiting Primers," AFML-TR-79-4073, June 1979.

86.   D.H. Kaelble, and P.J. Dynes, "Nondestructive Tests for Shear
        Strength Degradation of a Graphite-Epoxy Composite," <u>Composite
        Materials: Testing and Design (Fourth Conference), ASTM STP 617,</u>
        American Society for Testing and Materials, 190-200 (1977).

87.   C.E. Browning, Personal Communication. Present Address: AFWAL,
        Wright-Patterson Air Force Base, Ohio.

88.   J.M. Whitney and C.E. Browning, "Some Anomalies Associated with
        Moisture Diffusion in Epoxy Matrix Composite Materials, " <u>Advanced
        Composites Materials - Environmental Effects, ASTM STP 658,</u> J.R.
        Vinson, ed. American Society for Testing and Materials, 43-60 (1978).

APPENDIX

10.1   Matrix Resin Preparation

      A.   CON-4D

          1.Materials

C-1000	- 100gm.	Carboxy terminated polybutadiene (Nippon-Soda)
Heloxy 69	- 7.2gm.	Resorcinol diglycidyl ether (Wilmington Chemical Co.)
AMC-2	- 0.5gm.	Cordoba Chemical Co.
Dicup	- 5.0gm.	Dicumylperoxide - Hercules

2.Procedure

The C-1000 is charged to a 300 ml beaker, the AMC-2 added and mixed. The mixture is heated with stirring to 80°C. The Heloxy 69 is added dropwise over a period of 1 hour with vigorous mixing. The temperature is maintained at 80°C. The reaction is followed by acid number. After 5-5 ½ hours reaction time the acid number is stabilized at 28-30. The batch is cooled to 60°C and Dicup is added. Stirring is continued for 15-20 minutes and the batch is cooled to room temperature and stored in a freezer until used. On the day it is used, the resin is warmed to room temperature and mixed with solvent.

      B.   CON-4V

          1.   Materials - same as CON-4D with the exception that Vulcup (Hercules) is used in place of Dicup.

          2.   Procedure - same as CON-4V

C. Thermid 600 - LR-600 was diluted with MEK to lower viscosity. AL-600 was diluted with ethanol.

10.2 Molding Procedure

A. Lay-up Sequence (typical) for Vacuum Bag Molding

1. Silicone rubber separator sheet

2. Two layers of fiberglass cloth

3. Top caul plate (1/8" aluminum)

4. FEP film

5. Fiberglass cloth bleeder ply

6. TX-1040 Teflon coated fiberglass (porous) cloth

7. Prepreg plies

8. TX-1040 Teflon coated fiberglass cloth.

9. Fiberglass cloth bleeder ply

10. FEP film

11. Bottom caul plate ($\frac{1}{4}$" aluminum)

Coroprene strips are used to contain the lay-up during molding. A thermocouple is placed next to the lay-up to monitor the curing temperature.

B. Procedure - CON-4

The Mini-Clave loaded with a lay-up is inserted into a room temperature hydraulic press. A clamp force of 5-15 tons is applied to seal the Mini-Clave. A vacuum is applied to the Mini-Clave and the cure cycle started. A typical time-temperature pressure cycle for CON-4 is given below:

1. Start; T=room; vacuum on (30"Hg)

120

2. Heat to 200°F in 25-30 minutes; hold at 200°F for 30 min.

3. Heat to 275°F in ~ 15 minutes; hold at 275°F for 2 hours; additional pressure (N_2) 0-35 psi is applied when T=275°F.

4. Heat to 350°F in ~ 45 minutes; hold at 350°F for 4 hours.

5. Turn off heaters; allow to cool to room temperature overnight.

6. The panel is removed from the Mini-Clave and the bleeder plies and TX-1040 sheets removed simultaneously from each side of the panel.

C. Procedure - Epoxy

1. Start @ R.T.; vacuum on (30"Hg)

2. Heat to 107°C (225°F) in 40 minutes, hold @ 107°C (225°F) for 60 minutes.

3. Heat to 177°C (350°F) over a 60 minute period.

4. Hold at 177°C (350°F) for 60 minutes.

5. Cool to room temperature overnight.

6. Post cure 6 hours at 177°C (350°F).

10.3   Conversion Factors

To Convert From	To	Multiply By
Pounds/in.^{2} x 10^3 (KSI)	Megapascal (MPa)	6.894757
Pounds/in.^{2} x 10^6 (MSI)	Gegapascal (GPa)	6.894757
Foot lbs./in.	Joules/Meter (J/M)	53.3379

DAT FILM